Published for SISSA by Springer

Received: *May 6, 2022*
Accepted: *August 4, 2022*
Published: *June 14, 2023*

Cross-section measurements for the production of a Z boson in association with high-transverse-momentum jets in pp collisions at $\sqrt{s} = 13$ TeV with the ATLAS detector

The ATLAS collaboration

E-mail: atlas.publications@cern.ch

Abstract: Cross-section measurements for a Z boson produced in association with high-transverse-momentum jets ($p_{\mathrm{T}} \geq 100$ GeV) and decaying into a charged-lepton pair ($e^+e^-, \mu^+\mu^-$) are presented. The measurements are performed using proton–proton collisions at $\sqrt{s} = 13$ TeV corresponding to an integrated luminosity of 139 fb^{-1} collected by the ATLAS experiment at the LHC. Measurements of angular correlations between the Z boson and the closest jet are performed in events with at least one jet with $p_{\mathrm{T}} \geq 500$ GeV. Event topologies of particular interest are the collinear emission of a Z boson in dijet events and a boosted Z boson recoiling against a jet. Fiducial cross sections are compared with state-of-the-art theoretical predictions. The data are found to agree with next-to-next-to-leading-order predictions by NNLOJet and with the next-to-leading-order multi-leg generators MadGraph5_aMC@NLO and Sherpa.

Keywords: Electroweak Interaction, Hadron-Hadron Scattering

ArXiv ePrint: 2205.02597

https://doi.org/10.1007/JHEP06(2023)080

JHEP06(2023)080

Contents

1 Introduction

The measurement of Z-boson production[1] in association with jets, $Z+$jets, constitutes a powerful test of perturbative quantum chromodynamics (QCD) [1, 2] and, in the case of high-energy jets, it provides a way to probe the interplay between QCD and higher-order electroweak (EW) processes [3–6]. The large $Z+$jets production cross section and the easily identifiable decays of the Z boson to charged-lepton final states offer a clean experimental signature which can be measured precisely. Such processes also constitute non-negligible backgrounds in measurements of the Higgs boson [7, 8] and in searches for new phenomena [9–11], which often exploit the presence of high-p_{T} jets to enrich a data sample with potential signal. In those studies, predictions are used to extrapolate $Z+$jets backgrounds from control regions to the signal regions and to model the distributions of the final discriminants.

In the calculations of $Z+1$-jet production at leading order (LO), the Z boson recoils against a quark or a gluon. At next-to-leading order (NLO), real and virtual QCD and EW effects play a role in $Z+$jets production, such as in topologies corresponding to dijet events where a real Z boson is emitted from an incoming or outgoing quark leg [3–6].

[1] Throughout this paper, Z/γ^*-boson production is simply referred to as Z-boson production.

JHEP06(2023)080

Example Feynman diagrams for LO and NLO $Z+$jets production processes are shown in figure 1. The latter case can lead to production rate enhancements proportional to $\alpha_s \ln^2(p_{T,j1}/m_Z)$, where α_s is the strong coupling constant, $p_{T,j1}$ the transverse momentum of the leading jet, and m_Z the mass of the Z boson, and thus the effect can become very large for events with high-p_T jets. These events exhibit a collinear enhancement in the distribution of the angular distance between the Z boson and the closest jet. Although the enhancement can be probed in the region of small angular separation, this region also contains contributions where the Z boson is produced in association with larger numbers of jets, which must be included in the predictions. The measurements presented in this paper target QCD-only $Z+$jets production, treating EW $Z+2$-jets (EW Zjj) production [12] as a background. Measurements where the EW Zjj contribution is treated as signal and not subtracted as background are also performed and published in the HEPData entry [13] of this measurement.

The ATLAS Collaboration [14] at the Large Hadron Collider (LHC) [15] first measured angular distributions in high-p_T W boson production with jets ($W+$jets) in the 8 TeV pp-collision data set [16]. The first similar measurement in $Z+$jets events was published by the CMS Collaboration and used a partial 13 TeV data set corresponding to 35.9 fb^{-1} [17]. Both measurements highlight the fact that the collinear region, where the angular separation between the W/Z boson and the closest jet is small, represents a major challenge for contemporary Monte Carlo (MC) generators. The measurements presented in this paper include a wide range of new observables sensitive to the presence of high-p_T jets and to the collinear emission of a Z boson in dijet events. The statistical power of the full LHC Run-2 data set makes it possible to tighten the collinear selection, and to measure key observables separately for collinear and non-collinear topologies.

This publication focuses on events that contain a Z-boson candidate reconstructed from either an e^+e^- or $\mu^+\mu^-$ pair in association with hadronic jets defined as jets having transverse momentum greater than or equal to 100 GeV. The phase-space region with at least one associated jet is labelled as the *inclusive* region. In this region, the measured quantities are the transverse momentum of the leading jet ($p_{T,j1}$), the transverse momentum of the Z boson ($p_{T,\ell\ell}$), the scalar sum of the transverse momentum of all selected jets and leptons (H_T), and the jet multiplicity. A *high-p_T* region is selected by requiring the presence of a jet with $p_T \geq 500$ GeV. To test the prediction that this region is composed of two characteristic topologies, the soft radiation of a Z boson from a jet (*collinear* topology) and the hard scatter of a Z boson against a jet (*back-to-back* topology), the *high-p_T* region is split to cover different ranges of the angle between the Z boson and the closest jet, and selected key observables are measured separately for each region. In the *high-p_T* region, the following observables sensitive to the presence of collinear Z-boson emission are studied:

- $\Delta R^{\min}_{Z,j}$, the angular distance[2] between the Z boson and the closest jet. Real Z-boson radiation is expected to be enhanced at low values of $\Delta R^{\min}_{Z,j}$. At large values of

[2] ATLAS uses a right-handed coordinate system with its origin at the nominal interaction point (IP) in the centre of the detector and the z-axis along the beam pipe. The x-axis points from the IP to the centre of the LHC ring, and the y-axis points upwards. Cylindrical coordinates (r, ϕ) are used in the transverse plane, ϕ being the azimuthal angle around the z-axis. The pseudorapidity is defined in terms of the polar angle

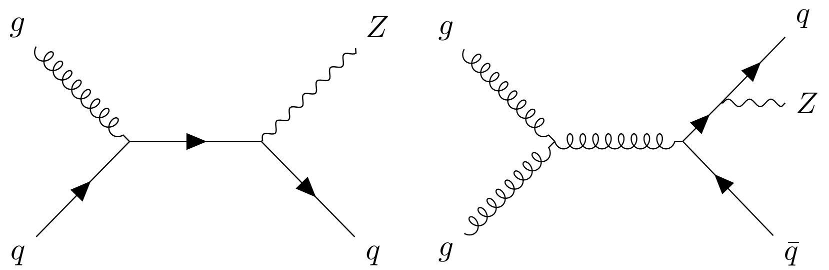

Figure 1. Representative Feynman diagrams for the production of a Z boson in association with high-p_{T} jets. The $Z+1$-jet events (left) are expected to populate the *back-to-back* region where the Z boson is balanced against a single high-p_{T} jet. In dijet events (right), the Z boson is expected to be radiated from the quark leg, with kinematics leading to small values of the angular distance between the Z boson and the closest jet, $\Delta R_{Z,j}^{\mathrm{min}}$, and therefore populating the *collinear* region.

$\Delta R_{Z,j}^{\mathrm{min}}$, the Z boson is balanced by a recoiling jet and large virtual EW corrections are expected. To enrich these two topologies, *collinear* and *back-to-back* regions are constructed by requiring $\Delta R_{Z,j}^{\mathrm{min}} \leq 1.4$ and $\Delta R_{Z,j}^{\mathrm{min}} \geq 2.0$, respectively.

- $r_{Z,j}$, the ratio of the Z-boson p_{T} to the closest-jet p_{T}, defined as

$$r_{Z,j} \equiv \frac{p_{\mathrm{T},\ell\ell}}{p_{\mathrm{T}}(\text{closest jet})}.$$

Collinear Z-boson radiation is expected to be dominated by soft Z bosons, resulting in very small values for this ratio.

- N_{jets}, the jet multiplicity. The *back-to-back* region is expected to be dominated by $Z+1$-jet events, whereas the *collinear* region would be dominated by $Z+2$-jets events.

The measurements of jet multiplicity and $r_{Z,j}$ are performed both in the full *high-p_{T}* region and separately in the *collinear* and *back-to-back* regions.

Measurements of jet multiplicity and $\Delta R_{Z,j}^{\mathrm{min}}$ are also performed in an alternative high-energy region, constructed by requiring the scalar sum of the transverse momentum of all selected jets, S_{T}, to be at least 600 GeV. This alternative region probes high-energy events but does not depend on the presence of a single very energetic object. In this region, called the *high-S_{T}* region, a large fraction of the events have higher jet multiplicity.

Predictions from the most recent generators combine NLO multi-leg matrix elements (ME) with a parton shower (PS) and hadronisation model [18–21]. Fixed-order parton-level theoretical predictions for $Z+$jets production at next-to-next-to-leading order (NNLO) are available for up to one associated jet [22–25]. In this paper, the cross-section measurements are compared with state-of-the-art multi-leg ME+PS generators and NNLO fixed-order

θ as $\eta = -\ln\tan(\theta/2)$. The angular distance is defined as $\Delta R \equiv \sqrt{(\Delta y)^2 + (\Delta\phi)^2}$. When dealing with massive jets and particles, the rapidity $y = (1/2)\ln[(E+p_z)/(E-p_z)]$ is used, where E is the jet/particle energy and p_z is the z-component of the jet/particle momentum.

JHEP06(2023)080

Z + jets predictions from NNLOJET [24, 25]. Virtual EW corrections were made available recently [26, 27] and are included in one of the SHERPA [19] predictions studied in this paper.

The paper is organised as follows. Section 2 contains a brief overview of the ATLAS detector. The data and simulated samples, as well as additional predictions used in the analysis, are described in section 3. The object definition and the event reconstruction at detector level are presented in section 4, while section 5 describes the background modelling and presents a comparison of measured and predicted yields at detector level. After background subtraction, the data are unfolded to particle level in a fiducial phase space with a procedure described in section 6. The experimental and theoretical systematic uncertainties are estimated in section 7. Section 8 presents the unfolded cross-section results and the comparisons with predictions. Conclusions are provided in section 9.

2 ATLAS detector

The ATLAS experiment at the LHC is a multipurpose particle detector with a forward–backward symmetric cylindrical geometry and a near 4π coverage in solid angle. It consists of an inner tracking detector surrounded by a thin superconducting solenoid providing a 2 T axial magnetic field, electromagnetic and hadron calorimeters, and a muon spectrometer. The inner tracking detector covers the pseudorapidity range $|\eta| < 2.5$. It consists of silicon pixel, silicon microstrip, and transition radiation tracking detectors. Lead/liquid-argon (LAr) sampling calorimeters provide electromagnetic (EM) energy measurements with high granularity. A steel/scintillator-tile hadron calorimeter covers the central pseudorapidity range ($|\eta| < 1.7$). The endcap and forward regions are instrumented with LAr calorimeters for both the EM and hadronic energy measurements up to $|\eta| = 4.9$. The muon spectrometer surrounds the calorimeters and is based on three large superconducting air-core toroidal magnets with eight coils each. The field integral of the toroids ranges between 2.0 and 6.0 T m across most of the detector. The muon spectrometer includes a system of precision tracking chambers and fast detectors for triggering. A two-level trigger system is used to select events. The first-level trigger is implemented in hardware and uses a subset of the detector information to accept events at a rate below 100 kHz. This is followed by a software-based trigger that reduces the accepted event rate to 1 kHz on average depending on the data-taking conditions. An extensive software suite [28] is used in the reconstruction and analysis of real and simulated data, in detector operations, and in the trigger and data acquisition systems of the experiment.

3 Data set and simulated event samples

The data used in this analysis were recorded with the ATLAS detector from 2015 to 2018 in pp collisions at $\sqrt{s} = 13$ TeV (full Run-2 data set) and correspond to a total integrated luminosity of 139 fb^{-1} [29]. The mean number of pp interactions per bunch crossing, including the hard scattering and other interactions in the same and neighbouring bunch crossings (pile-up), was $\langle\mu\rangle = 34$.

JHEP06(2023)080

Process	Generator	Order pQCD	References
Signal			
$Z \to \ell\ell$ ($\ell = e, \mu$)	SHERPA 2.2.11	0–2p NLO, 3–5p LO	[19, 32–42]
$Z \to \ell\ell$ ($\ell = e, \mu$)	MG5_aMC+Py8 FxFx	0–3p NLO	[19–21, 42–45]
$Z \to \ell\ell$ ($\ell = e, \mu$)	SHERPA 2.2.1	0–2p NLO, 3–4p LO	[18, 32–40]
$Z \to \ell\ell$ ($\ell = e, \mu$)	MG5_aMC+Py8 CKKWL	0–4p LO	[43, 46–48]
$Z \to \ell\ell$ ($\ell = e, \mu$)	NNLOJET@NNLO	1p NNLO	[24, 25]
$Z \to \ell\ell$ ($\ell = e, \mu$)	NNLOJET@NLO	1p NLO	[24, 25]
Backgrounds			
EW $Zjj(\to \ell\ell$ ($\ell = e, \mu$))	HERWIG 7.1.5, VBFNLO 3.0.0	NLO	[49–51]
$Z \to \tau\tau$	SHERPA 2.2.1	0–2p NLO, 3–4p LO	[18, 32–40]
W+jets	SHERPA 2.2.1	0–2p NLO, 3–4p LO	[18, 32–40]
$t\bar{t}$	POWHEG BOX v2 + PYTHIA 8.230	NLO	[52–55]
Single top (t-, Wt-, s-channel)	POWHEG BOX v2 + PYTHIA 8.230	NLO	[52–55]
$Z/W(\to qq)Z(\to \ell\ell)$	SHERPA 2.2.1	0–1p NLO, 2–3p LO	[18, 32–40]
$W(\to \ell\nu)Z(\to qq)$	SHERPA 2.2.1	0–1p NLO, 2–3p LO	[18, 32–40]
$W^{\pm}(\to qq)W^{\mp}(\to \ell\nu)$	SHERPA 2.2.1	0–1p NLO, 2–3p LO	[18, 32–40]
$\ell\ell\nu\nu, \ell\ell\ell\nu, \ell\ell\ell\ell$	SHERPA 2.2.2	0–1p NLO, 2–3p LO	[18, 32–40]
$V(\to \ell\ell) + \gamma$	SHERPA 2.2.8	0–1p NLO, 2–3p LO	[18, 32–40]

Table 1. Summary of the programs used to produce the signal and the various background samples. For every process the name of the program used is indicated in the second column. The third column reports the order of the QCD calculation in the matrix elements, where np denotes the number of real parton emissions. The SHERPA 2.2.11 Z + jets processes include virtual electroweak corrections.

MC simulation samples are used to estimate most of the contributions from background events, to unfold the data to particle level, and in comparisons with the unfolded data distributions. The generated samples were processed using the GEANT4-based ATLAS detector simulation [30, 31] and the same event-reconstruction algorithms are used for both the MC samples and the data. A summary of the MC generators and calculations used for the simulation of signal and background processes is provided in table 1.

The production of Z bosons in association with jets was simulated with the ATLAS configuration of SHERPA 2.2.11 [19], which includes matrix elements for up to five partons at LO and up to two partons at NLO. They are calculated with the Comix [32] and OPENLOOPS [33–35] libraries and matched with the SHERPA parton shower [36] using the MEPS@NLO prescription [37–40] with a set of tuned parameters ('tune') developed by the SHERPA authors. In contrast to SHERPA 2.2.1 [18], used previously in ATLAS publications, it includes a modified Catani–Seymour subtraction scheme [41], the Hessian NNPDF3.0NNLO PDF set [42] is used, and an analytic enhancement technique has been introduced [19]. The cross section in the *high-p_T* region has been considerably reduced relative to the prediction from the previous SHERPA version by switching to an improved matching scheme with a different treatment of unordered histories [40]. SHERPA 2.2.11 is also the only sample used in this paper which includes NLO virtual EW corrections [34, 35]. The samples were produced using three options for the combination of NLO EW and QCD corrections: an additive, a multiplicative, and an exponential scheme. The nominal prediction is derived via the additive scheme; a systematic uncertainty band is derived from the envelope of all schemes. In contrast to virtual EW corrections, EW parton showers are not included in any of the generators used in this paper. The SHERPA 2.2.11 $Z+$jets samples are used for the nominal unfolding of the data distributions, to estimate the systematic uncertainties and in comparisons with the cross-section measurements.

A second $Z+$jets sample, referred to as MG5_AMC+PY8 FXFX [19], was produced by using the MADGRAPH5_AMC@NLO 2.6.5 [43] program to generate matrix elements at NLO accuracy in QCD for up to three additional partons in the final state. The NNPDF3.1NNLO set [42] was used in the generation. The parton showering and subsequent hadronisation was performed using PYTHIA 8.240 [21] with the A14 tune [44] and the NNPDF2.3LO PDF set [45]. The jet multiplicities were merged using the FxFx prescription [20]. This prediction is compared with the unfolded cross-section measurements.

A third sample of $Z+$jets events and an event sample from $W+$jets processes were produced with the SHERPA 2.2.1 [18] generator using NLO matrix elements for up to two partons, and LO matrix elements for up to four partons, calculated with the Comix and OPENLOOPS libraries. They were matched with the SHERPA parton shower using the MEPS@NLO prescription with a set of tuned parameters developed by the SHERPA authors. The MC replica version of the NNPDF3.0NNLO set of PDFs was used. The SHERPA 2.2.1 $Z+$jets sample is used in comparisons with the unfolded cross-section measurements, as it was used as a standard in previous ATLAS Run-2 publications.

A fourth $Z+$jets sample, referred to as MG5_AMC+PY8 CKKWL, was generated using LO-accurate matrix elements with up to four final-state partons calculated by MADGRAPH5_AMC@NLO 2.2.2 [43]. The ME calculation employed the NNPDF3.0NLO PDF set and was interfaced to PYTHIA 8.186 [46] for the modelling of the parton shower, hadronisation, and underlying event. The overlap between matrix element and parton shower emissions was removed using the CKKW-L merging procedure [47, 48]. The A14 tune of PYTHIA was used with the NNPDF2.3LO PDF set. This sample is used to validate the unfolding method and in comparisons with the unfolded cross-section measurements.

Two additional $Z+$jets samples were generated with the NNLOJET program [24, 25], which computes fixed-order parton-level predictions for inclusive jet processes at higher orders in QCD. The NLO and NNLO predictions, referred to as NNLOJET@NLO and NNLOJET@NNLO, respectively, were calculated as higher-order corrections to the parton-level LO process of $Z+1$-jet production. The NNPDF3.1NNLO set was used with a central scale choice of $\mu_0 = \frac{1}{2}(E_{\mathrm{T},Z} + \Sigma_{i\in\mathrm{partons}} p_{\mathrm{T},i})$ with $E_{\mathrm{T},Z} = \sqrt{m_{\ell\ell}^2 + p_{\mathrm{T},Z}^2}$. These samples are pure QCD predictions at parton level. To match the fiducial selection of the measurement (see section 6), scale factors to correct from the Born level to the dressed-lepton level are computed and applied to these predictions. The slightly different overlap-removal procedure for jets and leptons used in these samples, due to the NNLOJET program design, is addressed by overlap-removal correction scale factors. Both sets of scale factors, deviating from unity at the percent level and computed separately for each bin of the measured observables, are published in the HEPData entry [13] of this measurement. Non-pertubative corrections are found to be consistent with zero when $p_{\mathrm{T},j1}$ exceeds 100 GeV and are not needed to match the fiducial selection of these measurements. These samples are used in comparisons with the unfolded cross-section measurements.

JHEP06(2023)080

The EW Zjj process is defined by the t-channel exchange of a weak boson and at tree level is calculated at $\mathcal{O}(\alpha_{\mathrm{EW}}^4)$ when including the decay of the Z boson [12]. In contrast, the strong Zjj process, which is covered by the $Z+$jets samples, has no weak boson exchanged in the t-channel and at tree level is calculated at $\mathcal{O}(\alpha_{\mathrm{EW}}^2\alpha_{\mathrm{s}}^2)$ when including the decay of the Z boson. The EW Zjj samples were produced in the vector-boson fusion (VBF) approximation with HERWIG 7.1.5 [49, 50] at NLO accuracy in the strong coupling, using VBFNLO 3.0.0 [51] to provide the loop amplitude. The MMHT2014LO PDF set [56] was used along with the default set of tuned parameters for parton showering, hadronisation and the underlying event. To account for the interference between strong Zjj and EW Zjj processes, a uniform modelling uncertainty of 25% in the EW Zjj cross section (40% in the collinear region), determined from simulation with MADGRAPH5_AMC@NLO 2.9.5, is applied [12].

The $t\bar{t}$ background in this measurement is derived with a data-driven method as described in section 5. The MC $t\bar{t}$ events used for intermediate steps of the method were modelled using the POWHEG BOX v2 [52–55] generator at NLO with the NNPDF3.0NLO PDF set and the h_{damp} parameter[3] set to 1.5 m_{top} [57]. The events were interfaced to PYTHIA 8.230 [21] to model the parton shower, hadronisation, and underlying event, with parameters set according to the A14 tune and using the NNPDF2.3LO set of PDFs. The $t\bar{t}$ sample is normalised to the cross-section prediction at NNLO accuracy, including the resummation of next-to-next-to-leading logarithmic (NNLL) soft-gluon terms calculated with TOP++ 2.0 [58–64].

Single top quark production in the s-channel, in the t-channel, and in association with a W boson (tW) was modelled using the POWHEG BOX v2 generator at NLO in QCD with the five-flavour scheme and the NNPDF3.0NLO set of PDFs. The diagram-removal scheme [65] was used to remove interference and overlap with $t\bar{t}$ production. The tW cross section is corrected to the theory prediction at approximate NNLO accuracy [66, 67], while the s- and t-channel cross sections are corrected to the prediction at NLO accuracy [68, 69].

Samples of diboson final states (VV) were produced with the SHERPA 2.2.1 or SHERPA 2.2.2 generator depending on the process, including off-shell effects and Higgs boson contributions where appropriate. Fully leptonic final states and semileptonic final states, where one boson decays leptonically and the other hadronically, were generated using matrix elements at NLO accuracy in QCD for up to one additional parton and at LO accuracy for up to three additional parton emissions. The matrix element calculations were matched and merged with the SHERPA parton shower as detailed above for SHERPA 2.2.1, and the NNPDF3.0NNLO set of PDFs was used.

The production of $V+\gamma$ final states was simulated with the SHERPA 2.2.8 [18] generator. Matrix elements at NLO QCD accuracy for up to one additional parton and LO accuracy for up to three additional parton emissions were matched and merged with the SHERPA parton shower as detailed above for SHERPA 2.2.1, and the NNPDF3.0NNLO set of PDFs was used.

[3]The h_{damp} parameter is a resummation damping factor and one of the parameters that control the matching of POWHEG matrix elements to the parton shower and thus effectively regulates the high-p_{T} radiation against which the $t\bar{t}$ system recoils.

Background events involving semileptonic decays of heavy quarks, hadrons misidentified as leptons, and, in the case of the electron channel, electrons from photon conversions are referred to collectively as 'multijet events'. The multijet background is estimated using data-driven techniques, as described in section 5.

For bottom and charm hadron decays, the EvtGen 1.7.0 program [70] was used for MG5_aMC+Py8 FxFx samples, and EvtGen 1.2.0 was used for all other MadGraph and Powheg samples. The effect of multiple interactions in the same and neighbouring bunch crossings (pile-up) was modelled by overlaying the simulated hard-scattering event with inelastic pp events generated with Pythia 8.186 [46] using the NNPDF2.3lo PDF and the A3 tune [71]. The small differences in lepton reconstruction, isolation, and trigger efficiencies between simulation and data are corrected in the simulation on an event-by-event basis by applying efficiency scale factors for each lepton [72–74].

4 Event reconstruction

Events are used if they were recorded during stable beam conditions and if they satisfy detector and data-quality requirements [75]. They are required to have a primary vertex, defined as the vertex with the highest sum of track p_{T}^2, with at least two associated tracks with $p_{\mathrm{T}} > 500\,\mathrm{MeV}$ [76]. Events are selected using triggers [77–79] that require at least two electrons or two muons, or the combination of at least one electron and one muon; the efficiencies for these triggers plateau in the region of $p_{\mathrm{T}} > 25\,\mathrm{GeV}$.

Electron candidates are reconstructed from inner-detector tracks which come from the primary vertex and are matched to clusters of energy deposits in the EM calorimeter. To fulfil the primary-vertex condition, the electron track's transverse impact parameter significance must satisfy $|d_0|/\sigma(d_0) < 5.0$, where d_0 is the transverse impact parameter and $\sigma(d_0)$ its uncertainty, and the longitudinal impact parameter z_0 must satisfy $|z_0 \sin(\theta)| < 0.5$ mm, where θ is the angle of the track to the beamline. Electron candidates must satisfy the 'Medium' likelihood-based identification requirements [72] based on EM shower shapes, track quality, and track–cluster matching. They must also satisfy the 'PflowLoose' [72] isolation requirement. Electron candidates are used in the analysis if they have $p_{\mathrm{T}} \geq 25$ GeV and $|\eta| < 1.37$ or $1.52 < |\eta| < 2.47$.

Muon candidates are identified by matching inner-detector tracks from the primary vertex to either full tracks or track segments reconstructed in the muon spectrometer. The candidates must satisfy the following primary-vertex requirements: the transverse impact parameter significance must satisfy $|d_0|/\sigma(d_0) < 3.0$ and the longitudinal impact parameter must satisfy $|z_0 \sin(\theta)| < 0.5$ mm, where d_0, $\sigma(d_0)$, z_0 and θ are as defined above for the electrons. Muons are required to pass 'Medium' identification requirements [73, 74] based on quality criteria applied to the inner-detector and muon-spectrometer tracks. Muon candidates with $p_{\mathrm{T}} \geq 300$ GeV must satisfy tighter identification requirements in the muon spectrometer in order to improve the muon-p_{T} resolution. Muons must also satisfy the 'PflowLoose' isolation requirement, built from tracking and calorimeter information, with a muon-p_{T}-dependent variable cone size ΔR [74]. Muon candidates are used in the analysis if they have $p_{\mathrm{T}} \geq 25$ GeV and $|\eta| < 2.4$.

JHEP06(2023)080

Jets of hadrons are reconstructed using a particle-flow algorithm [80] based on noise-suppressed positive-energy topological clusters in the calorimeter. Energy deposited in the calorimeter by charged particles is subtracted and replaced by the momenta of tracks which are matched to those topological clusters. The jets are clustered using the anti-k_t [81] algorithm implemented in the FASTJET package [82] with a radius parameter $R = 0.4$. They are further calibrated according to in situ measurements of the jet energy scale [83]. Analysis jets are required to have a calibrated $p_{\mathrm{T}} \geq 100$ GeV and $|y| < 2.5$.

Electrons, muons and jets are reconstructed and identified independently. An overlap-removal procedure is then applied to uniquely identify these objects in an event. For the lepton–jet overlap removal, softer jets with $p_{\mathrm{T}} \geq 30$ GeV and $|y| < 2.5$ are considered. Preselected jets with a high probability to have been initiated by an electron or a radiated photon such that ΔR between the jet and a lepton is smaller than 0.2 are removed. In a second step, leptons closer than $\Delta R = 0.4$ to any remaining jet are removed.

Events are selected if they contain a Z-boson candidate reconstructed from two same-flavour, opposite-charge leptons ($\ell = e, \mu$) and with dilepton invariant mass $71\,\mathrm{GeV} \leq m_{\ell\ell} \leq 111\,\mathrm{GeV}$. The selected events are also required to contain at least one analysis jet. Events which satisfy the above selection requirements define the *inclusive* $Z+$jets region. A dedicated *high-p_{T}* region is created by requiring the leading jet to have $p_{\mathrm{T},j1} \geq 500$ GeV. This latter region is split into the *collinear* region, where the angular distance between the Z boson and the closest jet must be $\Delta R_{Z,j}^{\mathrm{min}} \leq 1.4$, and the *back-to-back* region that requires $\Delta R_{Z,j}^{\mathrm{min}} \geq 2.0$. An alternative phase space is also defined by requiring $S_{\mathrm{T}} \geq 600$ GeV, labelled as the *high-S_{T}* region, where S_{T} is defined as the scalar sum of the p_{T} of the analysis jets.

5 Background estimation

Backgrounds from single-boson, diboson and single-top-quark processes are estimated using the MC samples described in section 3, while top-pair production and 'multijet event' contributions from semileptonic decays of heavy quarks, hadrons misidentified as leptons, and electrons from photon conversions are estimated from data. A summary of the composition and relative importance of the backgrounds in the various signal regions is given in table 2. The overall purity of the $Z+$jets selections (defined as the expected fraction of signal events after the final selection) ranges from 94% in the *inclusive* region to 87%, 86%, 87% and 88% in the *high-p_{T}*, *collinear*, *back-to-back* and *high-S_{T}* regions, respectively. Backgrounds are dominated by $t\bar{t}$, diboson and EW Zjj processes, with fractions of 2%–5% , 2%–6% and 1%–5%, respectively. The fraction of events arising from $Z \to \tau^+\tau^-$, $W+$jets, $V+\gamma$, and multijet backgrounds is below the percent level in all signal regions.

The $t\bar{t}$ background is evaluated with a data-driven methodology. A $t\bar{t}$-enriched control region is constructed with the same event selection as the signal region, but with $e^{\pm}\mu^{\mp}$ final states instead of the same-flavour e^+e^- or $\mu^+\mu^-$ pairs. This control region contains only percent-level contributions from $Z+$jets, $W+$jets, diboson, single-top and $Z \to \tau^+\tau^-$ events. The prediction for the $t\bar{t}$ distributions in the signal region is obtained by multiplying the corresponding measured distributions in the control region (after subtracting the non-$t\bar{t}$

$Z \to e^+e^-$	*Inclusive*	*High-p_{T}*	*Collinear*	*Back-to-back*	*High-S_{T}*
$Z+$jets	$1\,171\,000 \pm 49\,000$	$6\,150 \pm 310$	$2\,520 \pm 120$	$2\,520 \pm 150$	$18\,300 \pm 800$
$t\bar{t}$	$43\,400 \pm 1\,300$	209 ± 16	136 ± 13	47.2 ± 7.5	917 ± 41
Diboson	$19\,530 \pm 750$	428 ± 29	183 ± 16	167 ± 16	$1\,008 \pm 53$
EW Zjj	$13\,270 \pm 500$	312 ± 23	102 ± 11	135 ± 14	789 ± 43
Single-top	$2\,430 \pm 160$	27.9 ± 5.5	14.0 ± 3.8	9.8 ± 3.2	54.2 ± 8.2
$Z \to \tau\tau$	515 ± 37	4.6 ± 4.2	1.6 ± 2.1	2.2 ± 1.7	10.6 ± 6.2
$W+$jets	93 ± 16	3.4 ± 1.9	0.3 ± 0.6	2.9 ± 1.7	3.4 ± 1.9
$V+\gamma$	$1\,413 \pm 83$	14.2 ± 4.3	6.5 ± 2.6	5.1 ± 2.3	34.1 ± 7.3
Total predicted	$1\,252\,000 \pm 51\,000$	$7\,150 \pm 350$	$2\,970 \pm 130$	$2\,890 \pm 170$	$21\,100 \pm 880$
Data	$1\,312\,145$	$7\,539$	$2\,955$	$3\,231$	$21\,746$
$Z \to \mu^+\mu^-$	*Inclusive*	*High-p_{T}*	*Collinear*	*Back-to-back*	*High-S_{T}*
$Z+$jets	$1\,537\,000 \pm 63\,000$	$6\,700 \pm 300$	$2\,950 \pm 130$	$2\,420 \pm 120$	$23\,110 \pm 920$
$t\bar{t}$	$55\,400 \pm 1\,300$	209 ± 16	142 ± 12	39.1 ± 6.6	$1\,058 \pm 41$
Diboson	$24\,160 \pm 870$	438 ± 27	198 ± 16	157 ± 14	$1\,149 \pm 55$
EW Zjj	$17\,020 \pm 580$	328 ± 22	113 ± 12	134 ± 13	915 ± 45
Single-top	$3\,110 \pm 190$	29.1 ± 5.5	13.6 ± 3.8	11.2 ± 3.5	70.0 ± 9.2
$Z \to \tau\tau$	460 ± 33	3.5 ± 4.0	1.1 ± 2.3	1.8 ± 1.5	8.8 ± 5.4
$W+$jets	128 ± 14	1.9 ± 1.4	0.3 ± 0.5	1.5 ± 1.3	2.7 ± 2.0
$V+\gamma$	$1\,273 \pm 90$	2.5 ± 2.4	0.0 ± 0.7	2.2 ± 1.5	22.4 ± 5.5
Total predicted	$1\,638\,000 \pm 64\,000$	$7\,710 \pm 330$	$3\,420 \pm 140$	$2\,770 \pm 140$	$26\,300 \pm 1\,000$
Data	$1\,673\,057$	$7\,896$	$3\,372$	$3\,059$	$26\,567$

Table 2. Event yields in the different $Z+$jets signal regions in the electron and muon channels. Uncertainties correspond to the statistical and experimental systematic uncertainties added in quadrature. The $Z+$jets prediction is computed with SHERPA 2.2.11. The number of multijet events is negligible and not included.

contributions) by $ee/e\mu$ and $\mu\mu/e\mu$ scale factors [84]. These factors are computed bin by bin in the signal region for each distribution using simulation.

Diboson backgrounds are dominated by two contributions: semileptonic WZ and ZZ final states, and fully leptonic diboson final states where the decay products of a gauge boson are reconstructed as jets. The measured kinematics of the boson decay products, as well as the production of one or two additional jets, agrees with predictions from SHERPA, as demonstrated in refs. [85–89] within the modelling uncertainties described in section 7. The simulation of the EW Zjj events done with HERWIG+VBFNLO agrees with measurements performed in ($Z \to \ell^+\ell^-$)-enriched phase spaces [12]. Due to their good performance in previous measurements, simulations are used to describe the diboson and EW Zjj backgrounds in this analysis.

Multijet events are assessed with a data-driven approach using a template fit of the $m_{\ell\ell}$ distribution. The $m_{\ell\ell}$ template for this background is derived from data in a multijet-enriched control region, which is defined by either inverting or dropping the lepton selection requirements associated with isolation, identification and charge. The sub-percent contributions to the multijet template that do not originate from the multijet background are evaluated and subtracted using simulation. The fit is performed over the range

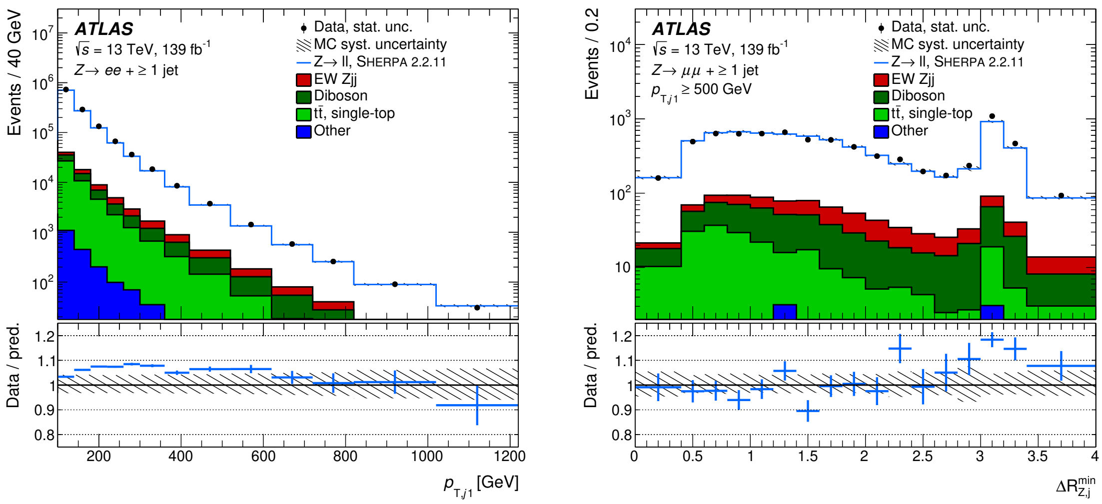

Figure 2. Distributions of the leading-jet p_{T} in the *inclusive* region in the electron channel (left) and the angular distance between the Z boson and the closest jet, $\Delta R^{\min}_{Z,j}$, in the *high*-p_{T} region in the muon channel (right). The signal and background samples are stacked to produce the figures. The $W+$jets, $Z \to \tau^-\tau^+$ and $V+\gamma$ processes are combined and labelled 'Other'. The bottom panel shows the ratio of the data to the total prediction. Experimental uncertainties (described in section 7) for the signal and background distributions are combined in the hatched band, and the data statistical uncertainty is shown as error bars.

51 GeV $\leq m_{\ell\ell} \leq$ 151 GeV. The contribution from multijet events in the analysis is then estimated in the invariant-mass interval of the signal region (71 GeV $\leq m_{\ell\ell} \leq$ 111 GeV). The resulting fraction of multijet events is at the sub-percent level and so is neglected in this analysis.

Figure 2 shows the data and predicted event yields as a function of $p_{\mathrm{T},j1}$ in the electron channel and as a function of $\Delta R^{\min}_{Z,j}$ in the *high*-p_{T} region in the muon channel. The SHERPA 2.2.11 predictions agree with the data in general, but do not describe it precisely in the full range of the measurements. The distributions are discussed in more detail in section 8.

6 Unfolding of detector effects

The cross-section measurements presented in this paper (see section 1) are performed within the fiducial acceptance region defined by the following requirements:

- Two same-flavour, opposite-charge leptons with $p_{\mathrm{T}} \geq 25$ GeV and $|\eta| < 2.5$
- 71 GeV $\leq m_{\ell\ell} \leq$ 111 GeV
- At least one jet, where jets must have $p_{\mathrm{T}} \geq 100$ GeV and $|y| < 2.5$.

The *high*-p_{T}, *collinear*, *back-to-back*, and *high*-S_{T} signal regions are defined in analogy to the detector-level definitions.

JHEP06(2023)080

The cross sections are defined at particle level, corresponding to 'dressed' electrons and muons. A dressed lepton is defined as the four-vector combination of a prompt lepton (that does not originate from the decay of a hadron or a τ-lepton, or from a photon conversion) and all prompt photons within a surrounding cone of size $\Delta R = 0.1$. The particle level also includes jets found by applying the anti-k_t algorithm with radius parameter $R = 0.4$ to final-state particles with decay length $c\tau > 10$ mm, excluding dressed Z-boson decay products. Overlap removal is also applied at particle level: jets with $p_{\mathrm{T}} \geq 30$ GeV within $\Delta R = 0.2$ of a dressed lepton are removed, followed by the removal of leptons within $\Delta R = 0.4$ of the remaining jets. This overlap removal is applied at particle level in order to best match the detector response, especially in the *collinear* region where the detector is not able to discriminate easily between nearby objects.

The fiducial cross sections are evaluated from the reconstructed kinematic observables for events that pass the selection described in section 4. The expected background components, as described in section 5, are subtracted from the distributions in data.

An iterative unfolding technique [90] with two iterations, as implemented in the RooUnfold package [91], is used to unfold the background-subtracted data to the particle level, thereby accounting for the impact of detector inefficiencies and resolution [72–74, 80, 83]. Before entering the iterative unfolding, the background-subtracted data are corrected for the expected fraction of events passing the detector-level selection but not the particle-level selection. The unfolding is carried out with the response matrices constructed from the SHERPA 2.2.11 $Z+$jets samples. The unfolded event yields are divided by the integrated luminosity of the data sample to provide the final fiducial cross sections [92]. The electron and muon channels are unfolded separately and then combined to measure the production cross section for a Z boson decaying into a single charged-lepton flavour ($Z \to \ell^+\ell^-$).

The binning of all observables is optimised to keep the statistical uncertainty below 10% and to maximize the purity, or the fraction of reconstructed events where the reconstructed and truth values fall in the same bin. The latter is kept above 60%, with typical values of $70-90\%$. In order to mitigate the modelling uncertainty due to migration effects across the lower edge of the $p_{\mathrm{T},j1}$ distribution, this observable is unfolded using two underflow bins within 60 GeV $\leq p_{\mathrm{T},j1} \leq$ 100 GeV. In a similar fashion, an underflow bin is added for the $p_{\mathrm{T},\ell\ell}$, H_{T} and jet multiplicity distributions for events where the leading jet does not pass the $p_{\mathrm{T}} \geq 100$ GeV selection but instead has 60 GeV $\leq p_{\mathrm{T},j1} \leq$ 100 GeV. The unfolding of $r_{Z,j}$ is performed in two dimensions using three bins for the p_{T} of the closest jet for each bin of $r_{Z,j}$.

7 Systematic uncertainties

Theory modelling uncertainties. Theoretical modelling uncertainties from the MC predictions are considered when unfolding the data and in the comparisons with the cross-section measurements.

Modelling uncertainties are taken into account by varying the QCD scales, the PDFs and, in the case of SHERPA 2.2.11, the virtual EW corrections. The effect of QCD scale uncertainties is defined by the envelope of variations resulting from changing the renormal-

JHEP06(2023)080

isation (μ_r) and factorisation (μ_f) scales by factors of two with an additional constraint of $0.5 \leq \mu_\mathrm{r}/\mu_\mathrm{f} \leq 2$. Uncertainties due to the PDF parameterisation are evaluated using sets of PDF variations [93]. The PDF uncertainties also include a comparison with the nominal MMHT2014NNLO [56] PDF and the CT14NNLO [94] PDFs. For SHERPA $Z+$jets and diboson processes, the PDF uncertainties also include a consistent variation of α_s in the PDF and in the hard scatter based on NNPDF3.0NLO [42]. The prediction from SHERPA 2.2.11 also considers uncertainties related to the NLO virtual EW corrections, derived from the envelope of the additive, multiplicative and exponentiated EW correction schemes [19]. The uncertainties associated with the virtual EW corrections are maximal and amount to 5% where the EW corrections are largest: in the *back-to-back* region with large $p_{\mathrm{T},\ell\ell}$ and $\Delta R^{\mathrm{min}}_{Z,j} \approx \pi$. In comparison, the effect of QCD scale uncertainties on SHERPA 2.2.11 predictions ranges between 10% and 60%, with average values near 25%. The corresponding range in MG5_AMC+PY8 FXFX is between 5% and 20%. The differences between these two generators and their uncertainties are further explored in ref. [19]. In the NNLOJET predictions, the QCD scale uncertainties are typically in the range between 5% and 10% and constitute the dominant systematic component. Due to computational limitations in the NNLOJET program, the predictions do not include PDF uncertainties.

The diboson predictions used in the background subtraction from data include PDF and scale uncertainties. The EW Zjj prediction includes the effects of scale, PDF and interference uncertainties, which amount to normalisation uncertainties of 9%, 2% and 25%–40% respectively (see section 3). The effects of scale and PDF uncertainties on the single-top predictions amount to a total normalisation uncertainty of about 4%, primarily from the normalisation to theory predictions at NNLO and NLO accuracies.

Systematic uncertainties in cross-section measurements. Systematic uncertainties in the measured cross sections stem from experimental, MC-modelling and unfolding uncertainties. The uncertainties are propagated to the data cross sections by varying the subtracted background and the MC inputs to the unfolding procedure (response matrix, fraction of unmatched events, reconstruction efficiency). They are treated as being correlated over kinematic regions, over distributions of observables and, where applicable, over channels and between signal and background processes.

Experimental uncertainties specific to each leptonic final state ($Z \to e^+e^-$ and $Z \to \mu^+\mu^-$): Systematic uncertainties in the lepton-candidate selection are related to the reconstruction, identification, isolation, and trigger [72, 73]. Uncertainties in the lepton calibrations can cause changes in the acceptance, owing to the migration of events across the p_T threshold and the $m_{\ell\ell}$ boundaries. The uncertainties in the electron energy scale and resolution are taken into account [95], as are those related to the muon momentum scale, inner-detector and muon-spectrometer resolution, and sagitta-bias correction [73].

Experimental uncertainties common to the electron and muon final states: Systematic uncertainties associated with jet reconstruction are addressed via jet-energy-scale (JES) variations in a 29-nuisance-parameter scheme and jet-energy-resolution (JER) variations in a 13-nuisance-parameter scheme [96, 97]. Imperfect modelling of the effects of pile-up leads to acceptance changes for different jet multiplicities. To assess this uncertainty, the average number of pile-up interactions is varied in simulation. The uncertainty in the combined 2015–2018 integrated luminosity is 1.7% [98], obtained using the LUCID-2 detector [99] for the primary luminosity measurements.

Modelling uncertainties: Distribution-shape variations from PDF, scale and EW uncertainties in the SHERPA 2.2.11 $Z+$jets simulation, computed as described above, are propagated to the unfolded cross sections via the response matrices and associated unmatched-events and efficiency corrections. Although the uncertainties in the simulation can be large, their effect on the cross-section measurement is minimised by the unfolding technique used. The systematic uncertainties in the modelling of background MC samples are propagated to the unfolded cross section via the background subtraction in the signal regions. The background-modelling uncertainty comes mainly from the diboson and EW Zjj backgrounds.

Systematic uncertainties associated with the unfolding procedure: Systematic uncertainties account for possible residual biases in the unfolding procedure, such as those due to the modelling of the signal events or the finite bin width used in each distribution. The limited size of a simulation sample can also create biases in the distribution used in the unfolding procedure. The following uncertainties from the unfolding procedure are considered:

- The statistical uncertainties of the MC inputs to the unfolding procedure are propagated to the unfolded cross sections with a 'toy' simulation method based on 1000 ensembles (pseudo-experiments) of unfolding inputs.
- The effects of the mismodelling of the data by the MC simulation on the results of unfolding procedure are derived by reweighting the SHERPA 2.2.11 $Z+$jets MC simulation at particle level for each unfolded observable, such that the MC simulation distribution matches the background-subtracted data at the reconstruction level. The reweighted MC simulation is unfolded with the non-reweighted response matrix and the uncertainty is obtained by comparing the unfolded result against the reweighted distribution at particle level (non-closure).
- An additional uncertainty is derived to account for more subtle differences between the SHERPA 2.2.11 and MG5_AMC+PY8 CKKWL generators (e.g. hadronisation models, additional soft objects, distributions in other kinematic dimensions) which are not accounted for by the previous method. A non-closure test is performed where the MG5_AMC+PY8 CKKWL samples are first reweighed to match SHERPA 2.2.11 particle-level distributions for each observable in turn and subsequently unfolded with SHERPA 2.2.11. The uncertainty is evaluated by comparing the unfolded result and the reweighted distribution at particle level.

The total fractional uncertainties of the unfolded differential cross sections in $p_{\mathrm{T},j1}$ and $\Delta R^{\mathrm{min}}_{Z,j}$ for the combined $Z \to \ell^+\ell^-$ measurement, performed as detailed in section 8, are shown in figure 3. Table 3 shows the breakdown of the total relative statistical and systematic uncertainties in the measured integrated cross sections for $Z+$jets production in the five kinematic search regions. In the *inclusive* and *high-*S_{T} regions, jet uncertainties

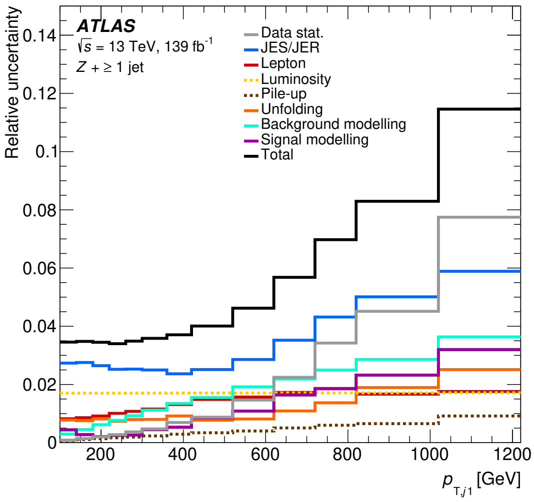

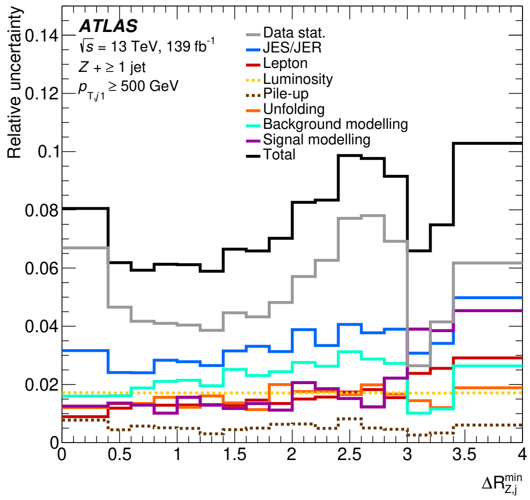

Figure 3. Fractional uncertainties in the measured differential cross-sections in $p_{\mathrm{T},j1}$ in the *inclusive* region (left) and in $\Delta R^{\mathrm{min}}_{Z,j}$ in the *high-*p_{T} region (right) from the combined $Z \to \ell^+\ell^-$ measurement.

Uncertainty source [%]	*Inclusive*	*High-*p_{T}	*Collinear*	*Back-to-back*	*High-*S_{T}
JES/JER	2.6	3.2	2.8	3.6	2.8
Lepton	0.9	1.6	1.4	2.0	1.1
Luminosity	1.7	1.7	1.7	1.7	1.7
Pile-up	0.1	0.4	0.4	0.4	0.4
Unfolding	0.5	1.0	1.1	1.4	0.8
Background modelling	0.5	2.0	2.0	1.9	1.7
Signal modelling	0.5	1.2	1.1	1.1	1.1
Total syst. uncertainty	3.4	4.8	4.4	5.3	4.2
Data stat. uncertainty	0.1	2.1	2.9	2.7	1.2
Total uncertainty	3.4	5.3	5.3	5.9	4.4

Table 3. Relative statistical and systematic uncertainties (in %) in the measured integrated cross sections for Z + jets production in the five search regions, computed by integrating over the respective jet-multiplicity distribution.

dominate with a relative contribution of 2.6% and 2.8%, respectively. In the *high-*p_{T} region and its *collinear* and *back-to-back* subregions the jet and data statistical uncertainties are largest, with relative contributions of 3.2% and 2.1% in the *high-*p_{T} region, respectively, 2.8% and 2.9% in the *collinear* region, and 3.6% and 2.7% in the *back-to-back* region.

8 Results

The integrated and differential fiducial cross sections are measured in the electron and muon channels separately, and the compatibility of the results from the two channels is tested. These results are then combined using the Best Linear Unbiased Estimate (BLUE)

JHEP06(2023)080

method [100]. In the combination, all systematic uncertainties except the lepton-related experimental uncertainties are treated as correlated between the electron and muon channels. Data and MC statistical uncertainties are treated as uncorrelated between channels. The combined measurements are consistent with both individual decay channels for the full set of observables. In general, the uncertainties in the measured cross sections are dominated by the systematic uncertainties and are smaller than the uncertainties in the predictions, except for NNLOJET@NNLO, which matches or exceeds the precision of the measurements in some kinematic regions.

Integrated fiducial cross sections for $Z+\text{jets}$ production are evaluated in the *inclusive*, *high-p_{T}*, *collinear*, *back-to-back* and *high-S_{T}* signal regions (see section 6) by summing over the respective unfolded jet-multiplicity distributions. The measured cross sections are compared with the predictions from SHERPA 2.2.11, MG5_AMC+PY8 FXFX, SHERPA 2.2.1 and with NNLO and NLO predictions from NNLOJET in table 4 and in figure 4. The prediction from SHERPA 2.2.11 uniquely includes NLO virtual EW corrections (see section 3). When these virtual corrections are removed from the SHERPA 2.2.11 prediction, its total cross sections for the *inclusive*, *high-p_{T}*, *collinear*, *back-to-back* and *high-S_{T}* regions increase by 0.065%, 6.9%, 3.8%, 11% and 3.0%, respectively. The cross sections predicted by the three generators and the NNLOJET predictions agree with the measured values within the theory uncertainties.

Differential cross sections are measured and compared in figures 5–11 with predictions from SHERPA 2.2.1, MG5_AMC+PY8 CKKWL, and the next-generation MC generators SHERPA 2.2.11 and MG5_AMC+PY8 FXFX, and with NLO and NNLO $Z+\text{jets}$ calculations from NNLOJET. In general, NNLOJET@NNLO and MG5_AMC+PY8 FXFX provide the most precise predictions.

The Z-boson and jet transverse momenta (two correlated quantities) are fundamental observables of the $Z+\text{jets}$ process and probe pertubative QCD over a wide range of scales. Moreover, understanding the kinematics of jets in events with vector bosons produced in association with several jets is essential for the modelling of backgrounds for other SM processes and searches beyond the SM. Figure 5 shows the differential cross section as a function of $p_{\mathrm{T},\ell\ell}$ and $p_{\mathrm{T},j1}$. The high-$p_{\mathrm{T},\ell\ell}$ region is dominated by the back-to-back topology and receives significant negative corrections due to EW effects. In contrast, events with a *high-p_{T}* jet typically result in both back-to-back and collinear topologies. The SHERPA 2.2.1 and MG5_AMC+PY8 CKKWL generators predict a harder $p_{\mathrm{T},j1}$ distribution than seen in the data, resulting in an overestimation of the cross section for high $p_{\mathrm{T},j1}$. In contrast, SHERPA 2.2.11 and MG5_AMC+PY8 FXFX show significantly better modelling of the $p_{\mathrm{T},j1}$ spectrum and are also in good agreement with the measured $p_{\mathrm{T},\ell\ell}$ spectrum. The smaller cross section from SHERPA 2.2.11 relative to SHERPA 2.2.1 in the *high-p_{T}* region is attributed to the improved matching scheme with a different treatment of unordered histories [19]. The prediction from MG5_AMC+PY8 FXFX models the data more precisely, due to the inclusion of NLO matrix elements with three partons. The NNLOJET@NNLO predictions describe the data very precisely, except for very large values of $p_{\mathrm{T},\ell\ell}$ (and $p_{\mathrm{T},j1}$), where negative NLO virtual EW corrections of 10%–20% are expected and the QCD-only calculation overestimates the data.

JHEP06(2023)080

Inclusive $Z+$jets					
Data	13.90	$\pm$ 0.01 (stat)	$\pm$ 0.47 (syst)		pb
SHERPA 2.2.11	13.3	$^{+0.2}_{-0.2}$ (PDF)	$^{+3.1}_{-1.8}$ (Scale)	$\pm \leq 0.1$ (EW)	pb
MG5_AMC+PY8 FXFX	14.5	$^{+0.1}_{-0.1}$ (PDF)	$^{+0.8}_{-1.2}$ (Scale)		pb
SHERPA 2.2.1	13.8	$^{+0.5}_{-0.5}$ (PDF)	$^{+5.2}_{-3.4}$ (Scale)		pb
NNLOJET@NNLO	13.83		$^{+0.18}_{-0.27}$ (Scale)		pb
NNLOJET@NLO	13.5		$^{+1.1}_{-0.9}$ (Scale)		pb
High-p_{T}: $p_{\mathrm{T},j1} \geq 500$ GeV					
Data	72.3	$\pm$ 1.5 (stat)	$\pm$ 3.5 (syst)		fb
SHERPA 2.2.11	69	$^{+2}_{-1}$ (PDF)	$^{+28}_{-17}$ (Scale)	$^{+2}_{-2}$ (EW)	fb
MG5_AMC+PY8 FXFX	78	$^{+4}_{-1}$ (PDF)	$^{+9}_{-12}$ (Scale)		fb
SHERPA 2.2.1	95	$^{+4}_{-3}$ (PDF)	$^{+40}_{-26}$ (Scale)		fb
NNLOJET@NNLO	76		$^{+10}_{-12}$ (Scale)		fb
NNLOJET@NLO	71		$^{+14}_{-11}$ (Scale)		fb
Collinear: *High-p_{T}* and $\Delta R^{\mathrm{min}}_{Z,j} \leq 1.4$					
Data	27.9	$\pm$ 0.8 (stat)	$\pm$ 1.2 (syst)		fb
SHERPA 2.2.11	28	$^{+1}_{-1}$ (PDF)	$^{+14}_{-8}$ (Scale)	$\pm \leq 1$ (EW)	fb
MG5_AMC+PY8 FXFX	29.6	$^{+1.3}_{-0.3}$ (PDF)	$^{+3.1}_{-4.3}$ (Scale)		fb
SHERPA 2.2.1	39	$^{+2}_{-1}$ (PDF)	$^{+18}_{-11}$ (Scale)		fb
NNLOJET@NNLO	27.0		$^{+5.7}_{-7.2}$ (Scale)		fb
NNLOJET@NLO	24.1		$^{+7.0}_{-5.1}$ (Scale)		fb
Back-to-back: *High-p_{T}* and $\Delta R^{\mathrm{min}}_{Z,j} \geq 2.0$					
Data	31.6	$\pm$ 0.8 (stat)	$\pm$ 1.7 (syst)		fb
SHERPA 2.2.11	28.1	$^{+0.6}_{-0.3}$ (PDF)	$^{+7.9}_{-4.9}$ (Scale)	$^{+1.4}_{-1.4}$ (EW)	fb
MG5_AMC+PY8 FXFX	34.4	$^{+1.6}_{-0.3}$ (PDF)	$^{+4.6}_{-5.6}$ (Scale)		fb
SHERPA 2.2.1	38	$^{+2}_{-1}$ (PDF)	$^{+15}_{-10}$ (Scale)		fb
NNLOJET@NNLO	35.3		$^{+1.9}_{-2.4}$ (Scale)		fb
NNLOJET@NLO	36.0		$^{+3.5}_{-3.3}$ (Scale)		fb
High-S_{T}: $S_{\mathrm{T}} \geq 600$ GeV					
Data	226.0	$\pm$ 2.6 (stat)	$\pm$ 9.5 (syst)		fb
SHERPA 2.2.11	220	$^{+10}_{-10}$ (PDF)	$^{+110}_{-60}$ (Scale)	$\pm \leq 10$ (EW)	fb
MG5_AMC+PY8 FXFX	247	$^{+10}_{-2}$ (PDF)	$^{+30}_{-37}$ (Scale)		fb
SHERPA 2.2.1	280	$^{+10}_{-10}$ (PDF)	$^{+130}_{-80}$ (Scale)		fb
NNLOJET@NNLO	223		$^{+43}_{-47}$ (Scale)		fb
NNLOJET@NLO	168		$^{+45}_{-33}$ (Scale)		fb

Table 4. Measured integrated fiducial cross sections for $Z+$jets production in the five signal regions and predictions from SHERPA 2.2.11, MG5_AMC+PY8 FXFX, SHERPA 2.2.1, NNLOJET@NNLO and NNLOJET@NLO. Systematic uncertainties in the measured and predicted cross sections are calculated as described in section 7.

Jet-multiplicity distributions provide an excellent probe of QCD. Whereas the $Z+1$-jet bin is most sensitive to PDF effects, those with higher jet multiplicities are more sensitive to perturbative QCD effects [101]. Jet-multiplicity distributions also probe the validity of predictions in the presence of jet vetoes, which are frequently used in searches that require a specific number of jets in the selection. These vetoes create additional logarithmic terms, which are not explicitly included in the theoretical predictions presented in this paper. Figure 6 shows the differential cross section as a function of the jet multiplicity in the *inclusive* and *high-p_{T}* regions. As expected [101], the jet multiplicity in the *inclusive* phase

JHEP06(2023)080

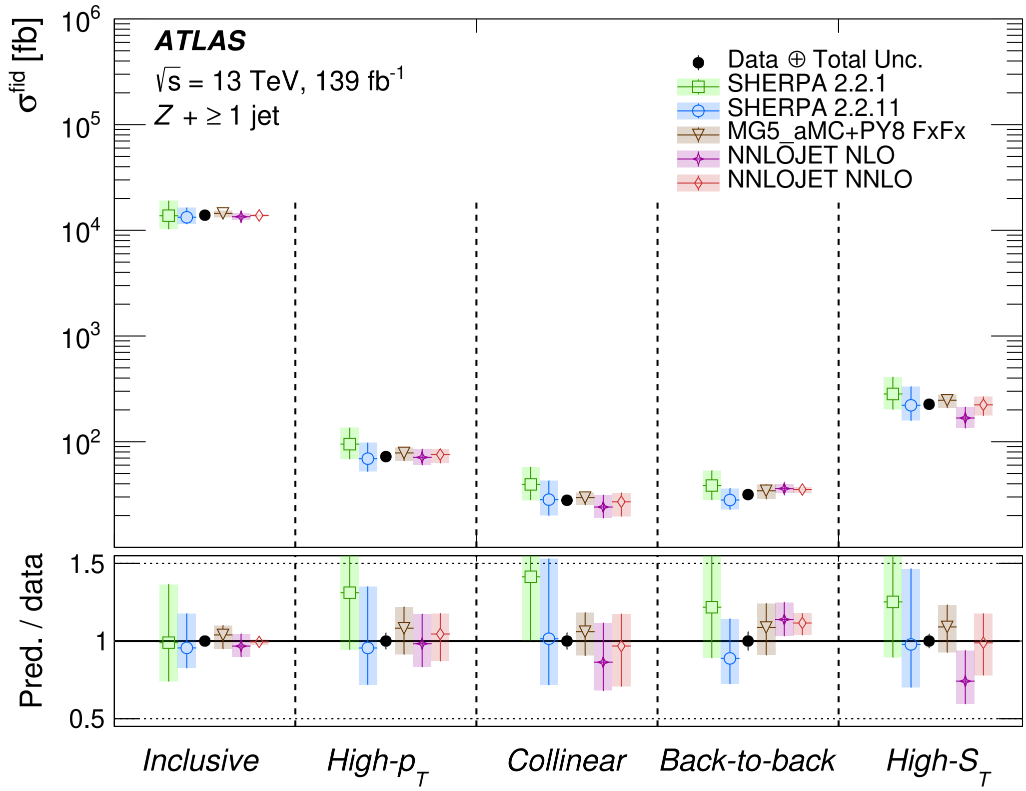

Figure 4. Summary of integrated fiducial cross-section results. The measured cross sections are shown with black points and the error bars represent the total uncertainty. Data are compared with predictions from MC generators and fixed-order calculations. The uncertainties in the predictions are found by adding in quadrature the uncertainties from the variations of the PDF (excluding NNLOJET predictions), QCD scales and, for SHERPA 2.2.11, virtual EW contributions, as explained in section 7.

space follows a downward staircase pattern, whereas in the *high-*p_{T} phase space, the cross section increases between 1-jet and 2-jet events followed by a downward pattern for higher jet multiplicities. While SHERPA 2.2.1 and MG5_AMC+PY8 CKKWL tend to overestimate the cross section for higher jet multiplicities, SHERPA 2.2.11 and MG5_AMC+PY8 FXFX agree with the data for both the *inclusive* and *high-*p_{T} regions, the latter generator at a higher level of precision. The NNLOJET predictions agree with the data in the *inclusive* and *high-*p_{T} phase spaces at high precision when it is expected from the order of the calculation, and at lower precision when the order of the calculation is exceeded.

The angular distance between the Z boson and the closest jet, $\Delta R^{\mathrm{min}}_{Z,j}$, and the ratio of the Z-boson transverse momentum to the closest-jet transverse momentum, $r_{Z,j}$, provide a way to distinguish between the presence of collinear Z-boson emission and back-to-back topologies. In the *high-*p_{T} selection, the collinear region is sensitive to logarithmic enhancements in production proportional to $\alpha_{\mathrm{s}} \ln^2(p_{\mathrm{T},j1}/m_Z)$, whereas the back-to-back region receives non-negligible virtual EW corrections. Figure 7 shows the differential cross sections as a function of $\Delta R^{\mathrm{min}}_{Z,j}$ and $r_{Z,j}$ in the *high-*p_{T} region. Both distributions show

JHEP06(2023)080

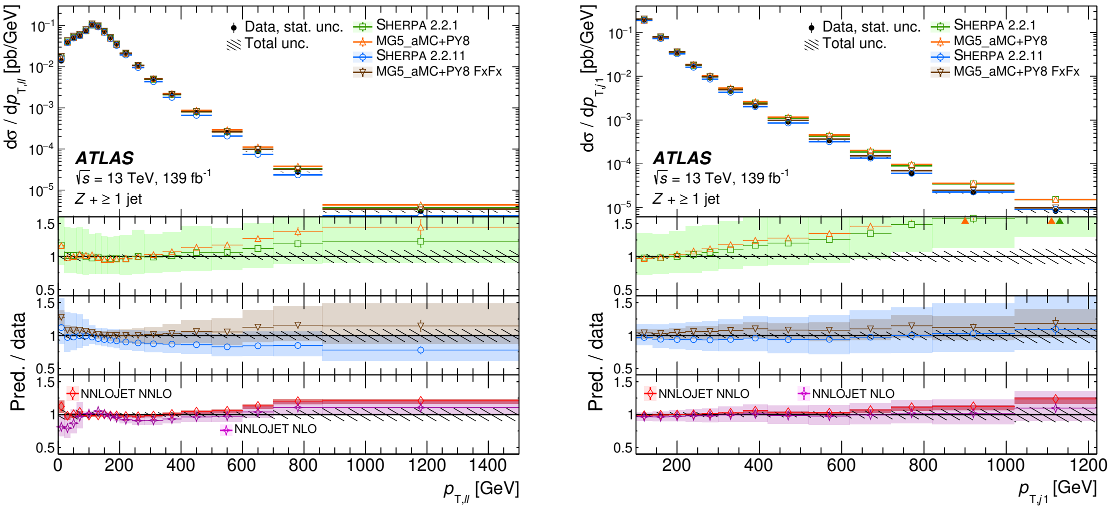

Figure 5. Differential cross section as a function of the transverse momentum of the Z boson (left) and of the transverse momentum of the leading jet (right) in the *inclusive* region. The unfolded data are shown with the black points where the statistical uncertainty is given as an error bar and the total uncertainty as a hatched region. The data are compared with predictions from MC generators and fixed-order calculations. In the ratio panels, the error bars correspond to the statistical uncertainty of the prediction and solid triangles indicate that the prediction is outside the vertical-axis range, while the total uncertainty of the unfolded data is represented as the hatched region. The uncertainties in the predictions, dominated by the scale uncertainties, are shown only in the ratio panels, except for MG5_aMC+Py8 CKKWL which is not included. They are found by adding in quadrature the uncertainties from the variations of the PDF (excluding NNLOjet predictions), QCD scales and, for Sherpa 2.2.11, virtual EW contributions, as explained in section 7.

an accumulation of events at low and high values of these two quantities: *collinear* events populate the figures at values $\Delta R^{\mathrm{min}}_{Z,j} \leq 1.4$ and $r_{Z,j} \leq 0.4$, while the *back-to-back* events are observed with $\Delta R^{\mathrm{min}}_{Z,j} \approx \pi$ and $r_{Z,j} \approx 1.0$. The collinear events are expected to be dominated by diagrams corresponding to the EW radiation of a Z boson from one of the legs of a dijet event. Consequently, they are expected to correspond to the accumulation of events with low values of $r_{Z,j}$. This hypothesis is validated in figure 8, which shows the measurement of the $r_{Z,j}$ distribution for the subset of *collinear* events defined by $\Delta R^{\mathrm{min}}_{Z,j} \leq 1.4$ where only the accumulation of low-$r_{Z,j}$ events is observed. In contrast, the measurement of the $r_{Z,j}$ distribution for the *back-to-back* selection defined by $\Delta R^{\mathrm{min}}_{Z,j} \geq 2.0$ is populated by events with $r_{Z,j} \approx 1$. The jet multiplicity is also measured separately for the *collinear* and *back-to-back* topologies as shown in figure 9. It is found that the *collinear* region is dominated by dijet events whereas the *back-to-back* region is dominated by $Z + 1$-jet events.

Figures 7–9 show that while still marginally in agreement with data within modelling uncertainties of up to 50%, Sherpa 2.2.1 central values increasingly overestimate the cross section with decreasing values of $\Delta R^{\mathrm{min}}_{Z,j}$. A similar trend is observed for

JHEP06(2023)080

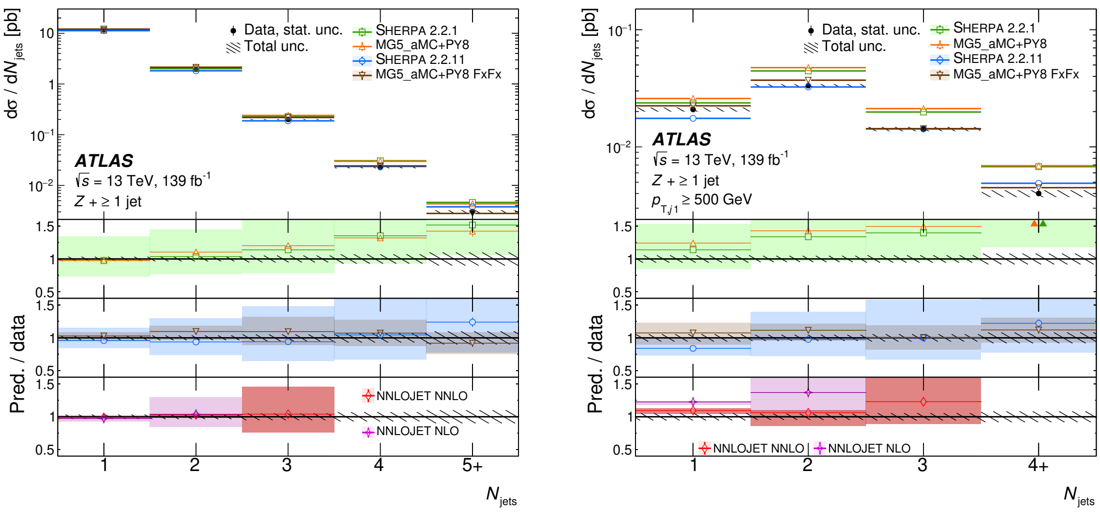

Figure 6. Differential cross section as a function of the jet multiplicity in the *inclusive* region (left) and *high-*p_{T} region (right). In each case, the last bin is inclusive in higher jet multiplicities. Further details are provided in the caption of figure 5.

MG5_aMC+Py8 CKKWL. The modelling is improved by the state-of-the-art generators MG5_aMC+Py8 FxFx and Sherpa 2.2.11. Good agreement of MG5_aMC+Py8 FxFx and Sherpa 2.2.11 with data even for very collinear events indicates that resummation of the additional logarithmic terms, e.g. via EW showers, is not needed at the present level of theoretical and experimental precision in the experimentally accessible kinematic regime. The NNLOjet@NNLO prediction models the data distribution in both the *collinear* and the *back-to-back* regions with high precision. The good performance in the *collinear* phase space is remarkable, as this region contains a large fraction of events with at least three jets, which are simulated only at LO in NNLOjet@NNLO and not at all by NNLOjet@NLO. The QCD-only calculation overestimates the cross section for exact *back-to-back* events in the *high-*p_{T} region, dominated by high-$p_{\mathrm{T},\ell\ell}$ events, consistent with the pattern observed in figure 5.

An alternative way to select a high-energy phase space is by requiring a large value of H_{T} or S_{T}. The former is often used as a dynamical scale choice, whereas the latter is more suited to selecting a phase space similar to the *high-*p_{T} region. Figure 10 shows the differential cross section as a function of H_{T}. The central values from Sherpa 2.2.1 increasingly overestimate the cross section with increasing H_{T}, while still marginally agreeing with the data within modelling uncertainties of up to 50%. The prediction from MG5_aMC+Py8 CKKWL shows a similar trend. In contrast, the state-of-the-art predictions from Sherpa 2.2.11, MG5_aMC+Py8 FxFx and NNLOjet@NNLO model the data well, the last with higher precision. Figure 11 shows the differential cross section as a function of $\Delta R^{\mathrm{min}}_{Z,j}$ and jet multiplicity in the *high-*S_{T} region. The *high-*S_{T} region probes high-energy events where the energy is typically shared by several jets. Compared to the *high-*p_{T} region, the jet multiplicity distribution is shifted towards higher values, and the

JHEP06(2023)080

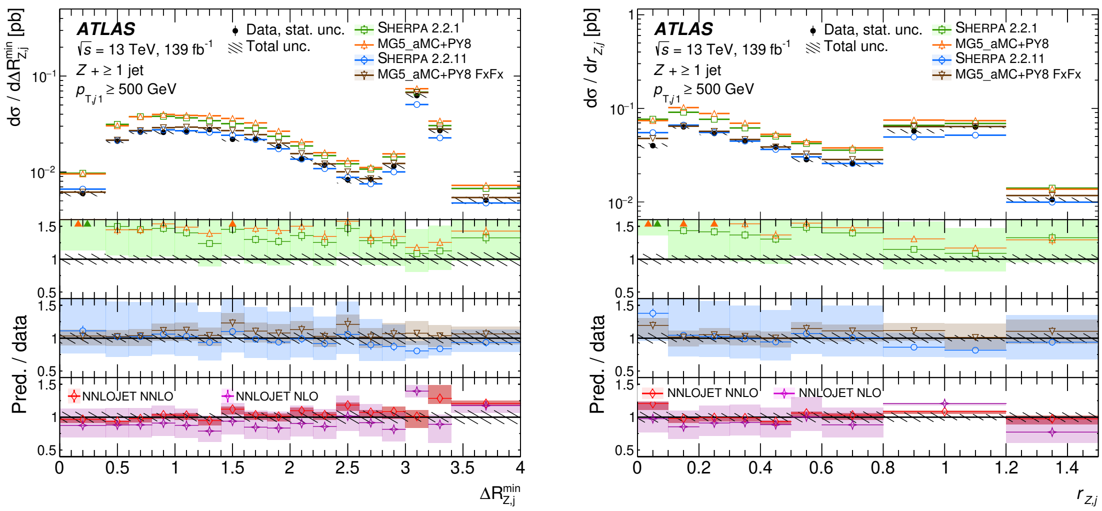

Figure 7. Differential cross section as a function of angular distance between the Z boson and the closest jet, $\Delta R^{\mathrm{min}}_{Z,j}$ (left) and of the ratio of Z-boson to closest-jet transverse momenta $r_{Z,j}$ (right) in the *high-p_{T}* region. For the NNLOJET predictions, the bins around $r_{Z,j} = 1$ are merged to be insensitive to the singularity in the fixed-order calculation. Further details are provided in the caption of figure 5.

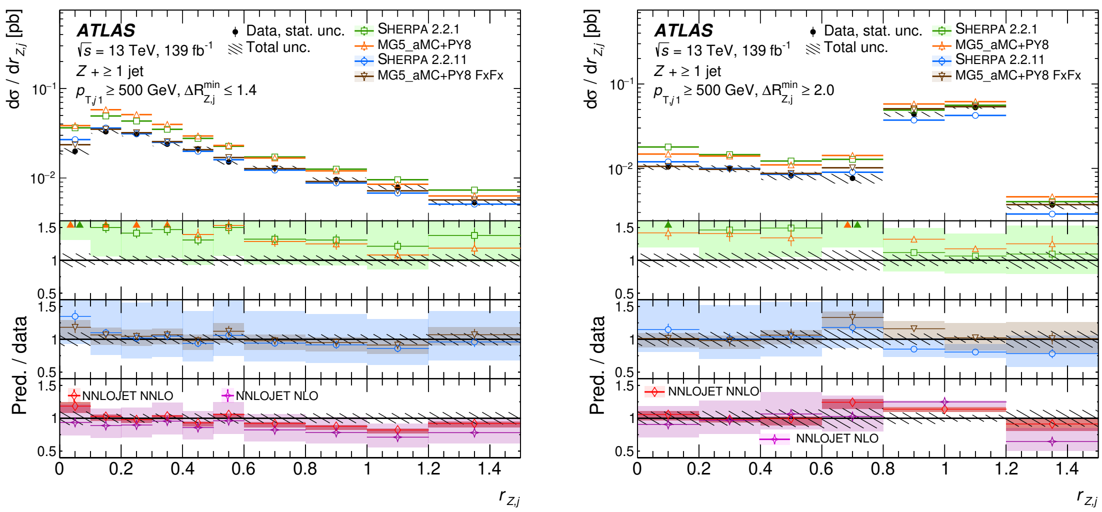

Figure 8. Differential cross section as a function of the ratio of Z-boson to closest-jet transverse momenta $r_{Z,j}$ in the *collinear* $\Delta R^{\mathrm{min}}_{Z,j} \leq 1.4$ region (left) and in the *back-to-back* $\Delta R^{\mathrm{min}}_{Z,j} \geq 2.0$ region (right). For the NNLOJET predictions, the bins around $r_{Z,j} = 1$ are merged to be insensitive to the singularity in the fixed-order calculation. Further details are provided in the caption of figure 5.

back-to-back peak in the $\Delta R^{\mathrm{min}}_{Z,j}$ distribution is suppressed relative to events where a jet is in closer proximity to the Z boson. As in the *high-p_{T}* region, SHERPA 2.2.1 is marginally consistent with the data within a large theoretical uncertainty, with the overestimation of the central values most pronounced in the *collinear* region and for higher jet multiplici-

JHEP06(2023)080

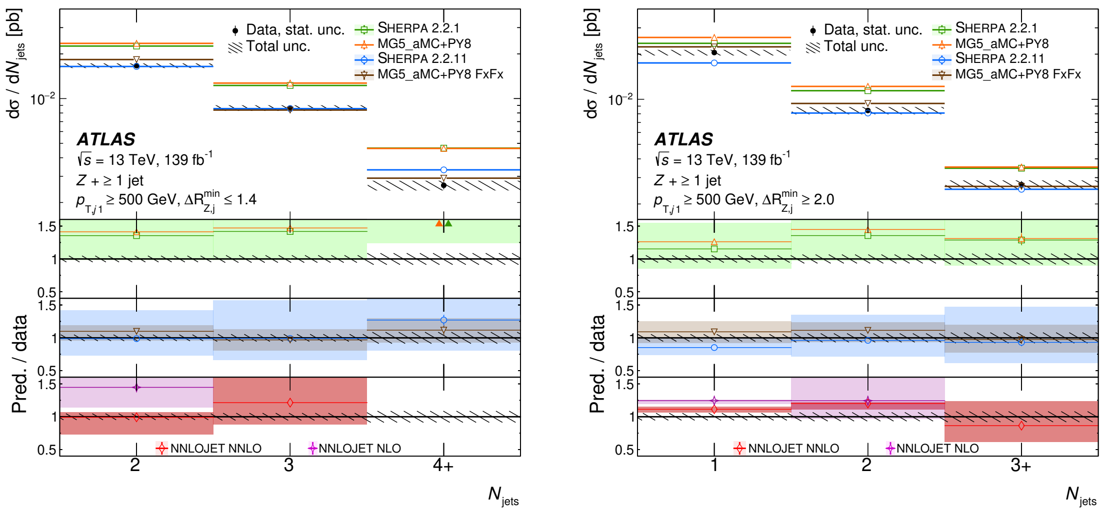

Figure 9. Differential cross section as a function of the jet multiplicity in the *collinear* $\Delta R_{Z,j}^{\mathrm{min}} \leq 1.4$ region (left) and in the *back-to-back* $\Delta R_{Z,j}^{\mathrm{min}} \geq 2.0$ region (right). In each case, the last bin is inclusive in higher jet multiplicities. In data, no events with exactly one jet are selected in the *collinear* region. Further details are provided in the caption of figure 5.

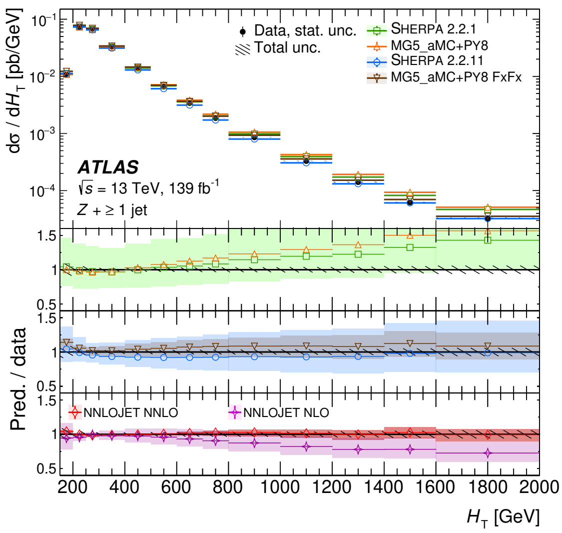

Figure 10. Differential cross section as a function of the transverse momenta scalar sum H_{T} in the *inclusive* region. Further details are provided in the caption of figure 5.

ties, with MG5_aMC+Py8 CKKWL showing a similar trend. Both Sherpa 2.2.11 and MG5_aMC+Py8 FxFx are consistent with the data, the latter at higher precision. The NNLOJet@NNLO prediction models this region well and with high precision, even though the fraction of events with at least three jets is larger than in the *high-p_{T}* phase space.

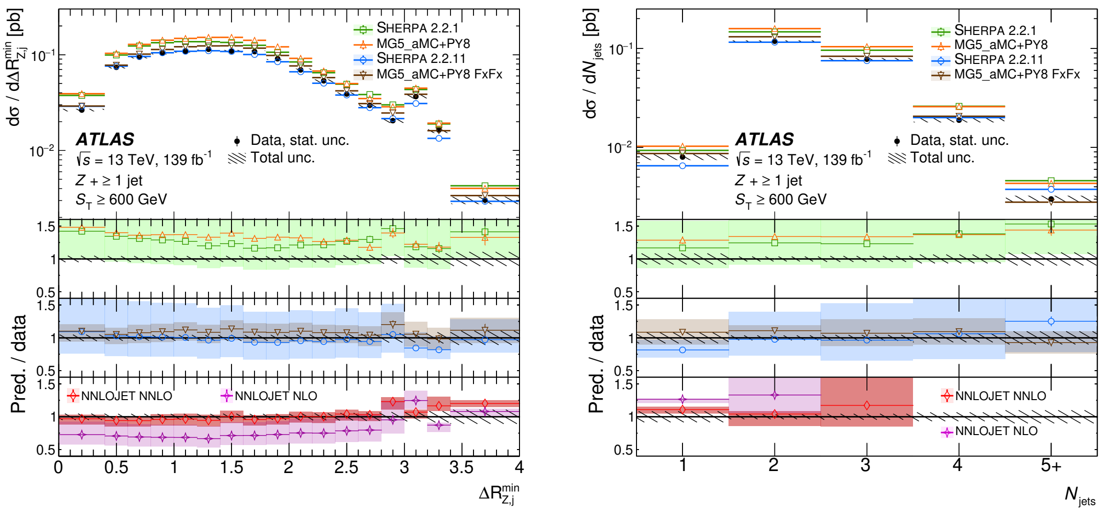

Figure 11. Differential cross section as a function of the angular distance $\Delta R^{\mathrm{min}}_{Z,j}$ between the Z boson and the closest jet (left) and of the jet multiplicity (right) in the *high*-S_{T} region. In the jet-multiplicity distribution, the last bin is inclusive in higher jet multiplicities. Further details are provided in the caption of figure 5.

9 Conclusions

This paper presents measurements of cross sections for a Z boson produced in association with high-transverse-momentum jets and decaying into a charged-lepton pair. The data were collected from pp collisions at $\sqrt{s} = 13$ TeV with the ATLAS detector at the LHC during 2015–2018 and correspond to an integrated luminosity of 139 fb^{-1}. Measurements were performed on events that contain a Z-boson candidate reconstructed from an e^+e^- pair or a $\mu^+\mu^-$ pair in association with hadronic jets defined as jets having transverse momentum greater than or equal to 100 GeV. Primarily, only the QCD component of $Z+$jets production is measured, treating the EW Zjj processes as a background. The paper focuses on selections with very high leading-jet p_{T} ($p_{\mathrm{T},j1} \geq 500$ GeV) and very high S_{T} ($S_{\mathrm{T}} \geq 600$ GeV), which are used to study two populations of events – collinear events and back-to-back events – with distinct patterns in distributions of $\Delta R^{\mathrm{min}}_{Z,j}$, $r_{Z,j}$, and jet multiplicity.

The data distributions were unfolded to the particle level and compared with state-of-the-art generator predictions and fixed-order calculations. Both Sherpa 2.2.1 and MG5_aMC+Py8 CKKWL overestimate the cross sections for large values of $p_{\mathrm{T},j1}$, H_{T} and S_{T}. The predictions from MG5_aMC+Py8 FxFx, with matrix elements for up to three partons at NLO, offer a significant improvement over MG5_aMC+Py8 CKKWL (which models up to four partons at LO) and in general match the data with high precision. Similarly, Sherpa 2.2.11, with the addition of a fifth parton at LO in the matrix element, the addition of NLO virtual EW corrections, and a different treatment of unordered histories in the parton shower, shows a significant improvement over Sherpa 2.2.1 and agrees with the data. The NNLO calculations at fixed order from NNLOJet describe the data

JHEP06(2023)080

cross sections at a very high level of precision, including in high-p_{T} regions where a sizeable fraction of the events have more than two jets. The calculation exhibits a harder $p_{\mathrm{T},\ell\ell}$ spectrum than the data in a region where larger negative EW corrections are expected.

Acknowledgments

We thank CERN for the very successful operation of the LHC, as well as the support staff from our institutions without whom ATLAS could not be operated efficiently.

We acknowledge the support of ANPCyT, Argentina; YerPhI, Armenia; ARC, Australia; BMWFW and FWF, Austria; ANAS, Azerbaijan; CNPq and FAPESP, Brazil; NSERC, NRC and CFI, Canada; CERN; ANID, Chile; CAS, MOST and NSFC, China; Minciencias, Colombia; MEYS CR, Czech Republic; DNRF and DNSRC, Denmark; IN2P3-CNRS and CEA-DRF/IRFU, France; SRNSFG, Georgia; BMBF, HGF and MPG, Germany; GSRI, Greece; RGC and Hong Kong SAR, China; ISF and Benoziyo Center, Israel; INFN, Italy; MEXT and JSPS, Japan; CNRST, Morocco; NWO, Netherlands; RCN, Norway; MEiN, Poland; FCT, Portugal; MNE/IFA, Romania; MESTD, Serbia; MSSR, Slovakia; ARRS and MIZŠ, Slovenia; DSI/NRF, South Africa; MICINN, Spain; SRC and Wallenberg Foundation, Sweden; SERI, SNSF and Cantons of Bern and Geneva, Switzerland; MOST, Taiwan; TENMAK, Türkiye; STFC, United Kingdom; DOE and NSF, United States of America. In addition, individual groups and members have received support from BCKDF, CANARIE, Compute Canada and CRC, Canada; PRIMUS 21/SCI/017 and UNCE SCI/013, Czech Republic; COST, ERC, ERDF, Horizon 2020 and Marie Skłodowska-Curie Actions, European Union; Investissements d'Avenir Labex, Investissements d'Avenir Idex and ANR, France; DFG and AvH Foundation, Germany; Herakleitos, Thales and Aristeia programmes co-financed by EU-ESF and the Greek NSRF, Greece; BSF-NSF and MINERVA, Israel; Norwegian Financial Mechanism 2014-2021, Norway; NCN and NAWA, Poland; La Caixa Banking Foundation, CERCA Programme Generalitat de Catalunya and PROMETEO and GenT Programmes Generalitat Valenciana, Spain; Göran Gustafssons Stiftelse, Sweden; The Royal Society and Leverhulme Trust, United Kingdom.

The crucial computing support from all WLCG partners is acknowledged gratefully, in particular from CERN, the ATLAS Tier-1 facilities at TRIUMF (Canada), NDGF (Denmark, Norway, Sweden), CC-IN2P3 (France), KIT/GridKA (Germany), INFN-CNAF (Italy), NL-T1 (Netherlands), PIC (Spain), ASGC (Taiwan), RAL (UK) and BNL (USA), the Tier-2 facilities worldwide and large non-WLCG resource providers. Major contributors of computing resources are listed in ref. [102].

A HepData material

The following tables will be included in the HEPData entry (link to entry):

1. Differential cross section of $p_{\mathrm{T},\ell\ell}$ in the *inclusive* region
2. Differential cross section of $p_{\mathrm{T},j1}$ in the *inclusive* region

JHEP06(2023)080

3. Differential cross section of jet multiplicity in the *inclusive* region
4. Differential cross section of jet multiplicity in the *high-*p_{T} region
5. Differential cross section of $\Delta R_{Z,j}^{\min}$ in the *high-*p_{T} region
6. Differential cross section of $r_{Z,j}$ in the *high-*p_{T} region
7. Differential cross section of $r_{Z,j}$ in the *collinear* region
8. Differential cross section of $r_{Z,j}$ in the *back-to-back* region
9. Differential cross section of jet multiplicity in the *collinear* region
10. Differential cross section of jet multiplicity in the *back-to-back* region
11. Differential cross section of H_{T} in the *inclusive* region
12. Differential cross section of $\Delta R_{Z,j}^{\min}$ in the *high-*S_{T} region
13. Differential cross section of jet multiplicity in the *high-*S_{T} region
14. Relative bin-by-bin systematic uncertainties of $p_{\mathrm{T},\ell\ell}$ in the *inclusive* region
15. Relative bin-by-bin systematic uncertainties of $p_{\mathrm{T},j1}$ in the *inclusive* region
16. Relative bin-by-bin systematic uncertainties of jet multiplicity in the *inclusive* region
17. Relative bin-by-bin systematic uncertainties of jet multiplicity in the *high-*p_{T} region
18. Relative bin-by-bin systematic uncertainties of $\Delta R_{Z,j}^{\min}$ in the *high-*p_{T} region
19. Relative bin-by-bin systematic uncertainties of $r_{Z,j}$ in the *high-*p_{T} region
20. Relative bin-by-bin systematic uncertainties of $r_{Z,j}$ in the *collinear* region
21. Relative bin-by-bin systematic uncertainties of $r_{Z,j}$ in the *back-to-back* region
22. Relative bin-by-bin systematic uncertainties of jet multiplicity in the *collinear* region
23. Relative bin-by-bin systematic uncertainties of jet multiplicity in the *back-to-back* region
24. Relative bin-by-bin systematic uncertainties of H_{T} in the *inclusive* region
25. Relative bin-by-bin systematic uncertainties of $\Delta R_{Z,j}^{\min}$ in the *high-*S_{T} region
26. Relative bin-by-bin systematic uncertainties of jet multiplicity in the *high-*S_{T} region
27. Bin-by-bin Born to dressed level leptons correction scale factor for $p_{\mathrm{T},\ell\ell}$ in the *inclusive* region
28. Bin-by-bin Born to dressed level leptons correction scale factor for $p_{\mathrm{T},j1}$ in the *inclusive* region
29. Bin-by-bin Born to dressed level leptons correction scale factor for the jet multiplicity in the *inclusive* region
30. Bin-by-bin Born to dressed level leptons correction scale factor for the jet multiplicity in the *high-*p_{T} region
31. Bin-by-bin Born to dressed level leptons correction scale factor for $\Delta R_{Z,j}^{\min}$ in the *high-*p_{T} region
32. Bin-by-bin Born to dressed level leptons correction scale factor for $r_{Z,j}$ in the *high-*p_{T} region
33. Bin-by-bin Born to dressed level leptons correction scale factor for $r_{Z,j}$ in the *collinear* region

JHEP06(2023)080

34. Bin-by-bin Born to dressed level leptons correction scale factor for $r_{Z,j}$ in the *back-to-back* region
35. Bin-by-bin Born to dressed level leptons correction scale factor for the jet multiplicity in the *collinear* region
36. Bin-by-bin Born to dressed level leptons correction scale factor for the jet multiplicity in the *back-to-back* region
37. Bin-by-bin Born to dressed level leptons correction scale factor for H_{T} in the *inclusive* region
38. Bin-by-bin Born to dressed level leptons correction scale factor for $\Delta R_{Z,j}^{\min}$ in the *high-S_{T}* region
39. Bin-by-bin Born to dressed level leptons correction scale factor for the jet multiplicity in the *high-S_{T}* region
40. Bin-by-bin overlap removal correction scale factor for $p_{\mathrm{T},\ell\ell}$ in the *inclusive* region
41. Bin-by-bin overlap removal correction scale factor for $p_{\mathrm{T},j1}$ in the *inclusive* region
42. Bin-by-bin overlap removal correction scale factor for the jet multiplicity in the *inclusive* region
43. Bin-by-bin overlap removal correction scale factor for the jet multiplicity in the *high-p_{T}* region
44. Bin-by-bin overlap removal correction scale factor for $\Delta R_{Z,j}^{\min}$ in the *high-p_{T}* region
45. Bin-by-bin overlap removal correction scale factor for $r_{Z,j}$ in the *high-p_{T}* region
46. Bin-by-bin overlap removal correction scale factor for $r_{Z,j}$ in the *collinear* region
47. Bin-by-bin overlap removal correction scale factor for $r_{Z,j}$ in the *back-to-back* region
48. Bin-by-bin overlap removal correction scale factor for the jet multiplicity in the *collinear* region
49. Bin-by-bin overlap removal correction scale factor for the jet multiplicity in the *back-to-back* region
50. Bin-by-bin overlap removal correction scale factor for H_{T} in the *inclusive* region
51. Bin-by-bin overlap removal correction scale factor for $\Delta R_{Z,j}^{\min}$ in the *high-S_{T}* region
52. Bin-by-bin overlap removal correction scale factor for the jet multiplicity in the *high-S_{T}* region
53. Differential cross section of $p_{\mathrm{T},\ell\ell}$ in the *inclusive* region, where the EW Zjj contribution is not subtracted as background
54. Differential cross section of $p_{\mathrm{T},j1}$ in the *inclusive* region, where the EW Zjj contribution is not subtracted as background
55. Differential cross section of jet multiplicity in the *inclusive* region, where the EW Zjj contribution is not subtracted as background
56. Differential cross section of jet multiplicity in the *high-p_{T}* region, where the EW Zjj contribution is not subtracted as background
57. Differential cross section of $\Delta R_{Z,j}^{\min}$ in the *high-p_{T}* region, where the EW Zjj contribution is not subtracted as background

JHEP06(2023)080

58. Differential cross section of $r_{Z,j}$ in the *high-p_{T}* region, where the EW Zjj contribution is not subtracted as background
59. Differential cross section of $r_{Z,j}$ in the *collinear* region, where the EW Zjj contribution is not subtracted as background
60. Differential cross section of $r_{Z,j}$ in the *back-to-back* region, where the EW Zjj contribution is not subtracted as background
61. Differential cross section of jet multiplicity in the *collinear* region, where the EW Zjj contribution is not subtracted as background
62. Differential cross section of jet multiplicity in the *back-to-back* region, where the EW Zjj contribution is not subtracted as background
63. Differential cross section of H_{T} in the *inclusive* region, where the EW Zjj contribution is not subtracted as background
64. Differential cross section of $\Delta R^{\mathrm{min}}_{Z,j}$ in the *high-S_{T}* region, where the EW Zjj contribution is not subtracted as background
65. Differential cross section of jet multiplicity in the *high-S_{T}* region, where the EW Zjj contribution is not subtracted as background
66. Relative bin-by-bin systematic uncertainties of $p_{\mathrm{T},\ell\ell}$ in the *inclusive* region, where the EW Zjj contribution is not subtracted as background
67. Relative bin-by-bin systematic uncertainties of $p_{\mathrm{T},j1}$ in the *inclusive* region, where the EW Zjj contribution is not subtracted as background
68. Relative bin-by-bin systematic uncertainties of jet multiplicity in the *inclusive* region, where the EW Zjj contribution is not subtracted as background
69. Relative bin-by-bin systematic uncertainties of jet multiplicity in the *high-p_{T}* region, where the EW Zjj contribution is not subtracted as background
70. Relative bin-by-bin systematic uncertainties of $\Delta R^{\mathrm{min}}_{Z,j}$ in the *high-p_{T}* region, where the EW Zjj contribution is not subtracted as background
71. Relative bin-by-bin systematic uncertainties of $r_{Z,j}$ in the *high-p_{T}* region, where the EW Zjj contribution is not subtracted as background
72. Relative bin-by-bin systematic uncertainties of $r_{Z,j}$ in the *collinear* region, where the EW Zjj contribution is not subtracted as background
73. Relative bin-by-bin systematic uncertainties of $r_{Z,j}$ in the *back-to-back* region, where the EW Zjj contribution is not subtracted as background
74. Relative bin-by-bin systematic uncertainties of jet multiplicity in the *collinear* region, where the EW Zjj contribution is not subtracted as background
75. Relative bin-by-bin systematic uncertainties of jet multiplicity in the *back-to-back* region, where the EW Zjj contribution is not subtracted as background
76. Relative bin-by-bin systematic uncertainties of H_{T} in the *inclusive* region, where the EW Zjj contribution is not subtracted as background
77. Relative bin-by-bin systematic uncertainties of $\Delta R^{\mathrm{min}}_{Z,j}$ in the *high-S_{T}* region, where the EW Zjj contribution is not subtracted as background
78. Relative bin-by-bin systematic uncertainties of jet multiplicity in the *high-S_{T}* region, where the EW Zjj contribution is not subtracted as background

JHEP06(2023)080

References

[1] D.J. Gross and F. Wilczek, *Asymptotically Free Gauge Theories. I*, *Phys. Rev. D* **8** (1973) 3633 [INSPIRE].

[2] H.D. Politzer, *Asymptotic freedom: an approach to strong interactions*, *Phys. Rept.* **14** (1974) 129 [INSPIRE].

[3] M. Rubin, G.P. Salam and S. Sapeta, *Giant QCD K-factors beyond NLO*, *JHEP* **09** (2010) 084 [arXiv:1006.2144] [INSPIRE].

[4] J.R. Christiansen and S. Prestel, *Merging weak and QCD showers with matrix elements*, *Eur. Phys. J. C* **76** (2016) 39 [arXiv:1510.01517] [INSPIRE].

[5] R. Boughezal, C. Focke and X. Liu, *Jet vetoes versus giant K-factors in the exclusive $Z+1$-jet cross section*, *Phys. Rev. D* **92** (2015) 094002 [arXiv:1501.01059] [INSPIRE].

[6] J.R. Christiansen and T. Sjöstrand, *Weak gauge boson radiation in parton showers*, *JHEP* **04** (2014) 115 [arXiv:1401.5238] [INSPIRE].

[7] ATLAS collaboration, *Measurement of the associated production of a Higgs boson decaying into b-quarks with a vector boson at high transverse momentum in pp collisions at $\sqrt{s}=13$ TeV with the ATLAS detector*, *Phys. Lett. B* **816** (2021) 136204 [arXiv:2008.02508] [INSPIRE].

[8] ATLAS collaboration, *Measurement of the production cross section for a Higgs boson in association with a vector boson in the $H\to WW^*\to \ell\nu\ell\nu$ channel in pp collisions at $\sqrt{s}=13$ TeV with the ATLAS detector*, *Phys. Lett. B* **798** (2019) 134949 [arXiv:1903.10052] [INSPIRE].

[9] ATLAS collaboration, *Search for squarks and gluinos in final states with one isolated lepton, jets, and missing transverse momentum at $\sqrt{s}=13$ TeV with the ATLAS detector*, *Eur. Phys. J. C* **81** (2021) 600 [*Erratum ibid.* **81** (2021) 956] [arXiv:2101.01629] [INSPIRE].

[10] ATLAS collaboration, *Searches for electroweak production of supersymmetric particles with compressed mass spectra in $\sqrt{s}=13$ TeV pp collisions with the ATLAS detector*, *Phys. Rev. D* **101** (2020) 052005 [arXiv:1911.12606] [INSPIRE].

[11] CMS collaboration, *Search for a heavy vector resonance decaying to a Z boson and a Higgs boson in proton-proton collisions at $\sqrt{s}=13$ TeV*, *Eur. Phys. J. C* **81** (2021) 688 [arXiv:2102.08198] [INSPIRE].

[12] ATLAS collaboration, *Differential cross-section measurements for the electroweak production of dijets in association with a Z boson in proton–proton collisions at ATLAS*, *Eur. Phys. J. C* **81** (2021) 163 [arXiv:2006.15458] [INSPIRE].

[13] E. Maguire, L. Heinrich and G. Watt, *HEPData: a repository for high energy physics data*, *J. Phys. Conf. Ser.* **898** (2017) 102006 [arXiv:1704.05473] [INSPIRE].

[14] ATLAS collaboration, *The ATLAS Experiment at the CERN Large Hadron Collider*, 2008 *JINST* **3** S08003 [INSPIRE].

[15] L. Evans and P. Bryant, *LHC Machine*, 2008 *JINST* **3** S08001 [INSPIRE].

JHEP06(2023)080

[16] ATLAS collaboration, *Measurement of W boson angular distributions in events with high transverse momentum jets at $\sqrt{s} = 8$ TeV using the ATLAS detector*, Phys. Lett. B **765** (2017) 132 [arXiv:1609.07045] [INSPIRE].

[17] CMS collaboration, *Measurements of the differential cross sections of the production of Z + jets and γ + jets and of Z boson emission collinear with a jet in pp collisions at $\sqrt{s} = 13$ TeV*, JHEP **05** (2021) 285 [arXiv:2102.02238] [INSPIRE].

[18] SHERPA collaboration, *Event generation with Sherpa 2.2*, SciPost Phys. **7** (2019) 034 [arXiv:1905.09127] [INSPIRE].

[19] ATLAS collaboration, *Modelling and computational improvements to the simulation of single vector-boson plus jet processes for the ATLAS experiment*, JHEP **08** (2022) 089 [arXiv:2112.09588] [INSPIRE].

[20] R. Frederix and S. Frixione, *Merging meets matching in MC@NLO*, JHEP **12** (2012) 061 [arXiv:1209.6215] [INSPIRE].

[21] T. Sjöstrand et al., *An introduction to PYTHIA 8.2*, Comput. Phys. Commun. **191** (2015) 159 [arXiv:1410.3012] [INSPIRE].

[22] R. Boughezal et al., *Z-boson production in association with a jet at next-to-next-to-leading order in perturbative QCD*, Phys. Rev. Lett. **116** (2016) 152001 [arXiv:1512.01291] [INSPIRE].

[23] R. Boughezal, X. Liu and F. Petriello, *Phenomenology of the Z-boson plus jet process at NNLO*, Phys. Rev. D **94** (2016) 074015 [arXiv:1602.08140] [INSPIRE].

[24] A. Gehrmann-De Ridder et al., *Precise QCD predictions for the production of a Z boson in association with a hadronic jet*, Phys. Rev. Lett. **117** (2016) 022001 [arXiv:1507.02850] [INSPIRE].

[25] A. Gehrmann-De Ridder et al., *The NNLO QCD corrections to Z boson production at large transverse momentum*, JHEP **07** (2016) 133 [arXiv:1605.04295] [INSPIRE].

[26] S. Kallweit et al., *NLO QCD+EW predictions for V + jets including off-shell vector-boson decays and multijet merging*, JHEP **04** (2016) 021 [arXiv:1511.08692] [INSPIRE].

[27] S. Kallweit et al., *NLO electroweak automation and precise predictions for W+multijet production at the LHC*, JHEP **04** (2015) 012 [arXiv:1412.5157] [INSPIRE].

[28] ATLAS collaboration, *The ATLAS Collaboration Software and Firmware*, ATL-SOFT-PUB-2021-001 (2021).

[29] ATLAS collaboration, *Improved luminosity determination in pp collisions at $\sqrt{s} = 7$ TeV using the ATLAS detector at the LHC*, Eur. Phys. J. C **73** (2013) 2518 [arXiv:1302.4393] [INSPIRE].

[30] ATLAS collaboration, *The ATLAS Simulation Infrastructure*, Eur. Phys. J. C **70** (2010) 823 [arXiv:1005.4568] [INSPIRE].

[31] GEANT4 collaboration, *GEANT4 — a simulation toolkit*, Nucl. Instrum. Meth. A **506** (2003) 250 [INSPIRE].

[32] T. Gleisberg and S. Höche, *Comix, a new matrix element generator*, JHEP **12** (2008) 039 [arXiv:0808.3674] [INSPIRE].

[33] OPENLOOPS 2 collaboration, *OpenLoops 2*, Eur. Phys. J. C **79** (2019) 866 [arXiv:1907.13071] [INSPIRE].

[34] F. Cascioli, P. Maierhofer and S. Pozzorini, *Scattering Amplitudes with Open Loops*, Phys. Rev. Lett. **108** (2012) 111601 [arXiv:1111.5206] [INSPIRE].

[35] A. Denner, S. Dittmaier and L. Hofer, *Collier: a Fortran-based Complex One-Loop LIbrary in Extended Regularizations*, *Comput. Phys. Commun.* **212** (2017) 220 [arXiv:1604.06792] [INSPIRE].

[36] S. Schumann and F. Krauss, *A Parton shower algorithm based on Catani-Seymour dipole factorisation*, *JHEP* **03** (2008) 038 [arXiv:0709.1027] [INSPIRE].

[37] S. Höche, F. Krauss, M. Schönherr and F. Siegert, *A critical appraisal of NLO+PS matching methods*, *JHEP* **09** (2012) 049 [arXiv:1111.1220] [INSPIRE].

[38] S. Höche, F. Krauss, M. Schönherr and F. Siegert, *QCD matrix elements + parton showers: The NLO case*, *JHEP* **04** (2013) 027 [arXiv:1207.5030] [INSPIRE].

[39] S. Catani, F. Krauss, R. Kuhn and B.R. Webber, *QCD matrix elements + parton showers*, *JHEP* **11** (2001) 063 [hep-ph/0109231] [INSPIRE].

[40] S. Höche, F. Krauss, S. Schumann and F. Siegert, *QCD matrix elements and truncated showers*, *JHEP* **05** (2009) 053 [arXiv:0903.1219] [INSPIRE].

[41] S. Catani, S. Dittmaier, M.H. Seymour and Z. Trócsányi, *The Dipole formalism for next-to-leading order QCD calculations with massive partons*, *Nucl. Phys. B* **627** (2002) 189 [hep-ph/0201036] [INSPIRE].

[42] R.D. Ball, *Parton distributions for the LHC Run II*, *JHEP* **04** (2015) 040 [arXiv:1410.8849] [INSPIRE].

[43] J. Alwall et al., *The automated computation of tree-level and next-to-leading order differential cross sections, and their matching to parton shower simulations*, *JHEP* **07** (2014) 079 [arXiv:1405.0301] [INSPIRE].

[44] ATLAS collaboration, *ATLAS Pythia 8 tunes to* 7 *TeV data*, ATL-PHYS-PUB-2014-021 (2014).

[45] R.D. Ball et al., *Parton distributions with LHC data*, *Nucl. Phys. B* **867** (2013) 244 [arXiv:1207.1303] [INSPIRE].

[46] T. Sjostrand, S. Mrenna and P.Z. Skands, *A brief introduction to PYTHIA 8.1*, *Comput. Phys. Commun.* **178** (2008) 852 [arXiv:0710.3820] [INSPIRE].

[47] L. Lönnblad, *Correcting the color dipole cascade model with fixed order matrix elements*, *JHEP* **05** (2002) 046 [hep-ph/0112284] [INSPIRE].

[48] L. Lönnblad and S. Prestel, *Matching tree-level matrix elements with interleaved showers*, *JHEP* **03** (2012) 019 [arXiv:1109.4829] [INSPIRE].

[49] M. Bähr et al., *Herwig++ physics and manual*, *Eur. Phys. J. C* **58** (2008) 639 [arXiv:0803.0883] [INSPIRE].

[50] J. Bellm et al., *Herwig 7.0/Herwig++ 3.0 release note*, *Eur. Phys. J. C* **76** (2016) 196 [arXiv:1512.01178] [INSPIRE].

[51] J. Baglio et al., *VBFNLO: a parton level Monte Carlo for processes with electroweak bosons — Manual for Version 2.7.0*, arXiv:1107.4038 [INSPIRE].

[52] S. Frixione, P. Nason and G. Ridolfi, *A Positive-weight next-to-leading-order Monte Carlo for heavy flavour hadroproduction*, *JHEP* **09** (2007) 126 [arXiv:0707.3088] [INSPIRE].

[53] P. Nason, *A New method for combining NLO QCD with shower Monte Carlo algorithms*, *JHEP* **11** (2004) 040 [hep-ph/0409146] [INSPIRE].

[54] S. Frixione, P. Nason and C. Oleari, *Matching NLO QCD computations with Parton Shower simulations: the POWHEG method*, *JHEP* **11** (2007) 070 [arXiv:0709.2092] [INSPIRE].

[55] S. Alioli, P. Nason, C. Oleari and E. Re, *A general framework for implementing NLO calculations in shower Monte Carlo programs: the POWHEG BOX*, *JHEP* **06** (2010) 043 [arXiv:1002.2581] [INSPIRE].

[56] L.A. Harland-Lang, A.D. Martin, P. Motylinski and R.S. Thorne, *Parton distributions in the LHC era: MMHT 2014 PDFs*, *Eur. Phys. J. C* **75** (2015) 204 [arXiv:1412.3989] [INSPIRE].

[57] ATLAS collaboration, *Studies on top-quark Monte Carlo modelling for Top2016*, ATL-PHYS-PUB-2016-020 (2016).

[58] M. Beneke, P. Falgari, S. Klein and C. Schwinn, *Hadronic top-quark pair production with NNLL threshold resummation*, *Nucl. Phys. B* **855** (2012) 695 [arXiv:1109.1536] [INSPIRE].

[59] M. Cacciari et al., *Top-pair production at hadron colliders with next-to-next-to-leading logarithmic soft-gluon resummation*, *Phys. Lett. B* **710** (2012) 612 [arXiv:1111.5869] [INSPIRE].

[60] P. Bärnreuther, M. Czakon and A. Mitov, *Percent Level Precision Physics at the Tevatron: First Genuine NNLO QCD Corrections to $q\bar{q} \to t\bar{t} + X$*, *Phys. Rev. Lett.* **109** (2012) 132001 [arXiv:1204.5201] [INSPIRE].

[61] M. Czakon and A. Mitov, *NNLO corrections to top-pair production at hadron colliders: the all-fermionic scattering channels*, *JHEP* **12** (2012) 054 [arXiv:1207.0236] [INSPIRE].

[62] M. Czakon and A. Mitov, *NNLO corrections to top pair production at hadron colliders: the quark-gluon reaction*, *JHEP* **01** (2013) 080 [arXiv:1210.6832] [INSPIRE].

[63] M. Czakon, P. Fiedler and A. Mitov, *Total Top-Quark Pair-Production Cross Section at Hadron Colliders Through $O(\alpha_S^4)$*, *Phys. Rev. Lett.* **110** (2013) 252004 [arXiv:1303.6254] [INSPIRE].

[64] M. Czakon and A. Mitov, *Top++: A program for the calculation of the top-pair cross-section at hadron colliders*, *Comput. Phys. Commun.* **185** (2014) 2930 [arXiv:1112.5675] [INSPIRE].

[65] S. Frixione et al., *Single-top hadroproduction in association with a W boson*, *JHEP* **07** (2008) 029 [arXiv:0805.3067] [INSPIRE].

[66] N. Kidonakis, *Two-loop soft anomalous dimensions for single top quark associated production with a W^- or H^-*, *Phys. Rev. D* **82** (2010) 054018 [arXiv:1005.4451] [INSPIRE].

[67] N. Kidonakis, *Top Quark Production*, DOI:10.3204/DESY-PROC-2013-03/Kidonakis [arXiv:1311.0283] [INSPIRE].

[68] P. Kant et al., *HatHor for single top-quark production: Updated predictions and uncertainty estimates for single top-quark production in hadronic collisions*, *Comput. Phys. Commun.* **191** (2015) 74 [arXiv:1406.4403] [INSPIRE].

[69] M. Aliev et al., *HATHOR: HAdronic Top and Heavy quarks crOss section calculatoR*, *Comput. Phys. Commun.* **182** (2011) 1034 [arXiv:1007.1327] [INSPIRE].

[70] D.J. Lange, *The EvtGen particle decay simulation package*, *Nucl. Instrum. Meth. A* **462** (2001) 152 [INSPIRE].

[71] ATLAS collaboration, *The Pythia 8 A3 tune description of ATLAS minimum bias and inelastic measurements incorporating the Donnachie–Landshoff diffractive model*, ATL-PHYS-PUB-2016-017 (2016).

[72] ATLAS collaboration, *Electron and photon performance measurements with the ATLAS detector using the 2015–2017 LHC proton-proton collision data*, 2019 *JINST* **14** P12006 [arXiv:1908.00005] [INSPIRE].

JHEP06(2023)080

[73] ATLAS collaboration, *Muon reconstruction performance of the ATLAS detector in proton–proton collision data at* $\sqrt{s} = 13$ *TeV*, *Eur. Phys. J. C* **76** (2016) 292 [arXiv:1603.05598] [INSPIRE].

[74] ATLAS collaboration, *Muon reconstruction and identification efficiency in ATLAS using the full Run 2 pp collision data set at* $\sqrt{s} = 13$ *TeV*, *Eur. Phys. J. C* **81** (2021) 578 [arXiv:2012.00578] [INSPIRE].

[75] ATLAS collaboration, *ATLAS data quality operations and performance for 2015–2018 data-taking*, 2020 *JINST* **15** P04003 [arXiv:1911.04632] [INSPIRE].

[76] ATLAS collaboration, *Performance of primary vertex reconstruction in proton-proton collisions at* $\sqrt{s} = 7$ *TeV in the ATLAS experiment*, ATLAS-CONF-2010-069 (2010) [INSPIRE].

[77] ATLAS collaboration, *Performance of electron and photon triggers in ATLAS during LHC Run 2*, *Eur. Phys. J. C* **80** (2020) 47 [arXiv:1909.00761] [INSPIRE].

[78] ATLAS collaboration, *Performance of the ATLAS muon triggers in Run 2*, 2020 *JINST* **15** P09015 [arXiv:2004.13447] [INSPIRE].

[79] ATLAS collaboration, *The ATLAS inner detector trigger performance in pp collisions at 13 TeV during LHC Run 2*, *Eur. Phys. J. C* **82** (2022) 206 [arXiv:2107.02485] [INSPIRE].

[80] ATLAS collaboration, *Jet reconstruction and performance using particle flow with the ATLAS Detector*, *Eur. Phys. J. C* **77** (2017) 466 [arXiv:1703.10485] [INSPIRE].

[81] M. Cacciari, G.P. Salam and G. Soyez, *The anti-*k_t *jet clustering algorithm*, *JHEP* **04** (2008) 063 [arXiv:0802.1189] [INSPIRE].

[82] M. Cacciari, G.P. Salam and G. Soyez, *FastJet User Manual*, *Eur. Phys. J. C* **72** (2012) 1896 [arXiv:1111.6097] [INSPIRE].

[83] ATLAS collaboration, *Jet energy scale and resolution measured in proton–proton collisions at* $\sqrt{s} = 13$ *TeV with the ATLAS detector*, *Eur. Phys. J. C* **81** (2021) 689 [arXiv:2007.02645] [INSPIRE].

[84] ATLAS collaboration, *Measurement of the production cross section of jets in association with a Z boson in pp collisions at* $\sqrt{s} = 7$ *TeV with the ATLAS detector*, *JHEP* **07** (2013) 032 [arXiv:1304.7098] [INSPIRE].

[85] ATLAS collaboration, *Measurement of ZZ production in the* $\ell\ell\nu\nu$ *final state with the ATLAS detector in pp collisions at* $\sqrt{s} = 13$ *TeV*, *JHEP* **10** (2019) 127 [arXiv:1905.07163] [INSPIRE].

[86] ATLAS collaboration, *Measurement of fiducial and differential* W^+W^- *production cross-sections at* $\sqrt{s} = 13$ *TeV with the ATLAS detector*, *Eur. Phys. J. C* **79** (2019) 884 [arXiv:1905.04242] [INSPIRE].

[87] ATLAS collaboration, *Measurement of* $W^{\pm}Z$ *production cross sections and gauge boson polarisation in pp collisions at* $\sqrt{s} = 13$ *TeV with the ATLAS detector*, *Eur. Phys. J. C* **79** (2019) 535 [arXiv:1902.05759] [INSPIRE].

[88] ATLAS collaboration, $ZZ \to \ell^+\ell^-\ell'^+\ell'^-$ *cross-section measurements and search for anomalous triple gauge couplings in 13 TeV pp collisions with the ATLAS detector*, *Phys. Rev. D* **97** (2018) 032005 [arXiv:1709.07703] [INSPIRE].

[89] ATLAS collaboration, *Measurement of* $WW/WZ \to \ell\nu qq'$ *production with the hadronically decaying boson reconstructed as one or two jets in pp collisions at* $\sqrt{s} = 8$ *TeV with ATLAS, and constraints on anomalous gauge couplings*, *Eur. Phys. J. C* **77** (2017) 563 [arXiv:1706.01702] [INSPIRE].

[90] G. D'Agostini, *A Multidimensional unfolding method based on Bayes' theorem*, Nucl. Instrum. Meth. A **362** (1995) 487 [INSPIRE].

[91] T. Adye, *Unfolding algorithms and tests using RooUnfold*, in the proceedings of the *PHYSTAT 2011*, (2011), p. 313–318 [DOI:10.5170/CERN-2011-006.313] [arXiv:1105.1160] [INSPIRE].

[92] ATLAS collaboration, *Measurements of the production cross section of a Z boson in association with jets in pp collisions at $\sqrt{s} = 13$ TeV with the ATLAS detector*, Eur. Phys. J. C **77** (2017) 361 [arXiv:1702.05725] [INSPIRE].

[93] J. Butterworth et al., *PDF4LHC recommendations for LHC Run II*, J. Phys. G **43** (2016) 023001 [arXiv:1510.03865] [INSPIRE].

[94] S. Dulat et al., *New parton distribution functions from a global analysis of quantum chromodynamics*, Phys. Rev. D **93** (2016) 033006 [arXiv:1506.07443] [INSPIRE].

[95] ATLAS collaboration, *Electron reconstruction and identification in the ATLAS experiment using the 2015 and 2016 LHC proton-proton collision data at $\sqrt{s} = 13$ TeV*, Eur. Phys. J. C **79** (2019) 639 [arXiv:1902.04655] [INSPIRE].

[96] ATLAS collaboration, *Jet energy scale measurements and their systematic uncertainties in proton-proton collisions at $\sqrt{s} = 13$ TeV with the ATLAS detector*, Phys. Rev. D **96** (2017) 072002 [arXiv:1703.09665] [INSPIRE].

[97] ATLAS collaboration, *Jet energy resolution in proton-proton collisions at $\sqrt{s} = 7$ TeV recorded in 2010 with the ATLAS detector*, Eur. Phys. J. C **73** (2013) 2306 [arXiv:1210.6210] [INSPIRE].

[98] ATLAS collaboration, *Luminosity determination in pp collisions at $\sqrt{s} = 13$ TeV using the ATLAS detector at the LHC*, ATLAS-CONF-2019-021 (2019).

[99] G. Avoni et al., *The new LUCID-2 detector for luminosity measurement and monitoring in ATLAS*, 2018 *JINST* **13** P07017 [INSPIRE].

[100] L. Lyons, D. Gibaut and P. Clifford, *How to combine correlated estimates of a single physical quantity*, Nucl. Instrum. Meth. A **270** (1988) 110 [INSPIRE].

[101] E. Gerwick, T. Plehn, S. Schumann and P. Schichtel, *Scaling patterns for QCD jets*, JHEP **10** (2012) 162 [arXiv:1208.3676] [INSPIRE].

[102] ATLAS collaboration, *ATLAS computing acknowledgements*, ATL-SOFT-PUB-2021-003 (2021)

JHEP06(2023)080

The ATLAS collaboration

G. Aad[101], B. Abbott[119], D.C. Abbott[102], K. Abeling[55], S.H. Abidi[29], A. Aboulhorma[35e], H. Abramowicz[150], H. Abreu[149], Y. Abulaiti[116], A.C. Abusleme Hoffman[136a], B.S. Acharya[68a,68b,o], B. Achkar[55], L. Adam[99], C. Adam Bourdarios[4], L. Adamczyk[84a], L. Adamek[154], S.V. Addepalli[26], J. Adelman[114], A. Adiguzel[21c], S. Adorni[56], T. Adye[133], A.A. Affolder[135], Y. Afik[36], M.N. Agaras[13], J. Agarwala[72a,72b], A. Aggarwal[99], C. Agheorghiesei[27c], J.A. Aguilar-Saavedra[129f], A. Ahmad[36], F. Ahmadov[38,w], W.S. Ahmed[103], X. Ai[48], G. Aielli[75a,75b], I. Aizenberg[167], M. Akbiyik[99], T.P.A. Åkesson[97], A.V. Akimov[37], K. Al Khoury[41], G.L. Alberghi[23b], J. Albert[163], P. Albicocco[53], M.J. Alconada Verzini[89], S. Alderweireldt[52], M. Aleksa[36], I.N. Aleksandrov[38], C. Alexa[27b], T. Alexopoulos[10], A. Alfonsi[113], F. Alfonsi[23b], M. Alhroob[119], B. Ali[131], S. Ali[147], M. Aliev[37], G. Alimonti[70a], C. Allaire[36], B.M.M. Allbrooke[145], P.P. Allport[20], A. Aloisio[71a,71b], F. Alonso[89], C. Alpigiani[137], E. Alunno Camelia[75a,75b], M. Alvarez Estevez[98], M.G. Alviggi[71a,71b], Y. Amaral Coutinho[81b], A. Ambler[103], C. Amelung[36], C.G. Ames[108], D. Amidei[105], S.P. Amor Dos Santos[129a], S. Amoroso[48], K.R. Amos[161], C.S. Amrouche[56], V. Ananiev[124], C. Anastopoulos[138], N. Andari[134], T. Andeen[11], J.K. Anders[19], S.Y. Andrean[47a,47b], A. Andreazza[70a,70b], S. Angelidakis[9], A. Angerami[41,y], A.V. Anisenkov[37], A. Annovi[73a], C. Antel[56], M.T. Anthony[138], E. Antipov[120], M. Antonelli[53], D.J.A. Antrim[17a], F. Anulli[74a], M. Aoki[82], J.A. Aparisi Pozo[161], M.A. Aparo[145], L. Aperio Bella[48], C. Appelt[18], N. Aranzabal[36], V. Araujo Ferraz[81a], C. Arcangeletti[53], A.T.H. Arce[51], E. Arena[91], J-F. Arguin[107], S. Argyropoulos[54], J.-H. Arling[48], A.J. Armbruster[36], O. Arnaez[154], H. Arnold[113], Z.P. Arrubarrena Tame[108], G. Artoni[74a,74b], H. Asada[110], K. Asai[117], S. Asai[152], N.A. Asbah[61], E.M. Asimakopoulou[159], J. Assahsah[35d], K. Assamagan[29], R. Astalos[28a], R.J. Atkin[33a], M. Atkinson[160], N.B. Atlay[18], H. Atmani[62b], P.A. Atmasiddha[105], K. Augsten[131], S. Auricchio[71a,71b], A.D. Auriol[20], V.A. Austrup[169], G. Avner[149], G. Avolio[36], K. Axiotis[56], M.K. Ayoub[14c], G. Azuelos[107,ac], D. Babal[28a], H. Bachacou[134], K. Bachas[151,q], A. Bachiu[34], F. Backman[47a,47b], A. Badea[61], P. Bagnaia[74a,74b], M. Bahmani[18], A.J. Bailey[161], V.R. Bailey[160], J.T. Baines[133], C. Bakalis[10], O.K. Baker[170], P.J. Bakker[113], E. Bakos[15], D. Bakshi Gupta[8], S. Balaji[146], R. Balasubramanian[113], E.M. Baldin[37], P. Balek[132], E. Ballabene[70a,70b], F. Balli[134], L.M. Baltes[63a], W.K. Balunas[32], J. Balz[99], E. Banas[85], M. Bandieramonte[128], A. Bandyopadhyay[24], S. Bansal[24], L. Barak[150], E.L. Barberio[104], D. Barberis[57b,57a], M. Barbero[101], G. Barbour[95], K.N. Barends[33a], T. Barillari[109], M-S. Barisits[36], J. Barkeloo[122], T. Barklow[142], R.M. Barnett[17a], P. Baron[121], D.A. Baron Moreno[100], A. Baroncelli[62a], G. Barone[29], A.J. Barr[125], L. Barranco Navarro[47a,47b], F. Barreiro[98], J. Barreiro Guimarães da Costa[14a], U. Barron[150], M.G. Barros Teixeira[129a], S. Barsov[37], F. Bartels[63a], R. Bartoldus[142], A.E. Barton[90], P. Bartos[28a], A. Basalaev[48], A. Basan[99], M. Baselga[49], I. Bashta[76a,76b], A. Bassalat[66,z], M.J. Basso[154], C.R. Basson[100], R.L. Bates[59], S. Batlamous[35e], J.R. Batley[32], B. Batool[140], M. Battaglia[135], M. Bauce[74a,74b],

JHEP06(2023)080

P. Bauer[24], A. Bayirli[21a], J.B. Beacham[51], T. Beau[126], P.H. Beauchemin[157], F. Becherer[54], P. Bechtle[24], H.P. Beck[19,p], K. Becker[165], C. Becot[48], A.J. Beddall[21d], V.A. Bednyakov[38], C.P. Bee[144], L.J. Beemster[15], T.A. Beermann[36], M. Begalli[81b,81d], M. Begel[29], A. Behera[144], J.K. Behr[48], C. Beirao Da Cruz E Silva[36], J.F. Beirer[55,36], F. Beisiegel[24], M. Belfkir[115b], G. Bella[150], L. Bellagamba[23b], A. Bellerive[34], P. Bellos[20], K. Beloborodov[37], K. Belotskiy[37], N.L. Belyaev[37], D. Benchekroun[35a], F. Bendebba[35a], Y. Benhammou[150], D.P. Benjamin[29], M. Benoit[29], J.R. Bensinger[26], S. Bentvelsen[113], L. Beresford[36], M. Beretta[53], D. Berge[18], E. Bergeaas Kuutmann[159], N. Berger[4], B. Bergmann[131], J. Beringer[17a], S. Berlendis[7], G. Bernardi[5], C. Bernius[142], F.U. Bernlochner[24], T. Berry[94], P. Berta[132], A. Berthold[50], I.A. Bertram[90], O. Bessidskaia Bylund[169], S. Bethke[109], A. Betti[44], A.J. Bevan[93], M. Bhamjee[33c], S. Bhatta[144], D.S. Bhattacharya[164], P. Bhattarai[26], V.S. Bhopatkar[6], R. Bi[128], R. Bi[29,af], R.M. Bianchi[128], O. Biebel[108], R. Bielski[122], N.V. Biesuz[73a,73b], M. Biglietti[76a], T.R.V. Billoud[131], M. Bindi[55], A. Bingul[21b], C. Bini[74a,74b], S. Biondi[23b,23a], A. Biondini[91], C.J. Birch-sykes[100], G.A. Bird[20,133], M. Birman[167], T. Bisanz[36], D. Biswas[168,k], A. Bitadze[100], K. Bjørke[124], I. Bloch[48], C. Blocker[26], A. Blue[59], U. Blumenschein[93], J. Blumenthal[99], G.J. Bobbink[113], V.S. Bobrovnikov[37], M. Boehler[54], D. Bogavac[36], A.G. Bogdanchikov[37], C. Bohm[47a], V. Boisvert[94], P. Bokan[48], T. Bold[84a], M. Bomben[5], M. Bona[93], M. Boonekamp[134], C.D. Booth[94], A.G. Borbély[59], H.M. Borecka-Bielska[107], L.S. Borgna[95], G. Borissov[90], D. Bortoletto[125], D. Boscherini[23b], M. Bosman[13], J.D. Bossio Sola[36], K. Bouaouda[35a], J. Boudreau[128], E.V. Bouhova-Thacker[90], D. Boumediene[40], R. Bouquet[5], A. Boveia[118], J. Boyd[36], D. Boye[29], I.R. Boyko[38], J. Bracinik[20], N. Brahimi[62d,62c], G. Brandt[169], O. Brandt[32], F. Braren[48], B. Brau[102], J.E. Brau[122], W.D. Breaden Madden[59], K. Brendlinger[48], R. Brener[167], L. Brenner[36], R. Brenner[159], S. Bressler[167], B. Brickwedde[99], D. Britton[59], D. Britzger[109], I. Brock[24], G. Brooijmans[41], W.K. Brooks[136f], E. Brost[29], P.A. Bruckman de Renstrom[85], B. Brüers[48], D. Bruncko[28b,*], A. Bruni[23b], G. Bruni[23b], M. Bruschi[23b], N. Bruscino[74a,74b], L. Bryngemark[142], T. Buanes[16], Q. Buat[137], P. Buchholz[140], A.G. Buckley[59], I.A. Budagov[38,*], M.K. Bugge[124], O. Bulekov[37], B.A. Bullard[61], S. Burdin[91], C.D. Burgard[48], A.M. Burger[40], B. Burghgrave[8], J.T.P. Burr[32], C.D. Burton[11], J.C. Burzynski[141], E.L. Busch[41], V. Büscher[99], P.J. Bussey[59], J.M. Butler[25], C.M. Buttar[59], J.M. Butterworth[95], W. Buttinger[133], C.J. Buxo Vazquez[106], A.R. Buzykaev[37], G. Cabras[23b], S. Cabrera Urbán[161], D. Caforio[58], H. Cai[128], Y. Cai[14a,14d], V.M.M. Cairo[36], O. Cakir[3a], N. Calace[36], P. Calafiura[17a], G. Calderini[126], P. Calfayan[67], G. Callea[59], L.P. Caloba[81b], D. Calvet[40], S. Calvet[40], T.P. Calvet[101], M. Calvetti[73a,73b], R. Camacho Toro[126], S. Camarda[36], D. Camarero Munoz[98], P. Camarri[75a,75b], M.T. Camerlingo[76a,76b], D. Cameron[124], C. Camincher[163], M. Campanelli[95], A. Camplani[42], V. Canale[71a,71b], A. Canesse[103], M. Cano Bret[79], J. Cantero[161], Y. Cao[160], F. Capocasa[26], M. Capua[43b,43a], A. Carbone[70a,70b], R. Cardarelli[75a], J.C.J. Cardenas[8], F. Cardillo[161], T. Carli[36], G. Carlino[71a], B.T. Carlson[128,r], E.M. Carlson[163,155a], L. Carminati[70a,70b], M. Carnesale[74a,74b], S. Caron[112], E. Carquin[136f], S. Carrá[70a,70b], G. Carratta[23b,23a],

F. Carrio Argos[33g], J.W.S. Carter[154], T.M. Carter[52], M.P. Casado[13,h], A.F. Casha[154], E.G. Castiglia[170], F.L. Castillo[63a], L. Castillo Garcia[13], V. Castillo Gimenez[161], N.F. Castro[129a,129e], A. Catinaccio[36], J.R. Catmore[124], V. Cavaliere[29], N. Cavalli[23b,23a], V. Cavasinni[73a,73b], E. Celebi[21a], F. Celli[125], M.S. Centonze[69a,69b], K. Cerny[121], A.S. Cerqueira[81a], A. Cerri[145], L. Cerrito[75a,75b], F. Cerutti[17a], A. Cervelli[23b], S.A. Cetin[21d], Z. Chadi[35a], D. Chakraborty[114], M. Chala[129f], J. Chan[168], W.S. Chan[113], W.Y. Chan[152], J.D. Chapman[32], B. Chargeishvili[148b], D.G. Charlton[20], T.P. Charman[93], M. Chatterjee[19], S. Chekanov[6], S.V. Chekulaev[155a], G.A. Chelkov[38,a], A. Chen[105], B. Chen[150], B. Chen[163], C. Chen[62a], H. Chen[14c], H. Chen[29], J. Chen[62c], J. Chen[26], S. Chen[152], S.J. Chen[14c], X. Chen[62c], X. Chen[14b,ab], Y. Chen[62a], C.L. Cheng[168], H.C. Cheng[64a], A. Cheplakov[38], E. Cheremushkina[48], E. Cherepanova[113], R. Cherkaoui El Moursli[35e], E. Cheu[7], K. Cheung[65], L. Chevalier[134], V. Chiarella[53], G. Chiarelli[73a], G. Chiodini[69a], A.S. Chisholm[20], A. Chitan[27b], Y.H. Chiu[163], M.V. Chizhov[38], K. Choi[11], A.R. Chomont[74a,74b], Y. Chou[102], E.Y.S. Chow[113], T. Chowdhury[33g], L.D. Christopher[33g], K.L. Chu[64a], M.C. Chu[64a], X. Chu[14a,14d], J. Chudoba[130], J.J. Chwastowski[85], D. Cieri[109], K.M. Ciesla[84a], V. Cindro[92], A. Ciocio[17a], F. Cirotto[71a,71b], Z.H. Citron[167,l], M. Citterio[70a], D.A. Ciubotaru[27b], B.M. Ciungu[154], A. Clark[56], P.J. Clark[52], J.M. Clavijo Columbie[48], S.E. Clawson[100], C. Clement[47a,47b], J. Clercx[48], L. Clissa[23b,23a], Y. Coadou[101], M. Cobal[68a,68c], A. Coccaro[57b], R.F. Coelho Barrue[129a], R. Coelho Lopes De Sa[102], S. Coelli[70a], H. Cohen[150], A.E.C. Coimbra[70a,70b], B. Cole[41], J. Collot[60], P. Conde Muiño[129a,129g], S.H. Connell[33c], I.A. Connelly[59], E.I. Conroy[125], F. Conventi[71a,ad], H.G. Cooke[20], A.M. Cooper-Sarkar[125], F. Cormier[162], L.D. Corpe[36], M. Corradi[74a,74b], E.E. Corrigan[97], F. Corriveau[103,v], A. Cortes-Gonzalez[18], M.J. Costa[161], F. Costanza[4], D. Costanzo[138], B.M. Cote[118], G. Cowan[94], J.W. Cowley[32], K. Cranmer[116], S. Crépé-Renaudin[60], F. Crescioli[126], M. Cristinziani[140], M. Cristoforetti[77a,77b,c], V. Croft[157], G. Crosetti[43b,43a], A. Cueto[36], T. Cuhadar Donszelmann[158], H. Cui[14a,14d], Z. Cui[7], A.R. Cukierman[142], W.R. Cunningham[59], F. Curcio[43b,43a], P. Czodrowski[36], M.M. Czurylo[63b], M.J. Da Cunha Sargedas De Sousa[62a], J.V. Da Fonseca Pinto[81b], C. Da Via[100], W. Dabrowski[84a], T. Dado[49], S. Dahbi[33g], T. Dai[105], C. Dallapiccola[102], M. Dam[42], G. D'amen[29], V. D'Amico[76a,76b], J. Damp[99], J.R. Dandoy[127], M.F. Daneri[30], M. Danninger[141], V. Dao[36], G. Darbo[57b], S. Darmora[6], S.J. Das[29], A. Dattagupta[122], S. D'Auria[70a,70b], C. David[155b], T. Davidek[132], D.R. Davis[51], B. Davis-Purcell[34], I. Dawson[93], K. De[8], R. De Asmundis[71a], M. De Beurs[113], S. De Castro[23b,23a], N. De Groot[112], P. de Jong[113], H. De la Torre[106], A. De Maria[14c], A. De Salvo[74a], U. De Sanctis[75a,75b], M. De Santis[75a,75b], A. De Santo[145], J.B. De Vivie De Regie[60], D.V. Dedovich[38], J. Degens[113], A.M. Deiana[44], F. Del Corso[23b,23a], J. Del Peso[98], F. Del Rio[63a], F. Deliot[134], C.M. Delitzsch[49], M. Della Pietra[71a,71b], D. Della Volpe[56], A. Dell'Acqua[36], L. Dell'Asta[70a,70b], M. Delmastro[4], P.A. Delsart[60], S. Demers[170], M. Demichev[38], S.P. Denisov[37], L. D'Eramo[114], D. Derendarz[85], F. Derue[126], P. Dervan[91], K. Desch[24], K. Dette[154], C. Deutsch[24], P.O. Deviveiros[36], F.A. Di Bello[74a,74b], A. Di Ciaccio[75a,75b], L. Di Ciaccio[4], A. Di Domenico[74a,74b], C. Di Donato[71a,71b], A. Di Girolamo[36], G. Di Gregorio[73a,73b], A. Di Luca[77a,77b], B. Di Micco[76a,76b], R. Di Nardo[76a,76b], C. Diaconu[101], F.A. Dias[113], T. Dias Do Vale[141], M.A. Diaz[136a,136b], F.G. Diaz Capriles[24], M. Didenko[161], E.B. Diehl[105], L. Diehl[54], S. Díez Cornell[48], C. Diez Pardos[140], C. Dimitriadi[24,159], A. Dimitrievska[17a], W. Ding[14b], J. Dingfelder[24], I-M. Dinu[27b], S.J. Dittmeier[63b], F. Dittus[36], F. Djama[101], T. Djobava[148b], J.I. Djuvsland[16], D. Dodsworth[26], C. Doglioni[100,97], J. Dolejsi[132], Z. Dolezal[132], M. Donadelli[81c], B. Dong[62c], J. Donini[40], A. D'Onofrio[14c], M. D'Onofrio[91], J. Dopke[133], A. Doria[71a], M.T. Dova[89], A.T. Doyle[59], M.A. Draguet[125], E. Drechsler[141], E. Dreyer[167], I. Drivas-koulouris[10], A.S. Drobac[157], D. Du[62a], T.A. du Pree[113], F. Dubinin[37], M. Dubovsky[28a], E. Duchovni[167], G. Duckeck[108], O.A. Ducu[36], D. Duda[109], A. Dudarev[36], M. D'uffizi[100], L. Duflot[66], M. Dührssen[36], C. Dülsen[169], A.E. Dumitriu[27b], M. Dunford[63a], S. Dungs[49], K. Dunne[47a,47b], A. Duperrin[101], H. Duran Yildiz[3a], M. Düren[58], A. Durglishvili[148b], B.L. Dwyer[114], G.I. Dyckes[17a], M. Dyndal[84a], S. Dysch[100], B.S. Dziedzic[85], Z.O. Earnshaw[145], B. Eckerova[28a], M.G. Eggleston[51], E. Egidio Purcino De Souza[81b], L.F. Ehrke[56], G. Eigen[16], K. Einsweiler[17a], T. Ekelof[159], P.A. Ekman[97], Y. El Ghazali[35b], H. El Jarrari[35e,147], A. El Moussaouy[35a], V. Ellajosyula[159], M. Ellert[159], F. Ellinghaus[169], A.A. Elliot[93], N. Ellis[36], J. Elmsheuser[29], M. Elsing[36], D. Emeliyanov[133], A. Emerman[41], Y. Enari[152], I. Ene[17a], S. Epari[13], J. Erdmann[49], A. Ereditato[19], P.A. Erland[85], M. Errenst[169], M. Escalier[66], C. Escobar[161], E. Etzion[150], G. Evans[129a], H. Evans[67], M.O. Evans[145], A. Ezhilov[37], S. Ezzarqtouni[35a], F. Fabbri[59], L. Fabbri[23b,23a], G. Facini[95], V. Fadeyev[135], R.M. Fakhrutdinov[37], S. Falciano[74a], P.J. Falke[24], S. Falke[36], J. Faltova[132], Y. Fan[14a], Y. Fang[14a,14d], G. Fanourakis[46], M. Fanti[70a,70b], M. Faraj[68a,68b], A. Farbin[8], A. Farilla[76a], T. Farooque[106], S.M. Farrington[52], F. Fassi[35e], D. Fassouliotis[9], M. Faucci Giannelli[75a,75b], W.J. Fawcett[32], L. Fayard[66], O.L. Fedin[37,a], G. Fedotov[37], M. Feickert[160], L. Feligioni[101], A. Fell[138], D.E. Fellers[122], C. Feng[62b], M. Feng[14b], M.J. Fenton[158], A.B. Fenyuk[37], L. Ferencz[48], S.W. Ferguson[45], J. Pretel[54], J. Ferrando[48], A. Ferrari[159], P. Ferrari[113], R. Ferrari[72a], D. Ferrere[56], C. Ferretti[105], F. Fiedler[99], A. Filipčič[92], E.K. Filmer[1], F. Filthaut[112], M.C.N. Fiolhais[129a,129c,b], L. Fiorini[161], F. Fischer[140], W.C. Fisher[106], T. Fitschen[20,66], I. Fleck[140], P. Fleischmann[105], T. Flick[169], L. Flores[127], M. Flores[33d], L.R. Flores Castillo[64a], F.M. Follega[77a,77b], N. Fomin[16], J.H. Foo[154], B.C. Forland[67], A. Formica[134], A.C. Forti[100], E. Fortin[101], A.W. Fortman[61], M.G. Foti[17a], L. Fountas[9], D. Fournier[66], H. Fox[90], P. Francavilla[73a,73b], S. Francescato[61], M. Franchini[23b,23a], S. Franchino[63a], D. Francis[36], L. Franco[112], L. Franconi[19], M. Franklin[61], G. Frattari[26], A.C. Freegard[93], P.M. Freeman[20], W.S. Freund[81b], N. Fritzsche[50], A. Froch[54], D. Froidevaux[36], J.A. Frost[125], Y. Fu[62a], M. Fujimoto[117], E. Fullana Torregrosa[161,*], J. Fuster[161], A. Gabrielli[23b,23a], A. Gabrielli[36], P. Gadow[48], G. Gagliardi[57b,57a], L.G. Gagnon[17a], G.E. Gallardo[125], E.J. Gallas[125], B.J. Gallop[133], R. Gamboa Goni[93], K.K. Gan[118], S. Ganguly[152], J. Gao[62a], Y. Gao[52], F.M. Garay Walls[136a,136b], B. Garcia[29,af], C. García[161], J.E. García Navarro[161], J.A. García Pascual[14a], M. Garcia-Sciveres[17a], R.W. Gardner[39], D. Garg[79], R.B. Garg[142], S. Gargiulo[54], C.A. Garner[154], V. Garonne[29], S.J. Gasiorowski[137], P. Gaspar[81b], G. Gaudio[72a], P. Gauzzi[74a,74b], I.L. Gavrilenko[37], A. Gavrilyuk[37], C. Gay[162], G. Gaycken[48], E.N. Gazis[10], A.A. Geanta[27b], C.M. Gee[135], J. Geisen[97], M. Geisen[99], C. Gemme[57b], M.H. Genest[60], S. Gentile[74a,74b], S. George[94], W.F. George[20], T. Geralis[46], L.O. Gerlach[55], P. Gessinger-Befurt[36], M. Ghasemi Bostanabad[163], M. Ghneimat[140], A. Ghosal[140], A. Ghosh[158], A. Ghosh[7], B. Giacobbe[23b], S. Giagu[74a,74b], N. Giangiacomi[154], P. Giannetti[73a], A. Giannini[62a], S.M. Gibson[94], M. Gignac[135], D.T. Gil[84b], A.K. Gilbert[84a], B.J. Gilbert[41], D. Gillberg[34], G. Gilles[113], N.E.K. Gillwald[48], L. Ginabat[126], D.M. Gingrich[2,ac], M.P. Giordani[68a,68c], P.F. Giraud[134], G. Giugliarelli[68a,68c], D. Giugni[70a], F. Giuli[36], I. Gkialas[9,i], L.K. Gladilin[37], C. Glasman[98], G.R. Gledhill[122], M. Glisic[122], I. Gnesi[43b,e], Y. Go[29,af], M. Goblirsch-Kolb[26], D. Godin[107], S. Goldfarb[104], T. Golling[56], M.G.D. Gololo[33g], D. Golubkov[37], J.P. Gombas[106], A. Gomes[129a,129b], G. Gomes Da Silva[140], A.J. Gomez Delegido[161], R. Goncalves Gama[55], R. Gonçalo[129a,129c], G. Gonella[122], L. Gonella[20], A. Gongadze[38], F. Gonnella[20], J.L. Gonski[41], S. González de la Hoz[161], S. Gonzalez Fernandez[13], R. Gonzalez Lopez[91], C. Gonzalez Renteria[17a], R. Gonzalez Suarez[159], S. Gonzalez-Sevilla[56], G.R. Gonzalvo Rodriguez[161], R.Y. González Andana[52], L. Goossens[36], N.A. Gorasia[20], P.A. Gorbounov[37], B. Gorini[36], E. Gorini[69a,69b], A. Gorišek[92], A.T. Goshaw[51], M.I. Gostkin[38], C.A. Gottardo[112], M. Gouighri[35b], V. Goumarre[48], A.G. Goussiou[137], N. Govender[33c], C. Goy[4], I. Grabowska-Bold[84a], K. Graham[34], E. Gramstad[124], S. Grancagnolo[18], M. Grandi[145], V. Gratchev[37,*], P.M. Gravila[27f], F.G. Gravili[69a,69b], H.M. Gray[17a], M. Greco[69a,69b], C. Grefe[24], I.M. Gregor[48], P. Grenier[142], C. Grieco[13], A.A. Grillo[135], K. Grimm[31,m], S. Grinstein[13,t], J.-F. Grivaz[66], E. Gross[167], J. Grosse-Knetter[55], C. Grud[105], A. Grummer[111], J.C. Grundy[125], L. Guan[105], W. Guan[168], C. Gubbels[162], J.G.R. Guerrero Rojas[161], G. Guerrieri[68a,68c], F. Guescini[109], R. Gugel[99], J.A.M. Guhit[105], A. Guida[48], T. Guillemin[4], E. Guilloton[165,133], S. Guindon[36], F. Guo[14a,14d], J. Guo[62c], L. Guo[66], Y. Guo[105], R. Gupta[48], S. Gurbuz[24], S.S. Gurdasani[54], G. Gustavino[36], M. Guth[56], P. Gutierrez[119], L.F. Gutierrez Zagazeta[127], C. Gutschow[95], C. Guyot[134], C. Gwenlan[125], C.B. Gwilliam[91], E.S. Haaland[124], A. Haas[116], M. Habedank[48], C. Haber[17a], H.K. Hadavand[8], A. Hadef[99], S. Hadzic[109], M. Haleem[164], J. Haley[120], J.J. Hall[138], G.D. Hallewell[101], L. Halser[19], K. Hamano[163], H. Hamdaoui[35e], M. Hamer[24], G.N. Hamity[52], J. Han[62b], K. Han[62a], L. Han[14c], L. Han[62a], S. Han[17a], Y.F. Han[154], K. Hanagaki[82], M. Hance[135], D.A. Hangal[41,y], M.D. Hank[39], R. Hankache[100], J.B. Hansen[42], J.D. Hansen[42], P.H. Hansen[42], K. Hara[156], D. Harada[56], T. Harenberg[169], S. Harkusha[37], Y.T. Harris[125], P.F. Harrison[165], N.M. Hartman[142], N.M. Hartmann[108], Y. Hasegawa[139], A. Hasib[52], S. Haug[19], R. Hauser[106], M. Havranek[131], C.M. Hawkes[20], R.J. Hawkings[36], S. Hayashida[110], D. Hayden[106], C. Hayes[105], R.L. Hayes[162], C.P. Hays[125], J.M. Hays[93], H.S. Hayward[91], F. He[62a], Y. He[153], Y. He[126], M.P. Heath[52], V. Hedberg[97], A.L. Heggelund[124], N.D. Hehir[93], C. Heidegger[54], K.K. Heidegger[54], W.D. Heidorn[80],

JHEP06(2023)080

J. Heilman[34], S. Heim[48], T. Heim[17a], J.G. Heinlein[127], J.J. Heinrich[122],
L. Heinrich[36], J. Hejbal[130], L. Helary[48], A. Held[116], S. Hellesund[124], C.M. Helling[162],
S. Hellman[47a,47b], C. Helsens[36], R.C.W. Henderson[90], L. Henkelmann[32],
A.M. Henriques Correia[36], H. Herde[142], Y. Hernández Jiménez[144], H. Herr[99],
M.G. Herrmann[108], T. Herrmann[50], G. Herten[54], R. Hertenberger[108], L. Hervas[36],
N.P. Hessey[155a], H. Hibi[83], E. Higón-Rodriguez[161], S.J. Hillier[20], I. Hinchliffe[17a],
F. Hinterkeuser[24], M. Hirose[123], S. Hirose[156], D. Hirschbuehl[169], T.G. Hitchings[100],
B. Hiti[92], J. Hobbs[144], R. Hobincu[27e], N. Hod[167], M.C. Hodgkinson[138],
B.H. Hodkinson[32], A. Hoecker[36], J. Hofer[48], D. Hohn[54], T. Holm[24], M. Holzbock[109],
L.B.A.H. Hommels[32], B.P. Honan[100], J. Hong[62c], T.M. Hong[128], Y. Hong[55],
J.C. Honig[54], A. Hönle[109], B.H. Hooberman[160], W.H. Hopkins[6], Y. Horii[110],
S. Hou[147], A.S. Howard[92], J. Howarth[59], J. Hoya[89], M. Hrabovsky[121],
A. Hrynevich[37], T. Hryn'ova[4], P.J. Hsu[65], S.-C. Hsu[137], Q. Hu[41,y], Y.F. Hu[14a,14d,ae],
D.P. Huang[95], S. Huang[64b], X. Huang[14c], Y. Huang[62a], Y. Huang[14a], Z. Huang[100],
Z. Hubacek[131], M. Huebner[24], F. Huegging[24], T.B. Huffman[125], M. Huhtinen[36],
S.K. Huiberts[16], R. Hulsken[103], N. Huseynov[12,a], J. Huston[106], J. Huth[61],
R. Hyneman[142], S. Hyrych[28a], G. Iacobucci[56], G. Iakovidis[29], I. Ibragimov[140],
L. Iconomidou-Fayard[66], P. Iengo[71a,71b], R. Iguchi[152], T. Iizawa[56], Y. Ikegami[82],
A. Ilg[19], N. Ilic[154], H. Imam[35a], T. Ingebretsen Carlson[47a,47b], G. Introzzi[72a,72b],
M. Iodice[76a], V. Ippolito[74a,74b], M. Ishino[152], W. Islam[168], C. Issever[18,48],
S. Istin[21a,ag], H. Ito[166], J.M. Iturbe Ponce[64a], R. Iuppa[77a,77b], A. Ivina[167],
J.M. Izen[45], V. Izzo[71a], P. Jacka[130,131], P. Jackson[1], R.M. Jacobs[48], B.P. Jaeger[141],
C.S. Jagfeld[108], G. Jäkel[169], K. Jakobs[54], T. Jakoubek[167], J. Jamieson[59],
K.W. Janas[84a], G. Jarlskog[97], A.E. Jaspan[91], T. Javůrek[36], M. Javurkova[102],
F. Jeanneau[134], L. Jeanty[122], J. Jejelava[148a,x], P. Jenni[54,f], C.E. Jessiman[34],
S. Jézéquel[4], J. Jia[144], X. Jia[61], X. Jia[14a,14d], Z. Jia[14c], Y. Jiang[62a], S. Jiggins[52],
J. Jimenez Pena[109], S. Jin[14c], A. Jinaru[27b], O. Jinnouchi[153], H. Jivan[33g],
P. Johansson[138], K.A. Johns[7], C.A. Johnson[67], D.M. Jones[32], E. Jones[165],
R.W.L. Jones[90], T.J. Jones[91], J. Jovicevic[15], X. Ju[17a], J.J. Junggeburth[36],
A. Juste Rozas[13,t], S. Kabana[136e], A. Kaczmarska[85], M. Kado[74a,74b], H. Kagan[118],
M. Kagan[142], A. Kahn[41], A. Kahn[127], C. Kahra[99], T. Kaji[166], E. Kajomovitz[149],
N. Kakati[167], C.W. Kalderon[29], A. Kamenshchikov[154], N.J. Kang[135], Y. Kano[110],
D. Kar[33g], K. Karava[125], M.J. Kareem[155b], E. Karentzos[54], I. Karkanias[151],
S.N. Karpov[38], Z.M. Karpova[38], V. Kartvelishvili[90], A.N. Karyukhin[37], E. Kasimi[151],
C. Kato[62d], J. Katzy[48], S. Kaur[34], K. Kawade[139], K. Kawagoe[88], T. Kawaguchi[110],
T. Kawamoto[134], G. Kawamura[55], E.F. Kay[163], F.I. Kaya[157], S. Kazakos[13],
V.F. Kazanin[37], Y. Ke[144], J.M. Keaveney[33a], R. Keeler[163], G.V. Kehris[61],
J.S. Keller[34], A.S. Kelly[95], D. Kelsey[145], J.J. Kempster[20], J. Kendrick[20],
K.E. Kennedy[41], O. Kepka[130], B.P. Kerridge[165], S. Kersten[169], B.P. Kerševan[92],
L. Keszeghova[28a], S. Ketabchi Haghighat[154], M. Khandoga[126], A. Khanov[120],
A.G. Kharlamov[37], T. Kharlamova[37], E.E. Khoda[137], T.J. Khoo[18], G. Khoriauli[164],
J. Khubua[148b], Y.A.R. Khwaira[66], M. Kiehn[36], A. Kilgallon[122], D.W. Kim[47a,47b],
E. Kim[153], Y.K. Kim[39], N. Kimura[95], A. Kirchhoff[55], D. Kirchmeier[50], C. Kirfel[24],

JHEP06(2023)080

J. Kirk[133], A.E. Kiryunin[109], T. Kishimoto[152], D.P. Kisliuk[154], C. Kitsaki[10],
O. Kivernyk[24], M. Klassen[63a], C. Klein[34], L. Klein[164], M.H. Klein[105], M. Klein[91],
U. Klein[91], P. Klimek[36], A. Klimentov[29], F. Klimpel[109], T. Klingl[24],
T. Klioutchnikova[36], F.F. Klitzner[108], P. Kluit[113], S. Kluth[109], E. Kneringer[78],
T.M. Knight[154], A. Knue[54], D. Kobayashi[88], R. Kobayashi[86], M. Kocian[142],
T. Kodama[152], P. Kodyš[132], D.M. Koeck[145], P.T. Koenig[24], T. Koffas[34], N.M. Köhler[36],
M. Kolb[134], I. Koletsou[4], T. Komarek[121], K. Köneke[54], A.X.Y. Kong[1], T. Kono[117],
N. Konstantinidis[95], B. Konya[97], R. Kopeliansky[67], S. Koperny[84a], K. Korcyl[85],
K. Kordas[151], G. Koren[150], A. Korn[95], S. Korn[55], I. Korolkov[13], N. Korotkova[37],
B. Kortman[113], O. Kortner[109], S. Kortner[109], W.H. Kostecka[114], V.V. Kostyukhin[140],
A. Kotsokechagia[66], A. Kotwal[51], A. Koulouris[36], A. Kourkoumeli-Charalampidi[72a,72b],
C. Kourkoumelis[9], E. Kourlitis[6], O. Kovanda[145], R. Kowalewski[163], W. Kozanecki[134],
A.S. Kozhin[37], V.A. Kramarenko[37], G. Kramberger[92], P. Kramer[99], M.W. Krasny[126],
A. Krasznahorkay[36], J.A. Kremer[99], T. Kresse[50], J. Kretzschmar[91], K. Kreul[18],
P. Krieger[154], F. Krieter[108], S. Krishnamurthy[102], A. Krishnan[63b], M. Krivos[132],
K. Krizka[17a], K. Kroeninger[49], H. Kroha[109], J. Kroll[130], J. Kroll[127],
K.S. Krowpman[106], U. Kruchonak[38], H. Krüger[24], N. Krumnack[80], M.C. Kruse[51],
J.A. Krzysiak[85], A. Kubota[153], O. Kuchinskaia[37], S. Kuday[3a], D. Kuechler[48],
J.T. Kuechler[48], S. Kuehn[36], T. Kuhl[48], V. Kukhtin[38], Y. Kulchitsky[37,a],
S. Kuleshov[136d,136b], M. Kumar[33g], N. Kumari[101], M. Kuna[60], A. Kupco[130],
T. Kupfer[49], A. Kupich[37], O. Kuprash[54], H. Kurashige[83], L.L. Kurchaninov[155a],
Y.A. Kurochkin[37], A. Kurova[37], E.S. Kuwertz[36], M. Kuze[153], A.K. Kvam[102],
J. Kvita[121], T. Kwan[103], K.W. Kwok[64a], C. Lacasta[161], F. Lacava[74a,74b],
H. Lacker[18], D. Lacour[126], N.N. Lad[95], E. Ladygin[38], B. Laforge[126], T. Lagouri[136e],
S. Lai[55], I.K. Lakomiec[84a], N. Lalloue[60], J.E. Lambert[119], S. Lammers[67],
W. Lampl[7], C. Lampoudis[151], A.N. Lancaster[114], E. Lançon[29], U. Landgraf[54],
M.P.J. Landon[93], V.S. Lang[54], R.J. Langenberg[102], A.J. Lankford[158], F. Lanni[29],
K. Lantzsch[24], A. Lanza[72a], A. Lapertosa[57b,57a], J.F. Laporte[134], T. Lari[70a],
F. Lasagni Manghi[23b], M. Lassnig[36], V. Latonova[130], T.S. Lau[64a], A. Laudrain[99],
A. Laurier[34], S.D. Lawlor[94], Z. Lawrence[100], M. Lazzaroni[70a,70b], B. Le[100], B. Leban[92],
A. Lebedev[80], M. LeBlanc[36], T. LeCompte[6], F. Ledroit-Guillon[60], A.C.A. Lee[95],
G.R. Lee[16], L. Lee[61], S.C. Lee[147], S. Lee[47a,47b], L.L. Leeuw[33c], H.P. Lefebvre[94],
M. Lefebvre[163], C. Leggett[17a], K. Lehmann[141], G. Lehmann Miotto[36], W.A. Leight[102],
A. Leisos[151,s], M.A.L. Leite[81c], C.E. Leitgeb[48], R. Leitner[132], K.J.C. Leney[44],
T. Lenz[24], S. Leone[73a], C. Leonidopoulos[52], A. Leopold[143], C. Leroy[107], R. Les[106],
C.G. Lester[32], M. Levchenko[37], J. Levêque[4], D. Levin[105], L.J. Levinson[167],
D.J. Lewis[20], B. Li[14b], B. Li[62b], C. Li[62a], C-Q. Li[62c,62d], H. Li[62a], H. Li[62b],
H. Li[14c], H. Li[62b], J. Li[62c], K. Li[137], L. Li[62c], M. Li[14a,14d], Q.Y. Li[62a],
S. Li[62d,62c,d], T. Li[62b], X. Li[103], Z. Li[62b], Z. Li[125], Z. Li[103], Z. Li[91], Z. Liang[14a],
M. Liberatore[48], B. Liberti[75a], K. Lie[64c], J. Lieber Marin[81b], K. Lin[106],
R.A. Linck[67], R.E. Lindley[7], J.H. Lindon[2], A. Linss[48], E. Lipeles[127], A. Lipniacka[16],
T.M. Liss[160,aa], A. Lister[162], J.D. Little[4], B. Liu[14a], B.X. Liu[141], D. Liu[62d,62c],
J.B. Liu[62a], J.K.K. Liu[32], K. Liu[62d,62c], M. Liu[62a], M.Y. Liu[62a], P. Liu[14a],

Q. Liu[62d,137,62c], X. Liu[62a], Y. Liu[48], Y. Liu[14c,14d], Y.L. Liu[105], Y.W. Liu[62a], M. Livan[72a,72b], J. Llorente Merino[141], S.L. Lloyd[93], E.M. Lobodzinska[48], P. Loch[7], S. Loffredo[75a,75b], T. Lohse[18], K. Lohwasser[138], M. Lokajicek[130], J.D. Long[160], I. Longarini[74a,74b], L. Longo[69a,69b], R. Longo[160], I. Lopez Paz[36], A. Lopez Solis[48], J. Lorenz[108], N. Lorenzo Martinez[4], A.M. Lory[108], A. Lösle[54], X. Lou[47a,47b], X. Lou[14a,14d], A. Lounis[66], J. Love[6], P.A. Love[90], J.J. Lozano Bahilo[161], G. Lu[14a,14d], M. Lu[79], S. Lu[127], Y.J. Lu[65], H.J. Lubatti[137], C. Luci[74a,74b], F.L. Lucio Alves[14c], A. Lucotte[60], F. Luehring[67], I. Luise[144], O. Lukianchuk[66], O. Lundberg[143], B. Lund-Jensen[143], N.A. Luongo[122], M.S. Lutz[150], D. Lynn[29], H. Lyons[91], R. Lysak[130], E. Lytken[97], F. Lyu[14a], V. Lyubushkin[38], T. Lyubushkina[38], H. Ma[29], L.L. Ma[62b], Y. Ma[95], D.M. Mac Donell[163], G. Maccarrone[53], J.C. MacDonald[138], R. Madar[40], W.F. Mader[50], J. Maeda[83], T. Maeno[29], M. Maerker[50], V. Magerl[54], J. Magro[68a,68c], H. Maguire[138], D.J. Mahon[41], C. Maidantchik[81b], A. Maio[129a,129b,129d], K. Maj[84a], O. Majersky[28a], S. Majewski[122], N. Makovec[66], V. Maksimovic[15], B. Malaescu[126], Pa. Malecki[85], V.P. Maleev[37], F. Malek[60], D. Malito[43b,43a], U. Mallik[79], C. Malone[32], S. Maltezos[10], S. Malyukov[38], J. Mamuzic[13], G. Mancini[53], G. Manco[72a,72b], J.P. Mandalia[93], I. Mandić[92], L. Manhaes de Andrade Filho[81a], I.M. Maniatis[151], M. Manisha[134], J. Manjarres Ramos[50], D.C. Mankad[167], K.H. Mankinen[97], A. Mann[108], A. Manousos[78], B. Mansoulie[134], S. Manzoni[36], A. Marantis[151], G. Marchiori[5], M. Marcisovsky[130], L. Marcoccia[75a,75b], C. Marcon[97], M. Marinescu[20], M. Marjanovic[119], Z. Marshall[17a], S. Marti-Garcia[161], T.A. Martin[165], V.J. Martin[52], B. Martin dit Latour[16], L. Martinelli[74a,74b], M. Martinez[13,t], P. Martinez Agullo[161], V.I. Martinez Outschoorn[102], P. Martinez Suarez[13], S. Martin-Haugh[133], V.S. Martoiu[27b], A.C. Martyniuk[95], A. Marzin[36], S.R. Maschek[109], L. Masetti[99], T. Mashimo[152], J. Masik[100], A.L. Maslennikov[37], L. Massa[23b], P. Massarotti[71a,71b], P. Mastrandrea[73a,73b], A. Mastroberardino[43b,43a], T. Masubuchi[152], T. Mathisen[159], A. Matic[108], N. Matsuzawa[152], J. Maurer[27b], B. Maček[92], D.A. Maximov[37], R. Mazini[147], I. Maznas[151], M. Mazza[106], S.M. Mazza[135], C. Mc Ginn[29,af], J.P. Mc Gowan[103], S.P. Mc Kee[105], T.G. McCarthy[109], W.P. McCormack[17a], E.F. McDonald[104], A.E. McDougall[113], J.A. Mcfayden[145], G. Mchedlidze[148b], R.P. Mckenzie[33g], T.C. Mclachlan[48], D.J. Mclaughlin[95], K.D. McLean[163], S.J. McMahon[133], P.C. McNamara[104], R.A. McPherson[163,v], J.E. Mdhluli[33g], S. Meehan[36], T. Megy[40], S. Mehlhase[108], A. Mehta[91], B. Meirose[45], D. Melini[149], B.R. Mellado Garcia[33g], A.H. Melo[55], F. Meloni[48], E.D. Mendes Gouveia[129a], A.M. Mendes Jacques Da Costa[20], H.Y. Meng[154], L. Meng[90], S. Menke[109], M. Mentink[36], E. Meoni[43b,43a], C. Merlassino[125], L. Merola[71a,71b], C. Meroni[70a], G. Merz[105], O. Meshkov[37], J.K.R. Meshreki[140], J. Metcalfe[6], A.S. Mete[6], C. Meyer[67], J-P. Meyer[134], M. Michetti[18], R.P. Middleton[133], L. Mijović[52], G. Mikenberg[167], M. Mikestikova[130], M. Mikuž[92], H. Mildner[138], A. Milic[154], C.D. Milke[44], D.W. Miller[39], L.S. Miller[34], A. Milov[167], D.A. Milstead[47a,47b], T. Min[14c], A.A. Minaenko[37], I.A. Minashvili[148b], L. Mince[59], A.I. Mincer[116], B. Mindur[84a], M. Mineev[38], Y. Minegishi[152], Y. Mino[86], L.M. Mir[13], M. Miralles Lopez[161], M. Mironova[125], T. Mitani[166], A. Mitra[165], V.A. Mitsou[161],

JHEP06(2023)080

O. Miu[154], P.S. Miyagawa[93], Y. Miyazaki[88], A. Mizukami[82], J.U. Mjörnmark[97], T. Mkrtchyan[63a], M. Mlynarikova[114], T. Moa[47a,47b], S. Mobius[55], K. Mochizuki[107], P. Moder[48], P. Mogg[108], A.F. Mohammed[14a,14d], S. Mohapatra[41], G. Mokgatitswane[33g], B. Mondal[140], S. Mondal[131], K. Mönig[48], E. Monnier[101], L. Monsonis Romero[161], J. Montejo Berlingen[36], M. Montella[118], F. Monticelli[89], N. Morange[66], A.L. Moreira De Carvalho[129a], M. Moreno Llácer[161], C. Moreno Martinez[13], P. Morettini[57b], S. Morgenstern[165], M. Morii[61], M. Morinaga[152], V. Morisbak[124], A.K. Morley[36], F. Morodei[74a,74b], L. Morvaj[36], P. Moschovakos[36], B. Moser[36], M. Mosidze[148b], T. Moskalets[54], P. Moskvitina[112], J. Moss[31,n], E.J.W. Moyse[102], S. Muanza[101], J. Mueller[128], D. Muenstermann[90], R. Müller[19], G.A. Mullier[97], J.J. Mullin[127], D.P. Mungo[70a,70b], J.L. Munoz Martinez[13], D. Munoz Perez[161], F.J. Munoz Sanchez[100], M. Murin[100], W.J. Murray[165,133], A. Murrone[70a,70b], J.M. Muse[119], M. Muškinja[17a], C. Mwewa[29], A.G. Myagkov[37,a], A.J. Myers[8], A.A. Myers[128], G. Myers[67], M. Myska[131], B.P. Nachman[17a], O. Nackenhorst[49], A. Nag[50], K. Nagai[125], K. Nagano[82], J.L. Nagle[29,af], E. Nagy[101], A.M. Nairz[36], Y. Nakahama[82], K. Nakamura[82], H. Nanjo[123], R. Narayan[44], E.A. Narayanan[111], I. Naryshkin[37], M. Naseri[34], C. Nass[24], G. Navarro[22a], J. Navarro-Gonzalez[161], R. Nayak[150], P.Y. Nechaeva[37], F. Nechansky[48], T.J. Neep[20], A. Negri[72a,72b], M. Negrini[23b], C. Nellist[112], C. Nelson[103], K. Nelson[105], S. Nemecek[130], M. Nessi[36,g], M.S. Neubauer[160], F. Neuhaus[99], J. Neundorf[48], R. Newhouse[162], P.R. Newman[20], C.W. Ng[128], Y.S. Ng[18], Y.W.Y. Ng[158], B. Ngair[35e], H.D.N. Nguyen[107], R.B. Nickerson[125], R. Nicolaidou[134], J. Nielsen[135], M. Niemeyer[55], N. Nikiforou[36], V. Nikolaenko[37,a], I. Nikolic-Audit[126], K. Nikolopoulos[20], P. Nilsson[29], H.R. Nindhito[56], A. Nisati[74a], N. Nishu[2], R. Nisius[109], J-E. Nitschke[50], E.K. Nkadimeng[33g], S.J. Noacco Rosende[89], T. Nobe[152], D.L. Noel[32], Y. Noguchi[86], T. Nommensen[146], M.A. Nomura[29], M.B. Norfolk[138], R.R.B. Norisam[95], B.J. Norman[34], J. Novak[92], T. Novak[48], O. Novgorodova[50], L. Novotny[131], R. Novotny[111], L. Nozka[121], K. Ntekas[158], E. Nurse[95], F.G. Oakham[34,ac], J. Ocariz[126], A. Ochi[83], I. Ochoa[129a], S. Oda[88], S. Oerdek[159], A. Ogrodnik[84a], A. Oh[100], C.C. Ohm[143], H. Oide[153], R. Oishi[152], M.L. Ojeda[48], Y. Okazaki[86], M.W. O'Keefe[91], Y. Okumura[152], A. Olariu[27b], L.F. Oleiro Seabra[129a], S.A. Olivares Pino[136e], D. Oliveira Damazio[29], D. Oliveira Goncalves[81a], J.L. Oliver[158], M.J.R. Olsson[158], A. Olszewski[85], J. Olszowska[85,*], Ö.O. Öncel[54], D.C. O'Neil[141], A.P. O'Neill[19], A. Onofre[129a,129e], P.U.E. Onyisi[11], M.J. Oreglia[39], G.E. Orellana[89], D. Orestano[76a,76b], N. Orlando[13], R.S. Orr[154], V. O'Shea[59], R. Ospanov[62a], G. Otero y Garzon[30], H. Otono[88], P.S. Ott[63a], G.J. Ottino[17a], M. Ouchrif[35d], J. Ouellette[29,af], F. Ould-Saada[124], M. Owen[59], R.E. Owen[133], K.Y. Oyulmaz[21a], V.E. Ozcan[21a], N. Ozturk[8], S. Ozturk[21d], J. Pacalt[121], H.A. Pacey[32], K. Pachal[51], A. Pacheco Pages[13], C. Padilla Aranda[13], G. Padovano[74a,74b], S. Pagan Griso[17a], G. Palacino[67], A. Palazzo[69a,69b], S. Palazzo[52], S. Palestini[36], M. Palka[84b], J. Pan[170], T. Pan[64a], D.K. Panchal[11], C.E. Pandini[113], J.G. Panduro Vazquez[94], P. Pani[48], G. Panizzo[68a,68c], L. Paolozzi[56], C. Papadatos[107], S. Parajuli[44], A. Paramonov[6], C. Paraskevopoulos[10], D. Paredes Hernandez[64b], T.H. Park[154], M.A. Parker[32], F. Parodi[57b,57a], E.W. Parrish[114], V.A. Parrish[52], J.A. Parsons[41], U. Parzefall[54], B. Pascual Dias[107], L. Pascual Dominguez[150], V.R. Pascuzzi[17a], F. Pasquali[113], E. Pasqualucci[74a], S. Passaggio[57b], F. Pastore[94], P. Pasuwan[47a,47b], J.R. Pater[100], J. Patton[91], T. Pauly[36], J. Pearkes[142], M. Pedersen[124], R. Pedro[129a], S.V. Peleganchuk[37], O. Penc[130], C. Peng[64b], H. Peng[62a], M. Penzin[37], B.S. Peralva[81a,81d], A.P. Pereira Peixoto[60], L. Pereira Sanchez[47a,47b], D.V. Perepelitsa[29,af], E. Perez Codina[155a], M. Perganti[10], L. Perini[70a,70b,*], H. Pernegger[36], S. Perrella[36], A. Perrevoort[112], O. Perrin[40], K. Peters[48], R.F.Y. Peters[100], B.A. Petersen[36], T.C. Petersen[42], E. Petit[101], V. Petousis[131], C. Petridou[151], A. Petrukhin[140], M. Pettee[17a], N.E. Pettersson[36], A. Petukhov[37], K. Petukhova[132], A. Peyaud[134], R. Pezoa[136f], L. Pezzotti[36], G. Pezzullo[170], T. Pham[104], P.W. Phillips[133], M.W. Phipps[160], G. Piacquadio[144], E. Pianori[17a], F. Piazza[70a,70b], R. Piegaia[30], D. Pietreanu[27b], A.D. Pilkington[100], M. Pinamonti[68a,68c], J.L. Pinfold[2], B.C. Pinheiro Pereira[129a], C. Pitman Donaldson[95], D.A. Pizzi[34], L. Pizzimento[75a,75b], A. Pizzini[113], M.-A. Pleier[29], V. Plesanovs[54], V. Pleskot[132], E. Plotnikova[38], G. Poddar[4], R. Poettgen[97], R. Poggi[56], L. Poggioli[126], I. Pogrebnyak[106], D. Pohl[24], I. Pokharel[55], S. Polacek[132], G. Polesello[72a], A. Poley[141,155a], R. Polifka[131], A. Polini[23b], C.S. Pollard[125], Z.B. Pollock[118], V. Polychronakos[29], D. Ponomarenko[37], L. Pontecorvo[36], S. Popa[27a], G.A. Popeneciu[27d], D.M. Portillo Quintero[155a], S. Pospisil[131], P. Postolache[27c], K. Potamianos[125], I.N. Potrap[38], C.J. Potter[32], H. Potti[1], T. Poulsen[48], J. Poveda[161], G. Pownall[48], M.E. Pozo Astigarraga[36], A. Prades Ibanez[161], M.M. Prapa[46], D. Price[100], M. Primavera[69a], M.A. Principe Martin[98], M.L. Proffitt[137], N. Proklova[37], K. Prokofiev[64c], G. Proto[75a,75b], S. Protopopescu[29], J. Proudfoot[6], M. Przybycien[84a], J.E. Puddefoot[138], D. Pudzha[37], P. Puzo[66], D. Pyatiizbyantseva[37], J. Qian[105], Y. Qin[100], T. Qiu[93], A. Quadt[55], M. Queitsch-Maitland[24], G. Rabanal Bolanos[61], D. Rafanoharana[54], F. Ragusa[70a,70b], J.L. Rainbolt[39], J.A. Raine[56], S. Rajagopalan[29], E. Ramakoti[37], K. Ran[14a,14d], V. Raskina[126], D.F. Rassloff[63a], S. Rave[99], B. Ravina[59], I. Ravinovich[167], M. Raymond[36], A.L. Read[124], N.P. Readioff[138], D.M. Rebuzzi[72a,72b], G. Redlinger[29], K. Reeves[45], J.A. Reidelsturz[169], D. Reikher[150], A. Reiss[99], A. Rej[140], C. Rembser[36], A. Renardi[48], M. Renda[27b], M.B. Rendel[109], A.G. Rennie[59], S. Resconi[70a], M. Ressegotti[57b,57a], E.D. Resseguie[17a], S. Rettie[95], B. Reynolds[118], E. Reynolds[17a], M. Rezaei Estabragh[169], O.L. Rezanova[37], P. Reznicek[132], E. Ricci[77a,77b], R. Richter[109], S. Richter[47a,47b], E. Richter-Was[84b], M. Ridel[126], P. Rieck[116], P. Riedler[36], M. Rijssenbeek[144], A. Rimoldi[72a,72b], M. Rimoldi[48], L. Rinaldi[23b,23a], T.T. Rinn[29], M.P. Rinnagel[108], G. Ripellino[143], I. Riu[13], P. Rivadeneira[48], J.C. Rivera Vergara[163], F. Rizatdinova[120], E. Rizvi[93], C. Rizzi[56], B.A. Roberts[165], B.R. Roberts[17a], S.H. Robertson[103,v], M. Robin[48], D. Robinson[32], C.M. Robles Gajardo[136f], M. Robles Manzano[99], A. Robson[59], A. Rocchi[75a,75b], C. Roda[73a,73b], S. Rodriguez Bosca[63a], Y. Rodriguez Garcia[22a], A. Rodriguez Rodriguez[54], A.M. Rodríguez Vera[155b], S. Roe[36], J.T. Roemer[158], A.R. Roepe-Gier[119], J. Roggel[169], O. Røhne[124], R.A. Rojas[163], B. Roland[54], C.P.A. Roland[67], J. Roloff[29], A. Romaniouk[37], E. Romano[72a,72b], M. Romano[23b], A.C. Romero Hernandez[160], N. Rompotis[91], L. Roos[126], S. Rosati[74a], B.J. Rosser[39], E. Rossi[4], E. Rossi[71a,71b], L.P. Rossi[57b], L. Rossini[48], R. Rosten[118], M. Rotaru[27b], B. Rottler[54], D. Rousseau[66], D. Rousso[32], G. Rovelli[72a,72b], A. Roy[160], A. Rozanov[101], Y. Rozen[149], X. Ruan[33g], A. Rubio Jimenez[161], A.J. Ruby[91], T.A. Ruggeri[1], F. Rühr[54], A. Ruiz-Martinez[161], A. Rummler[36], Z. Rurikova[54], N.A. Rusakovich[38], H.L. Russell[163], J.P. Rutherfoord[7], E.M. Rüttinger[138], K. Rybacki[90], M. Rybar[132], E.B. Rye[124], A. Ryzhov[37], J.A. Sabater Iglesias[56], P. Sabatini[161], L. Sabetta[74a,74b], H.F-W. Sadrozinski[135], F. Safai Tehrani[74a], B. Safarzadeh Samani[145], M. Safdari[142], S. Saha[103], M. Sahinsoy[109], M. Saimpert[134], M. Saito[152], T. Saito[152], D. Salamani[36], G. Salamanna[76a,76b], A. Salnikov[142], J. Salt[161], A. Salvador Salas[13], D. Salvatore[43b,43a], F. Salvatore[145], A. Salzburger[36], D. Sammel[54], D. Sampsonidis[151], D. Sampsonidou[62d,62c], J. Sánchez[161], A. Sanchez Pineda[4], V. Sanchez Sebastian[161], H. Sandaker[124], C.O. Sander[48], J.A. Sandesara[102], M. Sandhoff[169], C. Sandoval[22b], D.P.C. Sankey[133], A. Sansoni[53], L. Santi[74a,74b], C. Santoni[40], H. Santos[129a,129b], S.N. Santpur[17a], A. Santra[167], K.A. Saoucha[138], J.G. Saraiva[129a,129d], J. Sardain[101], O. Sasaki[82], K. Sato[156], C. Sauer[63b], F. Sauerburger[54], E. Sauvan[4], P. Savard[154,ac], R. Sawada[152], C. Sawyer[133], L. Sawyer[96], I. Sayago Galvan[161], C. Sbarra[23b], A. Sbrizzi[23b,23a], T. Scanlon[95], J. Schaarschmidt[137], P. Schacht[109], D. Schaefer[39], U. Schäfer[99], A.C. Schaffer[66], D. Schaile[108], R.D. Schamberger[144], E. Schanet[108], C. Scharf[18], V.A. Schegelsky[37], D. Scheirich[132], F. Schenck[18], M. Schernau[158], C. Scheulen[55], C. Schiavi[57b,57a], Z.M. Schillaci[26], E.J. Schioppa[69a,69b], M. Schioppa[43b,43a], B. Schlag[99], K.E. Schleicher[54], S. Schlenker[36], K. Schmieden[99], C. Schmitt[99], S. Schmitt[48], L. Schoeffel[134], A. Schoening[63b], P.G. Scholer[54], E. Schopf[125], M. Schott[99], J. Schovancova[36], S. Schramm[56], F. Schroeder[169], H-C. Schultz-Coulon[63a], M. Schumacher[54], B.A. Schumm[135], Ph. Schune[134], A. Schwartzman[142], T.A. Schwarz[105], Ph. Schwemling[134], R. Schwienhorst[106], A. Sciandra[135], G. Sciolla[26], F. Scuri[73a], F. Scutti[104], C.D. Sebastiani[91], K. Sedlaczek[49], P. Seema[18], S.C. Seidel[111], A. Seiden[135], B.D. Seidlitz[41], T. Seiss[39], C. Seitz[48], J.M. Seixas[81b], G. Sekhniaidze[71a], S.J. Sekula[44], L. Selem[4], N. Semprini-Cesari[23b,23a], S. Sen[51], D. Sengupta[56], V. Senthilkumar[161], L. Serin[66], L. Serkin[68a,68b], M. Sessa[76a,76b], H. Severini[119], S. Sevova[142], F. Sforza[57b,57a], A. Sfyrla[56], E. Shabalina[55], R. Shaheen[143], J.D. Shahinian[127], N.W. Shaikh[47a,47b], D. Shaked Renous[167], L.Y. Shan[14a], M. Shapiro[17a], A. Sharma[36], A.S. Sharma[162], P. Sharma[79], S. Sharma[48], P.B. Shatalov[37], K. Shaw[145], S.M. Shaw[100], Q. Shen[62c], P. Sherwood[95], L. Shi[95], C.O. Shimmin[170], Y. Shimogama[166], J.D. Shinner[94], I.P.J. Shipsey[125], S. Shirabe[60], M. Shiyakova[38], J. Shlomi[167], M.J. Shochet[39], J. Shojaii[104], D.R. Shope[143], S. Shrestha[118], E.M. Shrif[33g], M.J. Shroff[163], P. Sicho[130], A.M. Sickles[160], E. Sideras Haddad[33g], O. Sidiropoulou[36], A. Sidoti[23b], F. Siegert[50], Dj. Sijacki[15], R. Sikora[84a], F. Sili[89], J.M. Silva[20], M.V. Silva Oliveira[36], S.B. Silverstein[47a], S. Simion[66], R. Simoniello[36], E.L. Simpson[59], N.D. Simpson[97], S. Simsek[21d], S. Sindhu[55], P. Sinervo[154], V. Sinetckii[37], S. Singh[141], S. Singh[154], S. Sinha[48], S. Sinha[33g], M. Sioli[23b,23a], I. Siral[122], S.Yu. Sivoklokov[37,*], J. Sjölin[47a,47b], A. Skaf[55], E. Skorda[97], P. Skubic[119], M. Slawinska[85], V. Smakhtin[167], B.H. Smart[133], J. Smiesko[132], S.Yu. Smirnov[37], Y. Smirnov[37], L.N. Smirnova[37,a],

O. Smirnova[97], E.A. Smith[39], H.A. Smith[125], J.L. Smith[91], R. Smith[142], M. Smizanska[90], K. Smolek[131], A. Smykiewicz[85], A.A. Snesarev[37], H.L. Snoek[113], S. Snyder[29], R. Sobie[163,v], A. Soffer[150], C.A. Solans Sanchez[36], E.Yu. Soldatov[37], U. Soldevila[161], A.A. Solodkov[37], S. Solomon[54], A. Soloshenko[38], K. Solovieva[54], O.V. Solovyanov[37], V. Solovyev[37], P. Sommer[36], A. Sonay[13], W.Y. Song[155b], A. Sopczak[131], A.L. Sopio[95], F. Sopkova[28b], V. Sothilingam[63a], S. Sottocornola[72a,72b], R. Soualah[115c], Z. Soumaimi[35e], D. South[48], S. Spagnolo[69a,69b], M. Spalla[109], F. Spanò[94], D. Sperlich[54], G. Spigo[36], M. Spina[145], S. Spinali[90], D.P. Spiteri[59], M. Spousta[132], E.J. Staats[34], A. Stabile[70a,70b], R. Stamen[63a], M. Stamenkovic[113], A. Stampekis[20], M. Standke[24], E. Stanecka[85], B. Stanislaus[17a], M.M. Stanitzki[48], M. Stankaityte[125], B. Stapf[48], E.A. Starchenko[37], G.H. Stark[135], J. Stark[101], D.M. Starko[155b], P. Staroba[130], P. Starovoitov[63a], S. Stärz[103], R. Staszewski[85], G. Stavropoulos[46], J. Steentoft[159], P. Steinberg[29], A.L. Steinhebel[122], B. Stelzer[141,155a], H.J. Stelzer[128], O. Stelzer-Chilton[155a], H. Stenzel[58], T.J. Stevenson[145], G.A. Stewart[36], M.C. Stockton[36], G. Stoicea[27b], M. Stolarski[129a], S. Stonjek[109], A. Straessner[50], J. Strandberg[143], S. Strandberg[47a,47b], M. Strauss[119], T. Strebler[101], P. Strizenec[28b], R. Ströhmer[164], D.M. Strom[122], L.R. Strom[48], R. Stroynowski[44], A. Strubig[47a,47b], S.A. Stucci[29], B. Stugu[16], J. Stupak[119], N.A. Styles[48], D. Su[142], S. Su[62a], W. Su[62d,137,62c], X. Su[62a,66], K. Sugizaki[152], V.V. Sulin[37], M.J. Sullivan[91], D.M.S. Sultan[77a,77b], L. Sultanaliyeva[37], S. Sultansoy[3b], T. Sumida[86], S. Sun[105], S. Sun[168], O. Sunneborn Gudnadottir[159], M.R. Sutton[145], M. Svatos[130], M. Swiatlowski[155a], T. Swirski[164], I. Sykora[28a], M. Sykora[132], T. Sykora[132], D. Ta[99], K. Tackmann[48,u], A. Taffard[158], R. Tafirout[155a], J.S. Tafoya Vargas[66], R.H.M. Taibah[126], R. Takashima[87], K. Takeda[83], E.P. Takeva[52], Y. Takubo[82], M. Talby[101], A.A. Talyshev[37], K.C. Tam[64b], N.M. Tamir[150], A. Tanaka[152], J. Tanaka[152], R. Tanaka[66], M. Tanasini[57b,57a], J. Tang[62c], Z. Tao[162], S. Tapia Araya[80], S. Tapprogge[99], A. Tarek Abouelfadl Mohamed[106], S. Tarem[149], K. Tariq[62b], G. Tarna[27b], G.F. Tartarelli[70a], P. Tas[132], M. Tasevsky[130], E. Tassi[43b,43a], A.C. Tate[160], G. Tateno[152], Y. Tayalati[35e], G.N. Taylor[104], W. Taylor[155b], H. Teagle[91], A.S. Tee[168], R. Teixeira De Lima[142], P. Teixeira-Dias[94], J.J. Teoh[154], K. Terashi[152], J. Terron[98], S. Terzo[13], M. Testa[53], R.J. Teuscher[154,v], N. Themistokleous[52], T. Theveneaux-Pelzer[18], O. Thielmann[169], D.W. Thomas[94], J.P. Thomas[20], E.A. Thompson[48], P.D. Thompson[20], E. Thomson[127], E.J. Thorpe[93], Y. Tian[55], V. Tikhomirov[37,a], Yu.A. Tikhonov[37], S. Timoshenko[37], E.X.L. Ting[1], P. Tipton[170], S. Tisserant[101], S.H. Tlou[33g], A. Tnourji[40], K. Todome[23b,23a], S. Todorova-Nova[132], S. Todt[50], M. Togawa[82], J. Tojo[88], S. Tokár[28a], K. Tokushuku[82], R. Tombs[32], M. Tomoto[82,110], L. Tompkins[142], P. Tornambe[102], E. Torrence[122], H. Torres[50], E. Torró Pastor[161], M. Toscani[30], C. Tosciri[39], D.R. Tovey[138], A. Traeet[16], I.S. Trandafir[27b], T. Trefzger[164], A. Tricoli[29], I.M. Trigger[155a], S. Trincaz-Duvoid[126], D.A. Trischuk[162], B. Trocmé[60], A. Trofymov[66], C. Troncon[70a], L. Truong[33c], M. Trzebinski[85], A. Trzupek[85], F. Tsai[144], M. Tsai[105], A. Tsiamis[151], P.V. Tsiareshka[37], S. Tsigaridas[155a], A. Tsirigotis[151,s], V. Tsiskaridze[144], E.G. Tskhadadze[148a], M. Tsopoulou[151], Y. Tsujikawa[86], I.I. Tsukerman[37], V. Tsulaia[17a],

JHEP06(2023)080

S. Tsuno[82], O. Tsur[149], D. Tsybychev[144], Y. Tu[64b], A. Tudorache[27b], V. Tudorache[27b], A.N. Tuna[36], S. Turchikhin[38], I. Turk Cakir[3a], R. Turra[70a], P.M. Tuts[41], S. Tzamarias[151], P. Tzanis[10], E. Tzovara[99], K. Uchida[152], F. Ukegawa[156], P.A. Ulloa Poblete[136c], G. Unal[36], M. Unal[11], A. Undrus[29], G. Unel[158], K. Uno[152], J. Urban[28b], P. Urquijo[104], G. Usai[8], R. Ushioda[153], M. Usman[107], Z. Uysal[21b], V. Vacek[131], B. Vachon[103], K.O.H. Vadla[124], T. Vafeiadis[36], C. Valderanis[108], E. Valdes Santurio[47a,47b], M. Valente[155a], S. Valentinetti[23b,23a], A. Valero[161], A. Vallier[101], J.A. Valls Ferrer[161], T.R. Van Daalen[137], P. Van Gemmeren[6], S. Van Stroud[95], I. Van Vulpen[113], M. Vanadia[75a,75b], W. Vandelli[36], M. Vandenbroucke[134], E.R. Vandewall[120], D. Vannicola[150], L. Vannoli[57b,57a], R. Vari[74a], E.W. Varnes[7], C. Varni[17a], T. Varol[147], D. Varouchas[66], L. Varriale[161], K.E. Varvell[146], M.E. Vasile[27b], L. Vaslin[40], G.A. Vasquez[163], F. Vazeille[40], T. Vazquez Schroeder[36], J. Veatch[31], V. Vecchio[100], M.J. Veen[113], I. Veliscek[125], L.M. Veloce[154], F. Veloso[129a,129c], S. Veneziano[74a], A. Ventura[69a,69b], A. Verbytskyi[109], M. Verducci[73a,73b], C. Vergis[24], M. Verissimo De Araujo[81b], W. Verkerke[113], J.C. Vermeulen[113], C. Vernieri[142], P.J. Verschuuren[94], M. Vessella[102], M.L. Vesterbacka[116], M.C. Vetterli[141,ac], A. Vgenopoulos[151], N. Viaux Maira[136f], T. Vickey[138], O.E. Vickey Boeriu[138], G.H.A. Viehhauser[125], L. Vigani[63b], M. Villa[23b,23a], M. Villaplana Perez[161], E.M. Villhauer[52], E. Vilucchi[53], M.G. Vincter[34], G.S. Virdee[20], A. Vishwakarma[52], C. Vittori[23b,23a], I. Vivarelli[145], V. Vladimirov[165], E. Voevodina[109], F. Vogel[108], P. Vokac[131], J. Von Ahnen[48], E. Von Toerne[24], B. Vormwald[36], V. Vorobel[132], K. Vorobev[37], M. Vos[161], J.H. Vossebeld[91], M. Vozak[113], L. Vozdecky[93], N. Vranjes[15], M. Vranjes Milosavljevic[15], M. Vreeswijk[113], R. Vuillermet[36], O. Vujinovic[99], I. Vukotic[39], S. Wada[156], C. Wagner[102], W. Wagner[169], S. Wahdan[169], H. Wahlberg[89], R. Wakasa[156], M. Wakida[110], V.M. Walbrecht[109], J. Walder[133], R. Walker[108], W. Walkowiak[140], A.M. Wang[61], A.Z. Wang[168], C. Wang[62a], C. Wang[62c], H. Wang[17a], J. Wang[64a], P. Wang[44], R.-J. Wang[99], R. Wang[61], R. Wang[6], S.M. Wang[147], S. Wang[62b], T. Wang[62a], W.T. Wang[79], W.X. Wang[62a], X. Wang[14c], X. Wang[160], X. Wang[62c], Y. Wang[62d], Y. Wang[14c], Z. Wang[105], Z. Wang[62d,51,62c], Z. Wang[105], A. Warburton[103], R.J. Ward[20], N. Warrack[59], A.T. Watson[20], M.F. Watson[20], G. Watts[137], B.M. Waugh[95], A.F. Webb[11], C. Weber[29], M.S. Weber[19], S.A. Weber[34], S.M. Weber[63a], C. Wei[62a], Y. Wei[125], A.R. Weidberg[125], J. Weingarten[49], M. Weirich[99], C. Weiser[54], C.J. Wells[48], T. Wenaus[29], B. Wendland[49], T. Wengler[36], N.S. Wenke[109], N. Wermes[24], M. Wessels[63a], K. Whalen[122], A.M. Wharton[90], A.S. White[61], A. White[8], M.J. White[1], D. Whiteson[158], L. Wickremasinghe[123], W. Wiedenmann[168], C. Wiel[50], M. Wielers[133], N. Wieseotte[99], C. Wiglesworth[42], L.A.M. Wiik-Fuchs[54], D.J. Wilbern[119], H.G. Wilkens[36], D.M. Williams[41], H.H. Williams[127], S. Williams[32], S. Willocq[102], P.J. Windischhofer[125], F. Winklmeier[122], B.T. Winter[54], M. Wittgen[142], M. Wobisch[96], A. Wolf[99], R. Wölker[125], J. Wollrath[158], M.W. Wolter[85], H. Wolters[129a,129c], V.W.S. Wong[162], A.F. Wongel[48], S.D. Worm[48], B.K. Wosiek[85], K.W. Woźniak[85], K. Wraight[59], J. Wu[14a,14d], M. Wu[64a], S.L. Wu[168], X. Wu[56], Y. Wu[62a], Z. Wu[134,62a], J. Wuerzinger[125], T.R. Wyatt[100], B.M. Wynne[52],

JHEP06(2023)080

S. Xella[42], L. Xia[14c], M. Xia[14b], J. Xiang[64c], X. Xiao[105], M. Xie[62a], X. Xie[62a], J. Xiong[17a], I. Xiotidis[145], D. Xu[14a], H. Xu[62a], H. Xu[62a], L. Xu[62a], R. Xu[127], T. Xu[105], W. Xu[105], Y. Xu[14b], Z. Xu[62b], Z. Xu[142], B. Yabsley[146], S. Yacoob[33a], N. Yamaguchi[88], Y. Yamaguchi[153], H. Yamauchi[156], T. Yamazaki[17a], Y. Yamazaki[83], J. Yan[62c], S. Yan[125], Z. Yan[25], H.J. Yang[62c,62d], H.T. Yang[17a], S. Yang[62a], T. Yang[64c], X. Yang[62a], X. Yang[14a], Y. Yang[44], Z. Yang[62a,105], W-M. Yao[17a], Y.C. Yap[48], H. Ye[14c], J. Ye[44], S. Ye[29], X. Ye[62a], I. Yeletskikh[38], M.R. Yexley[90], P. Yin[41], K. Yorita[166], C.J.S. Young[54], C. Young[142], M. Yuan[105], R. Yuan[62b,j], L. Yue[95], X. Yue[63a], M. Zaazoua[35e], B. Zabinski[85], E. Zaid[52], T. Zakareishvili[148b], N. Zakharchuk[34], S. Zambito[56], J. Zang[152], D. Zanzi[54], O. Zaplatilek[131], S.V. Zeißner[49], C. Zeitnitz[169], J.C. Zeng[160], D.T. Zenger Jr[26], O. Zenin[37], T. Ženiš[28a], S. Zenz[93], S. Zerradi[35a], D. Zerwas[66], B. Zhang[14c], D.F. Zhang[138], G. Zhang[14b], J. Zhang[6], K. Zhang[14a,14d], L. Zhang[14c], R. Zhang[168], S. Zhang[105], T. Zhang[152], X. Zhang[62c], X. Zhang[62b], Z. Zhang[66], H. Zhao[137], P. Zhao[51], T. Zhao[62b], Y. Zhao[135], Z. Zhao[62a], A. Zhemchugov[38], Z. Zheng[142], D. Zhong[160], B. Zhou[105], C. Zhou[168], H. Zhou[7], N. Zhou[62c], Y. Zhou[7], C.G. Zhu[62b], C. Zhu[14a,14d], H.L. Zhu[62a], H. Zhu[14a], J. Zhu[105], Y. Zhu[62a], X. Zhuang[14a], K. Zhukov[37], V. Zhulanov[37], N.I. Zimine[38], J. Zinsser[63b], M. Ziolkowski[140], L. Živković[15], A. Zoccoli[23b,23a], K. Zoch[56], T.G. Zorbas[138], O. Zormpa[46], W. Zou[41], L. Zwalinski[36]

[1] *Department of Physics, University of Adelaide, Adelaide; Australia*

[2] *Department of Physics, University of Alberta, Edmonton AB; Canada*

[3] [(a)] *Department of Physics, Ankara University, Ankara;* [(b)] *Division of Physics, TOBB University of Economics and Technology, Ankara; Türkiye*

[4] *LAPP, Univ. Savoie Mont Blanc, CNRS/IN2P3, Annecy; France*

[5] *APC, Université Paris Cité, CNRS/IN2P3, Paris; France*

[6] *High Energy Physics Division, Argonne National Laboratory, Argonne IL; United States of America*

[7] *Department of Physics, University of Arizona, Tucson AZ; United States of America*

[8] *Department of Physics, University of Texas at Arlington, Arlington TX; United States of America*

[9] *Physics Department, National and Kapodistrian University of Athens, Athens; Greece*

[10] *Physics Department, National Technical University of Athens, Zografou; Greece*

[11] *Department of Physics, University of Texas at Austin, Austin TX; United States of America*

[12] *Institute of Physics, Azerbaijan Academy of Sciences, Baku; Azerbaijan*

[13] *Institut de Física d'Altes Energies (IFAE), Barcelona Institute of Science and Technology, Barcelona; Spain*

[14] [(a)] *Institute of High Energy Physics, Chinese Academy of Sciences, Beijing;* [(b)] *Physics Department, Tsinghua University, Beijing;* [(c)] *Department of Physics, Nanjing University, Nanjing;* [(d)] *University of Chinese Academy of Science (UCAS), Beijing; China*

[15] *Institute of Physics, University of Belgrade, Belgrade; Serbia*

[16] *Department for Physics and Technology, University of Bergen, Bergen; Norway*

[17] [(a)] *Physics Division, Lawrence Berkeley National Laboratory, Berkeley CA;* [(b)] *University of California, Berkeley CA; United States of America*

[18] *Institut für Physik, Humboldt Universität zu Berlin, Berlin; Germany*

[19] *Albert Einstein Center for Fundamental Physics and Laboratory for High Energy Physics, University of Bern, Bern; Switzerland*

[20] *School of Physics and Astronomy, University of Birmingham, Birmingham; United Kingdom*

[21] [(a)] *Department of Physics, Bogazici University, Istanbul;* [(b)] *Department of Physics Engineering, Gaziantep University, Gaziantep;* [(c)] *Department of Physics, Istanbul University, Istanbul;* [(d)] *Istinye University, Sariyer, Istanbul; Türkiye*

JHEP06(2023)080

[22] [(a)] *Facultad de Ciencias y Centro de Investigaciónes, Universidad Antonio Nariño, Bogotá;* [(b)] *Departamento de Física, Universidad Nacional de Colombia, Bogotá; Colombia*
[23] [(a)] *Dipartimento di Fisica e Astronomia A. Righi, Università di Bologna, Bologna;* [(b)] *INFN Sezione di Bologna; Italy*
[24] *Physikalisches Institut, Universität Bonn, Bonn; Germany*
[25] *Department of Physics, Boston University, Boston MA; United States of America*
[26] *Department of Physics, Brandeis University, Waltham MA; United States of America*
[27] [(a)] *Transilvania University of Brasov, Brasov;* [(b)] *Horia Hulubei National Institute of Physics and Nuclear Engineering, Bucharest;* [(c)] *Department of Physics, Alexandru Ioan Cuza University of Iasi, Iasi;* [(d)] *National Institute for Research and Development of Isotopic and Molecular Technologies, Physics Department, Cluj-Napoca;* [(e)] *University Politehnica Bucharest, Bucharest;* [(f)] *West University in Timisoara, Timisoara; Romania*
[28] [(a)] *Faculty of Mathematics, Physics and Informatics, Comenius University, Bratislava;* [(b)] *Department of Subnuclear Physics, Institute of Experimental Physics of the Slovak Academy of Sciences, Kosice; Slovak Republic*
[29] *Physics Department, Brookhaven National Laboratory, Upton NY; United States of America*
[30] *Universidad de Buenos Aires, Facultad de Ciencias Exactas y Naturales, Departamento de Física, y CONICET, Instituto de Física de Buenos Aires (IFIBA), Buenos Aires; Argentina*
[31] *California State University, CA; United States of America*
[32] *Cavendish Laboratory, University of Cambridge, Cambridge; United Kingdom*
[33] [(a)] *Department of Physics, University of Cape Town, Cape Town;* [(b)] *iThemba Labs, Western Cape;* [(c)] *Department of Mechanical Engineering Science, University of Johannesburg, Johannesburg;* [(d)] *National Institute of Physics, University of the Philippines Diliman (Philippines);* [(e)] *University of South Africa, Department of Physics, Pretoria;* [(f)] *University of Zululand, KwaDlangezwa;* [(g)] *School of Physics, University of the Witwatersrand, Johannesburg; South Africa*
[34] *Department of Physics, Carleton University, Ottawa ON; Canada*
[35] [(a)] *Faculté des Sciences Ain Chock, Réseau Universitaire de Physique des Hautes Energies — Université Hassan II, Casablanca;* [(b)] *Faculté des Sciences, Université Ibn-Tofail, Kénitra;* [(c)] *Faculté des Sciences Semlalia, Université Cadi Ayyad, LPHEA-Marrakech;* [(d)] *LPMR, Faculté des Sciences, Université Mohamed Premier, Oujda;* [(e)] *Faculté des sciences, Université Mohammed V, Rabat;* [(f)] *Institute of Applied Physics, Mohammed VI Polytechnic University, Ben Guerir; Morocco*
[36] *CERN, Geneva; Switzerland*
[37] *Affiliated with an institute covered by a cooperation agreement with CERN*
[38] *Affiliated with an international laboratory covered by a cooperation agreement with CERN*
[39] *Enrico Fermi Institute, University of Chicago, Chicago IL; United States of America*
[40] *LPC, Université Clermont Auvergne, CNRS/IN2P3, Clermont-Ferrand; France*
[41] *Nevis Laboratory, Columbia University, Irvington NY; United States of America*
[42] *Niels Bohr Institute, University of Copenhagen, Copenhagen; Denmark*
[43] [(a)] *Dipartimento di Fisica, Università della Calabria, Rende;* [(b)] *INFN Gruppo Collegato di Cosenza, Laboratori Nazionali di Frascati; Italy*
[44] *Physics Department, Southern Methodist University, Dallas TX; United States of America*
[45] *Physics Department, University of Texas at Dallas, Richardson TX; United States of America*
[46] *National Centre for Scientific Research "Demokritos", Agia Paraskevi; Greece*
[47] [(a)] *Department of Physics, Stockholm University;* [(b)] *Oskar Klein Centre, Stockholm; Sweden*
[48] *Deutsches Elektronen-Synchrotron DESY, Hamburg and Zeuthen; Germany*
[49] *Fakultät Physik , Technische Universität Dortmund, Dortmund; Germany*
[50] *Institut für Kern- und Teilchenphysik, Technische Universität Dresden, Dresden; Germany*
[51] *Department of Physics, Duke University, Durham NC; United States of America*
[52] *SUPA — School of Physics and Astronomy, University of Edinburgh, Edinburgh; United Kingdom*
[53] *INFN e Laboratori Nazionali di Frascati, Frascati; Italy*
[54] *Physikalisches Institut, Albert-Ludwigs-Universität Freiburg, Freiburg; Germany*
[55] *II. Physikalisches Institut, Georg-August-Universität Göttingen, Göttingen; Germany*

JHEP06(2023)080

[56] *Département de Physique Nucléaire et Corpusculaire, Université de Genève, Genève; Switzerland*
[57] [(a)] *Dipartimento di Fisica, Università di Genova, Genova;* [(b)] *INFN Sezione di Genova; Italy*
[58] *II. Physikalisches Institut, Justus-Liebig-Universität Giessen, Giessen; Germany*
[59] *SUPA — School of Physics and Astronomy, University of Glasgow, Glasgow; United Kingdom*
[60] *LPSC, Université Grenoble Alpes, CNRS/IN2P3, Grenoble INP, Grenoble; France*
[61] *Laboratory for Particle Physics and Cosmology, Harvard University, Cambridge MA; United States of America*
[62] [(a)] *Department of Modern Physics and State Key Laboratory of Particle Detection and Electronics, University of Science and Technology of China, Hefei;* [(b)] *Institute of Frontier and Interdisciplinary Science and Key Laboratory of Particle Physics and Particle Irradiation (MOE), Shandong University, Qingdao;* [(c)] *School of Physics and Astronomy, Shanghai Jiao Tong University, Key Laboratory for Particle Astrophysics and Cosmology (MOE), SKLPPC, Shanghai;* [(d)] *Tsung-Dao Lee Institute, Shanghai; China*
[63] [(a)] *Kirchhoff-Institut für Physik, Ruprecht-Karls-Universität Heidelberg, Heidelberg;* [(b)] *Physikalisches Institut, Ruprecht-Karls-Universität Heidelberg, Heidelberg; Germany*
[64] [(a)] *Department of Physics, Chinese University of Hong Kong, Shatin, N.T., Hong Kong;* [(b)] *Department of Physics, University of Hong Kong, Hong Kong;* [(c)] *Department of Physics and Institute for Advanced Study, Hong Kong University of Science and Technology, Clear Water Bay, Kowloon, Hong Kong; China*
[65] *Department of Physics, National Tsing Hua University, Hsinchu; Taiwan*
[66] *IJCLab, Université Paris-Saclay, CNRS/IN2P3, 91405, Orsay; France*
[67] *Department of Physics, Indiana University, Bloomington IN; United States of America*
[68] [(a)] *INFN Gruppo Collegato di Udine, Sezione di Trieste, Udine;* [(b)] *ICTP, Trieste;* [(c)] *Dipartimento Politecnico di Ingegneria e Architettura, Università di Udine, Udine; Italy*
[69] [(a)] *INFN Sezione di Lecce;* [(b)] *Dipartimento di Matematica e Fisica, Università del Salento, Lecce; Italy*
[70] [(a)] *INFN Sezione di Milano;* [(b)] *Dipartimento di Fisica, Università di Milano, Milano; Italy*
[71] [(a)] *INFN Sezione di Napoli;* [(b)] *Dipartimento di Fisica, Università di Napoli, Napoli; Italy*
[72] [(a)] *INFN Sezione di Pavia;* [(b)] *Dipartimento di Fisica, Università di Pavia, Pavia; Italy*
[73] [(a)] *INFN Sezione di Pisa;* [(b)] *Dipartimento di Fisica E. Fermi, Università di Pisa, Pisa; Italy*
[74] [(a)] *INFN Sezione di Roma;* [(b)] *Dipartimento di Fisica, Sapienza Università di Roma, Roma; Italy*
[75] [(a)] *INFN Sezione di Roma Tor Vergata;* [(b)] *Dipartimento di Fisica, Università di Roma Tor Vergata, Roma; Italy*
[76] [(a)] *INFN Sezione di Roma Tre;* [(b)] *Dipartimento di Matematica e Fisica, Università Roma Tre, Roma; Italy*
[77] [(a)] *INFN-TIFPA;* [(b)] *Università degli Studi di Trento, Trento; Italy*
[78] *Universität Innsbruck, Department of Astro and Particle Physics, Innsbruck; Austria*
[79] *University of Iowa, Iowa City IA; United States of America*
[80] *Department of Physics and Astronomy, Iowa State University, Ames IA; United States of America*
[81] [(a)] *Departamento de Engenharia Elétrica, Universidade Federal de Juiz de Fora (UFJF), Juiz de Fora;* [(b)] *Universidade Federal do Rio De Janeiro COPPE/EE/IF, Rio de Janeiro;* [(c)] *Instituto de Física, Universidade de São Paulo, São Paulo;* [(d)] *Rio de Janeiro State University, Rio de Janeiro; Brazil*
[82] *KEK, High Energy Accelerator Research Organization, Tsukuba; Japan*
[83] *Graduate School of Science, Kobe University, Kobe; Japan*
[84] [(a)] *AGH University of Science and Technology, Faculty of Physics and Applied Computer Science, Krakow;* [(b)] *Marian Smoluchowski Institute of Physics, Jagiellonian University, Krakow; Poland*
[85] *Institute of Nuclear Physics Polish Academy of Sciences, Krakow; Poland*
[86] *Faculty of Science, Kyoto University, Kyoto; Japan*
[87] *Kyoto University of Education, Kyoto; Japan*
[88] *Research Center for Advanced Particle Physics and Department of Physics, Kyushu University, Fukuoka; Japan*
[89] *Instituto de Física La Plata, Universidad Nacional de La Plata and CONICET, La Plata; Argentina*
[90] *Physics Department, Lancaster University, Lancaster; United Kingdom*

JHEP06(2023)080

[91] *Oliver Lodge Laboratory, University of Liverpool, Liverpool; United Kingdom*
[92] *Department of Experimental Particle Physics, Jožef Stefan Institute and Department of Physics, University of Ljubljana, Ljubljana; Slovenia*
[93] *School of Physics and Astronomy, Queen Mary University of London, London; United Kingdom*
[94] *Department of Physics, Royal Holloway University of London, Egham; United Kingdom*
[95] *Department of Physics and Astronomy, University College London, London; United Kingdom*
[96] *Louisiana Tech University, Ruston LA; United States of America*
[97] *Fysiska institutionen, Lunds universitet, Lund; Sweden*
[98] *Departamento de Física Teorica C-15 and CIAFF, Universidad Autónoma de Madrid, Madrid; Spain*
[99] *Institut für Physik, Universität Mainz, Mainz; Germany*
[100] *School of Physics and Astronomy, University of Manchester, Manchester; United Kingdom*
[101] *CPPM, Aix-Marseille Université, CNRS/IN2P3, Marseille; France*
[102] *Department of Physics, University of Massachusetts, Amherst MA; United States of America*
[103] *Department of Physics, McGill University, Montreal QC; Canada*
[104] *School of Physics, University of Melbourne, Victoria; Australia*
[105] *Department of Physics, University of Michigan, Ann Arbor MI; United States of America*
[106] *Department of Physics and Astronomy, Michigan State University, East Lansing MI; United States of America*
[107] *Group of Particle Physics, University of Montreal, Montreal QC; Canada*
[108] *Fakultät für Physik, Ludwig-Maximilians-Universität München, München; Germany*
[109] *Max-Planck-Institut für Physik (Werner-Heisenberg-Institut), München; Germany*
[110] *Graduate School of Science and Kobayashi-Maskawa Institute, Nagoya University, Nagoya; Japan*
[111] *Department of Physics and Astronomy, University of New Mexico, Albuquerque NM; United States of America*
[112] *Institute for Mathematics, Astrophysics and Particle Physics, Radboud University/Nikhef, Nijmegen; Netherlands*
[113] *Nikhef National Institute for Subatomic Physics and University of Amsterdam, Amsterdam; Netherlands*
[114] *Department of Physics, Northern Illinois University, DeKalb IL; United States of America*
[115] [(a)] *New York University Abu Dhabi, Abu Dhabi;* [(b)] *United Arab Emirates University, Al Ain;* [(c)] *University of Sharjah, Sharjah; United Arab Emirates*
[116] *Department of Physics, New York University, New York NY; United States of America*
[117] *Ochanomizu University, Otsuka, Bunkyo-ku, Tokyo; Japan*
[118] *Ohio State University, Columbus OH; United States of America*
[119] *Homer L. Dodge Department of Physics and Astronomy, University of Oklahoma, Norman OK; United States of America*
[120] *Department of Physics, Oklahoma State University, Stillwater OK; United States of America*
[121] *Palacký University, Joint Laboratory of Optics, Olomouc; Czech Republic*
[122] *Institute for Fundamental Science, University of Oregon, Eugene, OR; United States of America*
[123] *Graduate School of Science, Osaka University, Osaka; Japan*
[124] *Department of Physics, University of Oslo, Oslo; Norway*
[125] *Department of Physics, Oxford University, Oxford; United Kingdom*
[126] *LPNHE, Sorbonne Université, Université Paris Cité, CNRS/IN2P3, Paris; France*
[127] *Department of Physics, University of Pennsylvania, Philadelphia PA; United States of America*
[128] *Department of Physics and Astronomy, University of Pittsburgh, Pittsburgh PA; United States of America*
[129] [(a)] *Laboratório de Instrumentação e Física Experimental de Partículas — LIP, Lisboa;* [(b)] *Departamento de Física, Faculdade de Ciências, Universidade de Lisboa, Lisboa;* [(c)] *Departamento de Física, Universidade de Coimbra, Coimbra;* [(d)] *Centro de Física Nuclear da Universidade de Lisboa, Lisboa;* [(e)] *Departamento de Física, Universidade do Minho, Braga;* [(f)] *Departamento de Física Teórica y del Cosmos, Universidad de Granada, Granada (Spain);* [(g)] *Departamento de Física, Instituto Superior Técnico, Universidade de Lisboa, Lisboa; Portugal*

[130] *Institute of Physics of the Czech Academy of Sciences, Prague; Czech Republic*
[131] *Czech Technical University in Prague, Prague; Czech Republic*
[132] *Charles University, Faculty of Mathematics and Physics, Prague; Czech Republic*
[133] *Particle Physics Department, Rutherford Appleton Laboratory, Didcot; United Kingdom*
[134] *IRFU, CEA, Université Paris-Saclay, Gif-sur-Yvette; France*
[135] *Santa Cruz Institute for Particle Physics, University of California Santa Cruz, Santa Cruz CA; United States of America*
[136] [(a)] *Departamento de Física, Pontificia Universidad Católica de Chile, Santiago;* [(b)] *Millennium Institute for Subatomic physics at high energy frontier (SAPHIR), Santiago;* [(c)] *Instituto de Investigación Multidisciplinario en Ciencia y Tecnología, y Departamento de Física, Universidad de La Serena;* [(d)] *Universidad Andres Bello, Department of Physics, Santiago;* [(e)] *Instituto de Alta Investigación, Universidad de Tarapacá, Arica;* [(f)] *Departamento de Física, Universidad Técnica Federico Santa María, Valparaíso; Chile*
[137] *Department of Physics, University of Washington, Seattle WA; United States of America*
[138] *Department of Physics and Astronomy, University of Sheffield, Sheffield; United Kingdom*
[139] *Department of Physics, Shinshu University, Nagano; Japan*
[140] *Department Physik, Universität Siegen, Siegen; Germany*
[141] *Department of Physics, Simon Fraser University, Burnaby BC; Canada*
[142] *SLAC National Accelerator Laboratory, Stanford CA; United States of America*
[143] *Department of Physics, Royal Institute of Technology, Stockholm; Sweden*
[144] *Departments of Physics and Astronomy, Stony Brook University, Stony Brook NY; United States of America*
[145] *Department of Physics and Astronomy, University of Sussex, Brighton; United Kingdom*
[146] *School of Physics, University of Sydney, Sydney; Australia*
[147] *Institute of Physics, Academia Sinica, Taipei; Taiwan*
[148] [(a)] *E. Andronikashvili Institute of Physics, Iv. Javakhishvili Tbilisi State University, Tbilisi;* [(b)] *High Energy Physics Institute, Tbilisi State University, Tbilisi;* [(c)] *University of Georgia, Tbilisi; Georgia*
[149] *Department of Physics, Technion, Israel Institute of Technology, Haifa; Israel*
[150] *Raymond and Beverly Sackler School of Physics and Astronomy, Tel Aviv University, Tel Aviv; Israel*
[151] *Department of Physics, Aristotle University of Thessaloniki, Thessaloniki; Greece*
[152] *International Center for Elementary Particle Physics and Department of Physics, University of Tokyo, Tokyo; Japan*
[153] *Department of Physics, Tokyo Institute of Technology, Tokyo; Japan*
[154] *Department of Physics, University of Toronto, Toronto ON; Canada*
[155] [(a)] *TRIUMF, Vancouver BC;* [(b)] *Department of Physics and Astronomy, York University, Toronto ON; Canada*
[156] *Division of Physics and Tomonaga Center for the History of the Universe, Faculty of Pure and Applied Sciences, University of Tsukuba, Tsukuba; Japan*
[157] *Department of Physics and Astronomy, Tufts University, Medford MA; United States of America*
[158] *Department of Physics and Astronomy, University of California Irvine, Irvine CA; United States of America*
[159] *Department of Physics and Astronomy, University of Uppsala, Uppsala; Sweden*
[160] *Department of Physics, University of Illinois, Urbana IL; United States of America*
[161] *Instituto de Física Corpuscular (IFIC), Centro Mixto Universidad de Valencia — CSIC, Valencia; Spain*
[162] *Department of Physics, University of British Columbia, Vancouver BC; Canada*
[163] *Department of Physics and Astronomy, University of Victoria, Victoria BC; Canada*
[164] *Fakultät für Physik und Astronomie, Julius-Maximilians-Universität Würzburg, Würzburg; Germany*
[165] *Department of Physics, University of Warwick, Coventry; United Kingdom*
[166] *Waseda University, Tokyo; Japan*
[167] *Department of Particle Physics and Astrophysics, Weizmann Institute of Science, Rehovot; Israel*
[168] *Department of Physics, University of Wisconsin, Madison WI; United States of America*

JHEP06(2023)080

[169] Fakultät für Mathematik und Naturwissenschaften, Fachgruppe Physik, Bergische Universität Wuppertal, Wuppertal; Germany
[170] Department of Physics, Yale University, New Haven CT; United States of America

[a] Also Affiliated with an institute covered by a cooperation agreement with CERN
[b] Also at Borough of Manhattan Community College, City University of New York, New York NY; United States of America
[c] Also at Bruno Kessler Foundation, Trento; Italy
[d] Also at Center for High Energy Physics, Peking University; China
[e] Also at Centro Studi e Ricerche Enrico Fermi; Italy
[f] Also at CERN, Geneva; Switzerland
[g] Also at Département de Physique Nucléaire et Corpusculaire, Université de Genève, Genève; Switzerland
[h] Also at Departament de Fisica de la Universitat Autonoma de Barcelona, Barcelona; Spain
[i] Also at Department of Financial and Management Engineering, University of the Aegean, Chios; Greece
[j] Also at Department of Physics and Astronomy, Michigan State University, East Lansing MI; United States of America
[k] Also at Department of Physics and Astronomy, University of Louisville, Louisville, KY; United States of America
[l] Also at Department of Physics, Ben Gurion University of the Negev, Beer Sheva; Israel
[m] Also at Department of Physics, California State University, East Bay; United States of America
[n] Also at Department of Physics, California State University, Sacramento; United States of America
[o] Also at Department of Physics, King's College London, London; United Kingdom
[p] Also at Department of Physics, University of Fribourg, Fribourg; Switzerland
[q] Also at Department of Physics, University of Thessaly; Greece
[r] Also at Department of Physics, Westmont College, Santa Barbara; United States of America
[s] Also at Hellenic Open University, Patras; Greece
[t] Also at Institucio Catalana de Recerca i Estudis Avancats, ICREA, Barcelona; Spain
[u] Also at Institut für Experimentalphysik, Universität Hamburg, Hamburg; Germany
[v] Also at Institute of Particle Physics (IPP); Canada
[w] Also at Institute of Physics, Azerbaijan Academy of Sciences, Baku; Azerbaijan
[x] Also at Institute of Theoretical Physics, Ilia State University, Tbilisi; Georgia
[y] Also at Lawrence Livermore National Laboratory, Livermore; United States of America
[z] Also at Physics Department, An-Najah National University, Nablus; Palestine
[aa] Also at The City College of New York, New York NY; United States of America
[ab] Also at The Collaborative Innovation Center of Quantum Matter (CICQM), Beijing; China
[ac] Also at TRIUMF, Vancouver BC; Canada
[ad] Also at Università di Napoli Parthenope, Napoli; Italy
[ae] Also at University of Chinese Academy of Sciences (UCAS), Beijing; China
[af] Also at University of Colorado Boulder, Department of Physics, Colorado; United States of America
[ag] Also at Yeditepe University, Physics Department, Istanbul; Türkiye
[*] Deceased